COMMONWEALTH OF AUSTRALIA
DEPARTMENT OF NATIONAL DEVELOPMENT
BUREAU OF MINERAL RESOURCES, GEOLOGY AND GEOPHYSICS

BULLETIN No. 109

Sedimentology of the Upper Devonian and Carboniferous Platform Sequence of the Bonaparte Gulf Basin

BY

J. J. VEEVERS

Issued under the Authority of the Hon. David Fairbairn,
Minister for National Development
1969

COMMONWEALTH OF AUSTRALIA

DEPARTMENT OF NATIONAL DEVELOPMENT

MINISTER: THE HON. DAVID FAIRBAIRN, D.F.C., M.P.

SECRETARY: R. W. BOSWELL, O.B.E.

BUREAU OF MINERAL RESOURCES, GEOLOGY AND GEOPHYSICS

DIRECTOR: N. H. FISHER

THIS BULLETIN WAS PREPARED IN THE GEOLOGICAL BRANCH

ASSISTANT DIRECTOR: J. N. CASEY

Published by the Bureau of Mineral Resources, Geology and Geophysics
Canberra, A.C.T.

Printed by Graphic Services Pty. Ltd., 60 Wyatt Street, Adelaide, S.A.

CORRIGENDUM

Table 3—the word duration should read deviation.

Plate 17, Figure 1—Caption should now read "Feldspar (bottom centre) and glauconite (top centre) . . . . . ."

Plate 21, Figure 2—This plate is wrong way round; the top is now to the left.

Plate 37, Figure 1—The nucleus of this oncolith has since been recognized tentatively as the codiacean alga litanaia.

CONTENTS

TABLES

ILLUSTRATIONS

FIGURES

PLATES

Between pages 46 and 47

20, fig. 1. Silicified crinoid ossicle. Septimus Limestone (photomicrograph)

20, fig. 2. Open valves of brachiopod shell filled with micrite lumps and drusy mosaic. Burt Range Formation (photomicrograph)

21, fig. 1. Another view of slide shown in Plate 20, figure 2, showing structure of drusy mosaic (photomicrograph)

21, fig. 2. Geopetal structure of brachiopod spiralia filled with fine sediment and drusy mosaic. Buttons Beds (photomicrograph)

22, fig. 1. Brachiopod filled with drusy mosaic and corals showing dolorhomb replacement. Westwood Member (photomicrograph)

22, fig. 2. *Girvanella* on surface of recrystallized spiriferid shell. Burt Range Formation (photomicrograph)

23, fig. 1. Recrystallized brachiopod shell in quartzose limestone. Burt Range Formation (photomicrograph)

23, fig. 2. Another view showing structure of drusy mosaic (photomicrograph)

24, fig. 1. Partly recrystallized brachiopod shell. Burt Range Formation (photomicrograph)

24, fig. 2. Partly recrystallized brachiopod valve. Burt Range Formation (photomicrograph)

25, fig. 1. Another view of slide shown in Plate 24, figure 2 (photomicrograph)

25, fig. 2. Microstylolite along edge of brachiopod valve. Burt Range Formation (photomicrograph)

26, fig. 1. Microstylolite on recrystallized brachiopod valve. Westwood Member (photomicrograph)

26, fig. 2. Detail of stromatolite (photomicrograph)

27, fig. 1. Bryozoon and crinoid ossicle. Septimus Limestone (photomicrograph)

27, fig. 2. Mash of corals, crinoid ossicles, brachiopods, and quartz grains. Burvill Beds (photomicrograph)

28, fig. 1. Endothyrid in quartzose limestone. Utting Calcarenite (photomicrograph)

28, fig. 2. Partly recrystallized brachiopod and hyperamminid. Burt Range Formation (photomicrograph)

29, fig. 1. The encrusting foraminiferan *(?)Wetheredella.* Ningbing Limestone (photomicrograph)

29, fig. 2. Recrystallized gastropod rimmed and filled with micrite. Westwood Member (photomicrograph)

30, fig. 1. Red alga, probably *Parachaetetes.* Buttons Beds (photomicrograph)

30, fig. 2. The alga(?) *Umbella.* Ningbing Limestone (photomicrograph)

Between pages 46 and 47

SUMMARY

The Upper Devonian and Carboniferous platform sequence of the Bonaparte Gulf Basin consists of 12,000 feet of marine conglomerate, quartz sandstone, limestone, and minor shale, disconformably overlain by 350 feet of Upper Carboniferous terrestrial quartz sandstone with minor conglomerate and siltstone.

The marine conglomerate is a marginal wedge, and consists essentially of well rounded fragments, up to boulder size, of metaquartzite and milky quartz in a matrix of quartz sandstone. Local variants contain fragments of igneous rocks derived from nearby sources. Basal breccia is found locally above unconformities, and an intraformational breccia of siltstone fragments is a common constituent of the Upper Carboniferous terrestrial formation.

The sandstone is a uniform argillaceous quartz sandstone with a pure orthoquartzite sand fraction, and occurs in two contrasting bed forms: cross-bedded sandstone, probably shaped by tidal currents flowing over a broad shelf; and flat-bedded sandstone, deposited near the shore. Granulometric studies seem to confirm that these sands are marine. Cross-bedding azimuths in the cross-bedded sandstone possibly indicate deposition in an arm of the sea from ebb tidal currents. A 90° change of direction of these currents from the early to the late Frasnian was probably caused by uplift in the southwestern part of the basin and consequent change in the shape and outline of the basin.

Carbonate rocks, chiefly limestone, were deposited during episodes of reduced supply of coarse terrigenous sediments. From field evidence, the well exposed Famennian limestone is known to be a reef complex. The other limestones are not so well exposed, so their depositional environment cannot be determined from field occurrence alone. Representative specimens of carbonate rocks were modally and chemically analysed, and this information was classified by a newly developed hierarchical agglomerative computer programme using an information statistic for the classification of mixed data. The Famennian reefal limestones are characterized by distinctive assemblages of groups defined numerically by petrographic and chemical attributes. Assemblages of numerical groups from other limestones were compared with those of the Famennian reefal sequence: two occurrences—one Frasnian, the other early Tournaisian—were identified as interfingering lagoonal/back reef facies, and a third (late Tournaisian and Visean) as non-reefal. The stratigraphical separation of older reefal (Frasnian to early Tournaisian) and younger non-reefal groups (late Tournaisian and Visean) can be interpreted unhesitatingly in terms of the tectonic history. The persistence of reefal limestones from the base of the Famennian to the end of the early Tournaisian and their earlier appearance during the dominantly terrigenous deposition of the Frasnian indicate the maintenance of a delicate balance of conditions in the sea favouring reef growth despite the intermittent influx of terrigenous sediment. The effect of the rapid uplift of the southwest margin of the basin in the mid-Tournaisian destroyed the balance and reefs did not reappear in the later Lower Carboniferous sea.

Associations among the modal and chemical attributes were found by a principal co-ordinate (or Q-factor) analysis. The composition of the analysed specimens may be expressed by varying proportions of the following four factors, each consisting of two negatively correlated attributes or sets of attributes:

(a) impurities (terrigenous minerals) versus pure calcite;

(b) dolomite versus skeletal matter;

(c) skeletal matter, excluding ostracods, versus lumps and algae; and

(d) conodonts and quartz versus skeletal matter, excluding conodonts and ostracods.

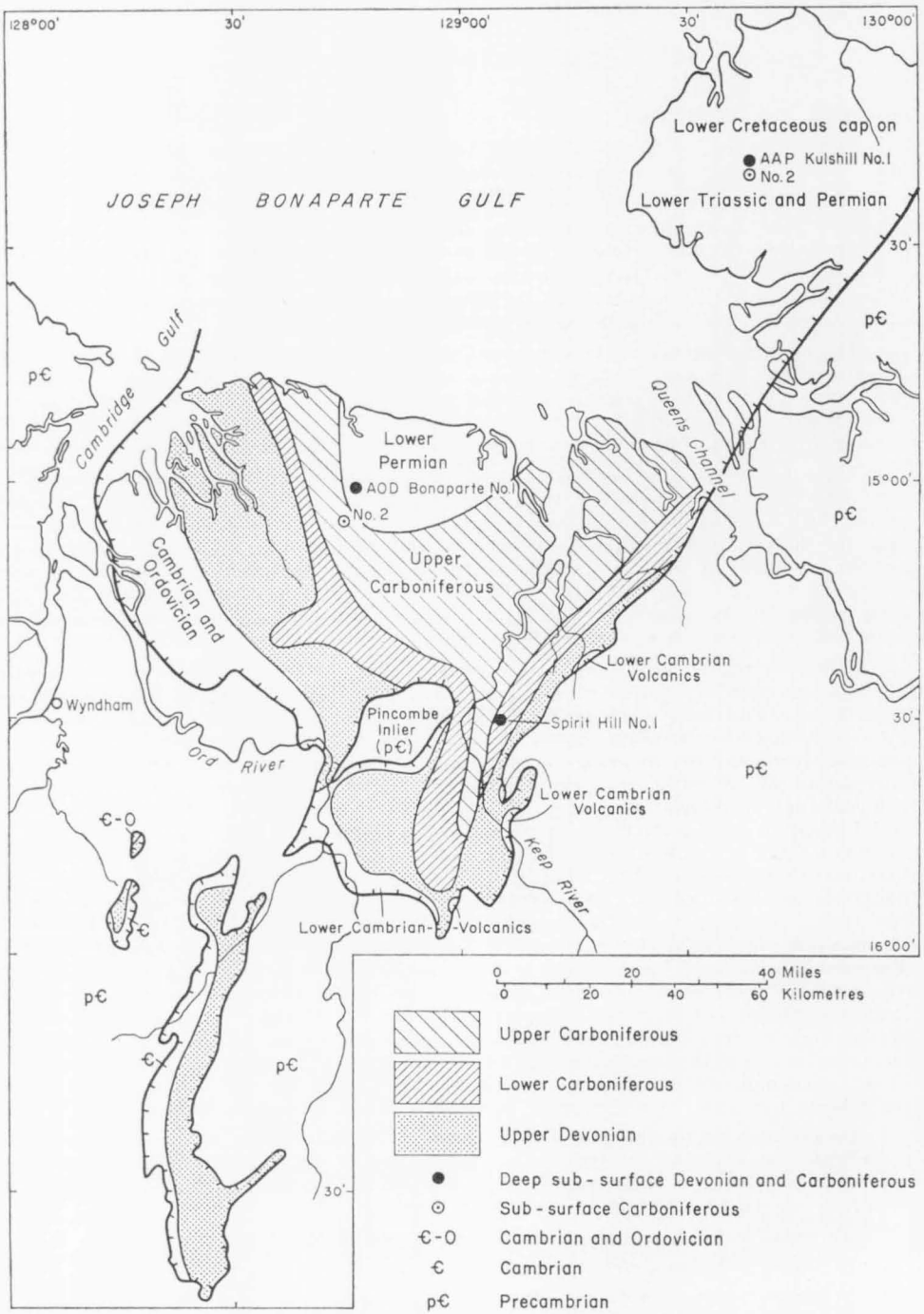

Figure 1. Solid geology of the southern part of the Bonaparte Gulf Basin

INTRODUCTION

The Upper Devonian and Lower Carboniferous sequence of the Bonaparte Gulf Basin (Figs 1, 2) comprises 12,000 feet of conglomerate, quartz sandstone, limestone, and shale deposited on a shallow-marine platform, and at least 14,000 feet of equivalent medium-grey siltstone, shale, and minor sandstone, deposited in a slightly deeper basin. The Upper Devonian and Lower Carboniferous sequence is unconformably overlain by 350 feet of Upper Carboniferous quartz sandstone, siltstone, and conglomerate, the Border Creek Formation, which is probably terrestrial.

A stratigraphical analysis of these sequences (Veevers & Roberts, 1968) was the main task of the current survey, which started in 1963. In the field, sedimentological studies sensu stricto necessarily took second place to stratigraphical analysis and as a result many of the studies reported below are incomplete. The excellence of the Bonaparte Gulf Basin as a study area comes from the concentration in a fairly small area of well exposed varied strata that have been little altered by subsequent movements and that generally contain abundant fossils which provide close stratigraphical and environmental control. Details of localities may be found in Veevers & Roberts (1968).

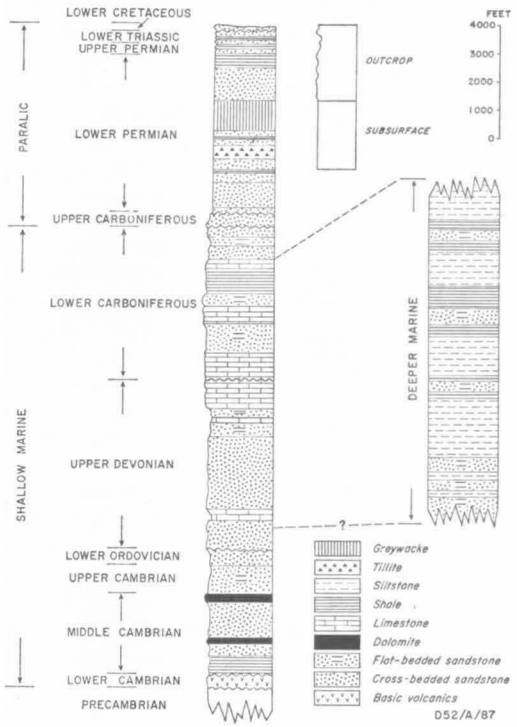

Figure 2. Diagrammatic composite stratigraphical sections

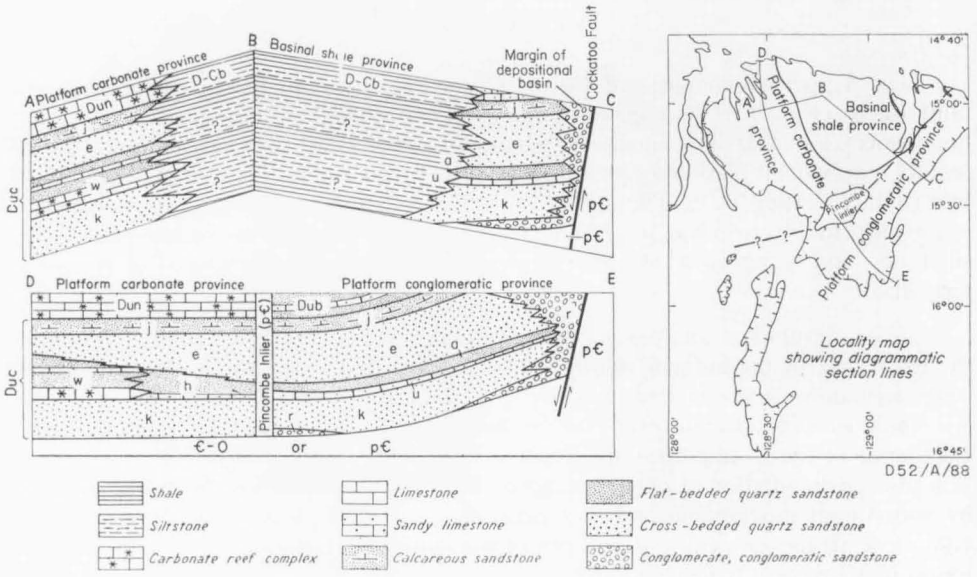

Figure 3. Upper Devonian facies

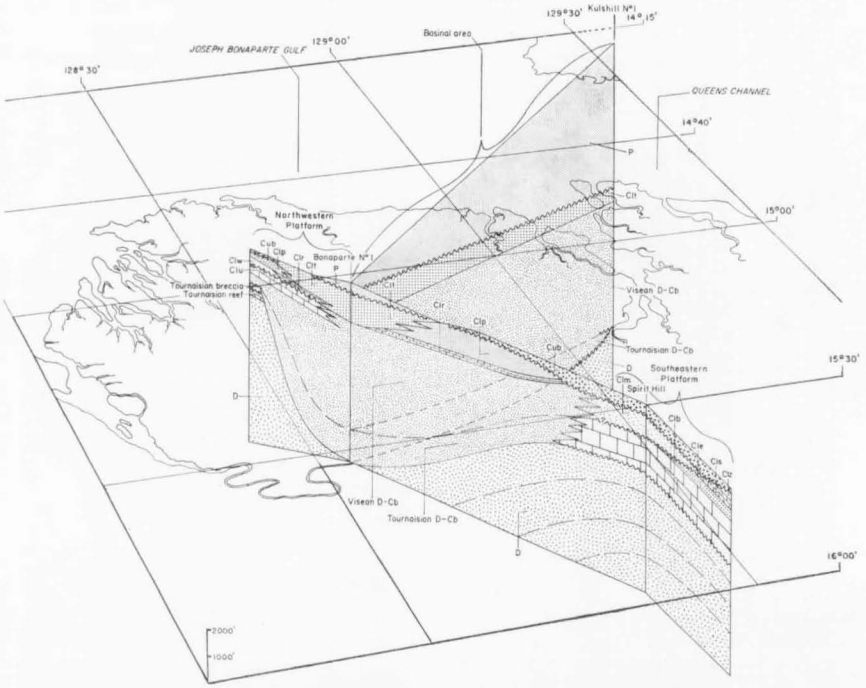

Figure 4. Distribution of Carboniferous formations

Summary of the Upper Devonian and Carboniferous Facies

As shown by the stratigraphical analysis (Veevers & Roberts, 1968), the Upper Devonian sequence (Fig. 3) is a marine shelf deposit in three facies: a platform conglomerate facies deposited near the shore; a platform carbonate facies deposited farther away from the shore; and a basinal shale facies deposited in a deeper part of the shelf. The Lower Carboniferous sequence (Fig. 4) is similar except that it lacks the platform conglomeratic facies of the Upper Devonian. The Upper Carboniferous is represented by a single formation, the Border Creek Formation, only 365 feet thick, of a single facies of presumed terrestrial quartz sandstone, conglomerate, and siltstone.

The sedimentology of these sequences will be published in three parts: (1) platform facies, comprising coarse terrigenous deposits (conglomerate, breccia, and sandstone) and carbonate sediments, all described in this Bulletin; (2) basinal shale facies; and (3) sedimentological synthesis.

COARSE TERRIGENOUS ROCKS

In this account, I have tried to avoid over-hasty interpretation of the environment of deposition. Most environmental indicators mean little by themselves, and the best interpretation is based on the combination of all the indicators available. Interpretations based on each group of sedimentological features (primary structures, petrography) are given throughout the text, and each interpretation is examined in terms of the various models of the environment of deposition. These are preliminary interpretations only, and firm conclusions are not drawn until all the features of the sediment have been described and discussed, and then related to the stratigraphy and palaeontology.

CONGLOMERATE AND BRECCIA

Conglomerate

Upper Devonian conglomerate occurs in the Ragged Range Conglomerate Member and in the conglomeratic phases of the Kellys Knob, Abney, and Cecil Sandstone Members in the Matheson Ridge/Cockatoo Spring area (Fig. 3). These occurrences follow the Cockatoo Fault system, and the Ivanhoe Fault system, or adjoin the Pincombe Inlier. The thickness of conglomerate in single beds or its total thickness through a section of conglomeratic sandstone decreases basinward of the fault system or away from the inlier; so the conglomerate is marginal and not basal. The conglomerate in these units, except the Abney Member, is interbedded with or passes laterally into cross-bedded sandstone. The Abney Member is the only unit of flat-bedded sandstone known to contain conglomerate. The Lower Carboniferous Milligans Beds at Spirit Hill contain thin lenses of conglomerate, which are also marginal. The conglomerate in the Upper Carboniferous Border Creek Formation is basal. The only other conglomerates in the basin are the limestone conglomerates in the fore-reef of the Ningbing Limestone and a thin bed of quartzite conglomerate in the back-reef; they are described in the second half of this Bulletin.

None of the units mentioned above consists entirely of conglomerate. As indicated by the name, the Ragged Range Conglomerate Member contains by far the greatest thickness of conglomerate: it constitutes all but 35 feet of the preserved 800 feet of Ragged Range Member at Conglomerate Hill in the Ragged Range and most of the estimated exposed 1,000 feet immediately north of Cockatoo Spring (Veevers & Roberts, 1968, fig. 15). In the northern part of the Ragged Range, 12 miles north of Conglomerate Hill, conglomerate constitutes a mere 75 feet in a total preserved thickness of 1,350 feet. The Lower Carboniferous sequence lacks conglomerate except for the pebbly sandstone at the base of the Waggon Creek Breccia (Veevers & Roberts, 1966), and the thin lenses in the Milligans Beds.

The Border Creek Formation contains lenticular beds of conglomerate, exemplified by a bed of conglomerate 65 feet thick at the southern end of Mount Septimus (section 150), which thins to a mere pebble bed a mile northward.

These conglomerates have a fairly uniform composition of well rounded pebbles, cobbles, and boulders of metaquartzite and, less commonly, of milky quartz; fragments of igneous rocks are rare. Local variants include fragments of basalt, up to 3 feet across, in the Ragged Range Member at Church Steeple Peak (Veevers & Roberts, 1968, pl. 2, fig. 2), grey siltstone breccia along the eastern

margin, and granitic detritus in the southern Ragged Range; and, in the Border Creek Formation, fragments of intraformational siltstone and mudstone. Rare pebbles of igneous rocks from the Ragged Range Member at Church Steeple Peak consist of porphyritic microgranite with well developed micrographic intergrowths, and porphyritic rhyolite or welded tuff. D. B. Dow (BMR, pers. comm.), who examined the rocks, considers that the microgranite could have come from the Bow River Granite or Castlereagh Hill Porphyry and the rhyolite or welded tuff from the Whitewater Volcanics; these formations are part of the Lamboo Complex in the East Kimberleys, and the nearest outcrops are only 25 miles south of Church Steeple Peak.

The matrix is a fairly uniform white to yellow quartz sandstone except in the Ragged Range Member, and in parts of the Kellys Knob Member, which are stained red with hematite. Variants in the matrix follow those of the clasts; so, for example, the granitic clasts in the southern Ragged Range have a matrix of arkose.

The proportion of clasts to matrix varies from the poorly consolidated conglomerate or virtually openwork gravel with little or no matrix in parts of the Ragged Range Member (notably at Church Steeple Peak and at Conglomerate Hill) and the Border Creek Formation, to the pebbly quartz sandstone of the conglomeratic phases of the Kellys Knob, Abney, and Cecil Members.

Most clasts are well rounded cobbles (64-256 mm.), which are sorted into crudely defined beds (Veevers & Roberts, 1968, pl. 2, fig. 1). In a few places, the clasts are poorly rounded and poorly sorted (Pl. 1, fig. 1).

Minor variants disregarded, the conglomerates are the mature orthoquartzite (oligomict) conglomerates of Pettijohn (1957, p. 256). According to Pettijohn, this kind of conglomerate does not form thick deposits, and 'they occur as sporadic pebbles or pebbly layers and lenses interbedded with strongly cross-bedded orthoquartzitic and proto-quartzitic sands'. This is true of the Bonaparte Basin conglomerates, with the notable exception of the thick and coarse conglomerates of the Ragged Range Member in the Conglomerate Hill area of the Ragged Range and in the Cockatoo Spring area. These thick conglomerates have the composition of orthoquartzite conglomerates, but the size and shape of Pettijohn's petromict conglomerates, whose chief constituents are metastable rocks. This anomalous composition is taken to indicate the overwhelming preponderance of orthoquartzite in the source area, either by cropping out over wide areas or by the removal by weathering of less stable rocks, so that regardless of the tectonic setting at the margin of the basin this was the only material available for deposition. Folk (1961, p. 123) has called attention to this kind of deposit, noting that 'orthoquartzites derived from re-worked sediments require no period of stability, in fact many of them are orogenic sediments'.

Environment of Deposition

The physical characters of the conglomerates merely indicate deposition in water; the only direct indication of the salinity of the water is provided by fossils. Part, if not all, of the Ragged Range Conglomerate Member was deposited in the sea, as indicated by the pelecypods and gastropods found in the sandstone matrix of the conglomerate near the base of the northern part of the Ragged Range (loc. 53/2), pelecypods found in sandstone interbedded with conglomerate in the middle part of the preserved section in the northern Ragged Range (loc. 52/1),

and pelecypods found immediately above the conglomerate bed at Church Steeple Peak (loc. 412/5). Since the strata enclosing the marine fossils are in no way different from those in the rest of the Ragged Range Member, the entire member is probably marine. For the same reason, the conglomeratic phases of the Kellys Knob, Abney, and Cecil Sandstone Members may also be inferred to be probably marine. The Border Creek Formation, on the other hand, has so far yielded no marine fossils—logs are its only known fossils—and it is regarded as probably terrestrial.

The marine conglomerate wedges of the Ragged Range, Kellys Knob, Abney, and Cecil Members are interpreted as being deposited along a shallow inshore area, which locally, as in the southern Ragged Range, subsided fast enough to allow the accumulation of thick conglomerate. This subsidence was probably caused by movements along the faults with which the conglomerates are associated. How much of the conglomerate was derived locally from the edge of the upthrown block and how much from farther away cannot be answered from the scanty evidence available because the quartzite composition of most clasts is not diagnostic of any particular part of the Precambrian source. Because of their chemical and mechanical instability, clasts of exceptional size and composition, such as the blocks of basalt 3 feet across in the Ragged Range Member of the Church Steeple Peak, and other basalt blocks and locally abundant grey siltstone pebbles and cobbles in the Ragged Range Member along the Cockatoo Fault System, indicate derivation from a nearby source: the Pincombe Inlier for the first example, and the upthrown block southeast of the Cockatoo Fault System for the second. Other diagnostic clasts in the Ragged Range Conglomerate at Church Steeple Peak are pebbles of porphyritic microgranite and porphyritic rhyolite or tuff, the nearest known outcrops of which are situated only 25 miles to the south.

The only abundant non-quartzose minerals and rock fragments found in the Ragged Range Conglomerate Member of the Ragged Range are those in the arkose and granite wash near the southern end of the Range (locs L7, L8), which have a ready source in the granitic rocks of the nearby Lamboo Complex. To the north, the Ragged Range Member consists with few exceptions—Traves (1955, p. 47) mentions some clasts of strongly weathered granite—of quartzite conglomerate and quartz sandstone. The conglomeratic phases of the Kellys Knob, Abney, and Cecil Members contain no obvious non-quartzitic clasts except for occasional pebbles of red micaceous quartz siltstone, which probably came from close by.

In the Border Creek Formation, the only known non-quartzitic clasts, except for the intraformational siltstone breccia, are deeply weathered cobbles of crystalline rock in the Spirit Hill area.

From the size of the biggest fragments—commonly up to 3 feet in parts of the Ragged Range Member and up to 1.5 feet in the other conglomeratic members of the Cockatoo Formation—we may infer that these conglomerates were deposited close inshore in front of a fairly high coast drained by streams capable of transporting boulders of this size. The terrestrial Border Creek Formation contains fragments of extra-basinal rock up to 1.5 feet across—the blocks of siltstone in this formation are probably intraformational—and these indicate the competency of the streams from which the Border Creek Formation is presumed to have been deposited. The intraformational blocks of siltstone and sandstone and the deep

cut-and-fill structures in the Border Creek Formation further testify to the rapid flow of the streams that crossed the area of deposition.

Breccia

The only breccias found, besides those in the Waggon Creek area (Veevers & Roberts, 1966), are the intraformational breccia of the Border Creek Formation and Kellys Knob Member and the basal breccia of the Buttons Beds in the Sorby Hills. The fore-reef breccia of the Ningbing Limestone is described in the second half of this Bulletin. The intraformational breccia of the Border Creek Formation consists dominantly of fragments of white siltstone from sand size up to 15 feet across in a sandstone matrix. The siltstone is identical with that found in beds within the formation. Blocks of intraformational sandstone were also found in breccia at Spirit Hill. The finer part of a breccia is shown in Plate 1, figure 2, and a channel cut into siltstone is shown in figure 51 of Veevers & Roberts (1968). The breccia is commonly found in cut-and-fill structures, and its origin is ascribed to the action of streams cutting new courses on an alluviated surface.

The breccia in the Buttons Beds of the Sorby Hills (loc. 402—see fig. 37 of Veevers & Roberts, 1968) was found in two beds each 1 foot thick, one immediately above the eroded surface of tilted Precambrian silicified siltstone, and the other 6 feet higher. The breccia consists of plates of silicified siltstone up to 3 inches long and rounded pebbles of milky quartz embedded in quartz sandstone (Pl. 2, fig. 1). Crude bedding is indicated by a parallel arrangement of some of the plates; other plates are oriented at high angles to the bedding. The breccia is succeeded by marine limestone. This basal breccia was deposited during the transgression of the sea over a surface of locally derived siltstone clasts and alluvium of milky quartz pebbles and quartz sand.

The Lower Carboniferous breccias of the Waggon Creek area are the subject of a separate report by Veevers & Roberts (1966), to which the reader is referred for details. In the Waggon Creek area of the southwestern Bonaparte Gulf Basin, two outcrops of breccia unconformably overlie the Cockatoo Formation. The western outcrop consists of pebbly sandstone overlain by dolomite breccia, which together are called the Waggon Creek Breccia. The sandstone contains pebbles of metaquartzite and quartz, and the breccia consists of angular blocks of dolomite up to 30 feet long, and rounded pebbles and boulders of quartz and metaquartzite in a sandy dolomite matrix. Marine fossils indicate a Visean age. The pebbly sandstone is probably beach rock, and the overlying breccia is a littoral talus breccia probably formed by the isolating and undermining by the sea of beds of dolomite in the otherwise soft Cockatoo Formation. A similar breccia, which crops out 2 miles to the east, was deposited under similar conditions during a brief marine incursion in the mid-Tournaisian.

SANDSTONE

The Upper Devonian and Carboniferous sandstone units of the Bonaparte Gulf Basin consist of two major kinds of sandstone, which for the sake of brevity will be referred to simply as cross-bedded sandstone and flat-bedded sandstone, after their dominant though not exclusive characteristic. The two kinds of sandstone are found interlayered in the Point Spring Sandstone; all the other sandstone units consist of one or the other kind. A key to the two kinds of sandstone, and their distributions among the formations, are given in Table 1.

TABLE 1: DIAGNOSTIC CHARACTERS OF CROSS-BEDDED AND FLAT-BEDDED SANDSTONES

Character	Cross-bedded Sandstone	Flat-bedded Sandstone
Sedimentary structures		
(1) thickness of beds	laminated to thick	laminated to thin
(2) flat-bedding	minor	dominant
(3) cross-bedding	dominant, chiefly *omikron*, with minor *iota* and *zeta* types	locally common: *xi*-type
(4) contortion	common, chiefly recumbent folds	absent
(5) others	ripple marks and parting lineation fairly rare; biogenic structures not seen	biogenic structures common
Other characters		
(6) grainsize	fine to coarse, locally conglomerate	fine to medium
(7) colour	white to yellow, locally red-brown	typically white, locally red-brown, greenish
(8) jointing	ubiquitous	rare
(9) fossils	rare, except for logs, fish plates, pelecypods	commonly abundant body and trace fossils
(10) grades laterally and vertically into	conglomerate	limestone and calcareous sandstone
Distribution	parts of Ragged Range Conglomerate Member	
	Kellys Knob Sandstone Member	Abney Sandstone Member
	Cecil Sandstone Member	Enga Sandstone
	Border Creek Foundation *	Zimmerman Sandstone
	both types interbedded	in Point Spring Sandstone

* Included in a third group distinguished by the presence of siltstone pellets and laths.

TABLE 2: GROSS FEATURES OF SANDSTONE FORMATIONS

The estimated original sizes and shapes of the sandstone units are specified by the criteria used by Krynine (1948)

	Length Along Strike (miles)	Width Across Strike (miles)	Area (miles^2)	Thickness (miles)	Volume (miles^3)	Size	Shape
			Mixed Cross-bedded and Flat-bedded Sandstone				
Ragged Range Conglomerate Member	130	10	1,300	0.2	260	medium	prismatic
Kellys Knob Member	90	90	8,100	0.2	1,620	large	tabular
Cecil Member	90	90	8,100	0.4	3,240	large	tabular
Border Creek Formation	70	50	3,500	0.1	350	large(?)	tabular
			Mixed Cross-bedded and Flat-bedded Sandstone				
Point Spring Sandstone	50	10	500	0.1	50	medium	tabular
			Flat-bedded Sandstone				
Abney Member	35	30	1,050	0.06	63	medium	tabular
Enga Sandstone	50	10	500	0.1	50	medium	tabular
Zimmerman Sandstone	5	3	15	0.1	1.5	small or medium	prismatic

Note: Due to subsequent erosion on the one hand and subsequent covering by younger units on the other, the original size and shape of these units are imperfectly known, and the figures in the table are minimum estimates.

The petrology of the two sandstones is not diagnostic, both being argillaceous quartz sandstone with a pure orthoquartzite sand fraction. A third kind of sandstone, represented by the Border Creek Formation, is separated from cross-bedded sandstone by the presence of siltstone pellets and laths.

According to Krynine's criteria (Table 2), three units of cross-bedded sandstone—the Kellys Knob Member, Cecil Member, and Border Creek Formation—are large tabular bodies; another three units—the Enga Sandstone and Abney Member (both flat-bedded sandstone) and the Point Spring Sandstone (mixed flat-bedded and cross-bedded sandstone)—are medium tabular bodies; the Ragged Range Member is a medium prismatic body; and the Zimmermann Sandstone is a small or medium prismatic body. With local exceptions (the Ragged Range Member is prismatic because it is marginal, the Zimmermann Sandstone because only a narrow belt of it is preserved), the cross-bedded sandstone units are large tabular bodies, and the flat-bedded sandstone units are medium tabular bodies.

Cross-bedded Sandstone

Primary Structures

As implied by the name, almost all outcrops of 'cross-bedded sandstone' are cross-bedded, and only a few are flat-bedded. Contorted bedding, ripple mark, and parting lineation are locally common but not so widespread as cross-bedding.

Cross-bedding

Almost all the cross-bedding seems to be of one kind, namely the omikron cross-bedding of Allen's (1963a) classification. As described in the terms used by Allen, the cross-beds are arranged in large scale sets, which in turn are grouped in cosets. The sets are tabular, being bounded by parallel plane surfaces or by thin flat-bedded layers, which are commonly hardened by subsequent deposits of iron oxide and silica. Cross-beds separated from each other by thin flat-bedded layers constitute parallel composite cosets (Karcz & Braun, 1964, fig. 5 (6)). In each coset, the cross-beds dip at about the same angle in virtually the same direction, so that in vertical sections at right angles to the cross-dip (section *bc* of the reference system of Potter & Pettijohn, 1963, fig. 4-2), the traces of the cross-bedding are even and parallel (Pl. 2, fig. 2). In sections parallel to the dip directions (section *ac* of Potter & Pettijohn), the traces of the cross-bedding are linear, curvilinear (concave upwards), or flexed (terms after Crook, 1965). Individual cross-beds are typically 0.1 foot thick, sets 1.5 feet thick, and cosets tens to hundreds of feet thick. Outcrops showing many of these features are illustrated in Plate 3, figures 1 and 2 (upper part). Another typical outcrop of cross-bedded sandstone, also of the Kellys Knob Member, is shown by Traves (1955, fig. 25).

Within the cross-bedded sandstone, rare solitary tabular cross-beds (alpha cross-beds) are separated by flat-bedded sandstone. In section 441 through the Point Spring Sandstone, a few solitary sets of cross-bedded sandstone lie within the uppermost 30 feet of a sequence of flat-bedded sandstone (interval 210-240 ft). This is one of the best localities in the Point Spring Sandstone to show the intermingling of the cross-bedded and flat-bedded sandstones. Care must be taken to ensure that the structures are seen in three dimensions; for example, in Figure 5 the thick set near the top appears to be solitary, but from other viewpoints the enclosing strata are seen to be cross-bedded too, but with a different direction of dip.

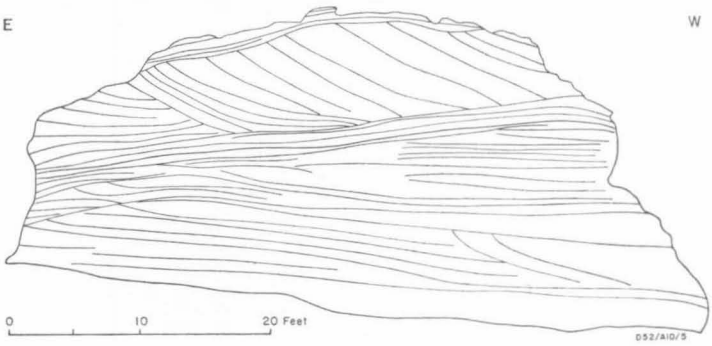

Figure 5. Cross-beds in probable Kellys Knob Member near Cape Domett (loc. 87-3). cf. Veevers & Roberts, 1968, pl. 14, fig. 2.

Solitary trough-shaped sets are found throughout most of the cross-bedded sandstone, but except in the bed of the Ord River (loc. 36) are not visibly abundant. This is probably because they are easily overlooked or misidentified as tabular cross-beds in single vertical sections; and it is only in wide expanses of horizontal sections (such as loc. 36) that trough cross-beds are seen to be fairly abundant. At locality 36, two types are found: zeta cross-beds (Pl. 4, fig. 1), which are semicylindrical bodies, and iota cross-beds (Pl. 4, fig. 2), which consist of pitching concordant cross-beds. In the uppermost 200 feet of section 36, the troughs are cut into sandstone, and are filled with a sandstone containing pebbles and cobbles of quartzite. The widest observed trough is 30 feet across, and it contains cobbles of quartzite up to 5 inches across. Narrower troughs contain smaller clasts. The correlation between size of clasts and width of troughs probably indicates the action of rapid currents which first cut a deep broad channel and then filled it with material coarser than that elsewhere in this section. Similar material fills troughs in the Border Creek Formation (Pl. 5, fig. 1).

An example of two troughs separated by a thin band of flat-bedded sandstone is shown in Plate 5, figure 2. The lower trough is filled with platy pebbles of Precambrian silicified siltstone, which are locally imbricated toward the right; the upper trough contains mainly rounded cobbles and boulders (up to 12 in. across) of Precambrian quartzite. The complete separation of the two kinds of clast indicates two source areas: (1) a nearby area of siltstone, from which clasts were too unstable mechanically to have been carried far; and (2) a broad and possibly more distant area of quartzite or quartzite gravel.

In the Border Creek Formation of the Weaber Range (top of section 25), troughs cut out of laminated sandstone are filled with parallel-bedded pebbly and cobbly sandstone (Pl. 5, fig. 1).

The last few examples have been of troughs with a fill coarser than the underlying rock. In the Border Creek Formation at Spirit Hill (Pl. 6, fig. 1), jointed medium to coarse-grained sandstone fills a steep-sided trough in conglomerate. The fill itself is a coset of omikron cross-bedding in turn cut into by shallow troughs.

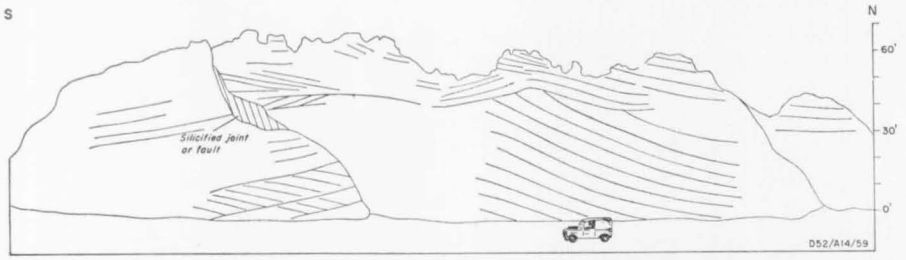

Figure 6. Set of cross-beds, at least 50 feet thick, in Kellys Knob Member, southwest tip of Hargreaves Hills (loc. 239B)

Thick Cross-bedded Sets. Thick cross-bedded sets (greater than 10 ft) were seen in the Kellys Knob Sandstone Member in the western part of the Hargreaves Hills and northwestward. A set at least 50 feet thick was found at locality 239B (Fig. 6); the lower part of the set is covered, so its complete thickness is unknown. The traces of the cross-bedding form catenary curves. The top of the main set is eroded and overlain by a similar set in which the cross-bedding is parallel to the erosion surface. Omikron cross-bedding is seen in other parts of the outcrop. Another thick set (Pl. 3, fig. 2, lower part) at least 25 feet thick, also with its lower part covered, lies beneath omikron cross-bedded cosets at locality 43/7, west of the Onslow Hills; the highest cross-dip, in this set (after removal of secondary tilt) is 50°, and part of this dip is probably attributable to intraformational folding. At locality 239C, on the western edge of the Hargreaves Hills (Fig. 7), the Kellys Knob Sandstone Member is exposed in a fault-bounded ridge on whose sides the traces of thick sets are visible. The thickest visible set is 30 feet, and like most other sets it is apparently of the omikron type. The main feature shown by this outcrop is the uniform northerly cross-dip. Closer detail of this kind of cross-bedding is shown in Plate 6, figure 2, a picture of an isolated outcrop of Kellys Knob Sandstone Member in the same area. Note the linear traces of cross-beds, and the northwesterly cross-dips.

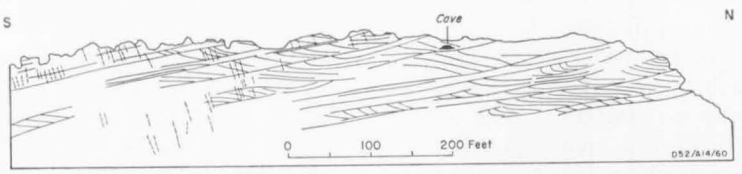

Figure 7. Looking west at fault block of Kellys Knob Member on the western edge of Hargreaves Hills (loc. 239c), half a mile north of locality 239B. The block has a secondary tilt of 10° to the south. All cross-dips are northward; the thickest set is 30 feet. The southern half of the block is crossed by joints normal to the bounding surfaces of the sets. In the northern part of the block, the cross-bedding in the upper parts of some sets has been steepened by contemporaneous contortion

A preliminary note on the interpretation of these thick sets is required before passing on to the description of other structures. Owing to their thickness alone, thick cross-bedded sets are commonly interpreted as aeolian deposits. In the same

way as omikron cross-beds may be deposited by the migration of straight-crested transverse ripples, either subaqueous or aeolian, so thick cross-bedded sets, at least those up to 100 feet thick, may be aeolian or subaqueous (Potter & Pettijohn, 1963, p. 86).

Intraformational Recumbent Folds

An example of a recumbent S-fold in cross-bedded sandstone is shown in Plate 7, figure 1. The beds are overfolded towards the southwest and the enclosing omikron cross-beds (not visible in the picture) cross-dip west-northwestward, roughly in the same direction as the overfolding, in agreement with McKee's et al. (1962) conclusions that S-folds, like other intraformational recumbent folds, are formed in clean water-saturated sand by the overriding force of a sand mass pushed forward by strong currents. In the figured example, the upper limb is preserved, whereas in most of the experimental folds of McKee et al. (1962) the upper limb was removed by stream-current planation.

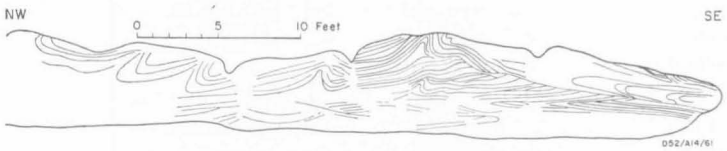

Figure 8. Series of recumbent folds in a cliff in Cecil Member in the Ord River (loc. 36-3)

A complex series of recumbent folds was found at locality 36/3 (Fig. 8). Six recumbent folds are visible; five of them have axes that dip at high angles to the northwest (or left), and the axis of the sixth fold (on the right) dips at a low angle to the southeast (or right), in general agreement with the resultant cross-dip azimuth of 75° of omikron cross-beds at this locality. Another point of interest centres on the recumbent fold in the middle. The left limb consists of concordant strata which are discordant in the right limb.

A recumbent fold near the left-hand edge of Plate 3, figure 2 (loc. 43/7) is oversteepened in the direction of lateral water stress as indicated by northwest-dipping omikron cross-beds.

Other Structures

Parting lineation was seen in a few places only. This structure is a characteristic of many flagstones and its rare appearance in the cross-bedded sandstone of the Bonaparte Gulf Basin is probably due to secondary rather than primary effects, such as poor cementation. Ripple marks are also uncommon, probably for similar reasons. Those that were seen are generally long and straight, symmetrical or asymmetrical, and parallel to the strike of nearby cross-bedding. Biogenic sedimentary structures were not seen in the cross-bedded sandstone.

Flat (horizontal) beds (Pl. 7, fig. 2; Veevers & Roberts, 1968, pl. 8, fig. 2) are found in places between cross-beds, but are everywhere subordinate to the cross-beds. Very thin flat beds are common interbedded with omikron cross-beds in composite sets.

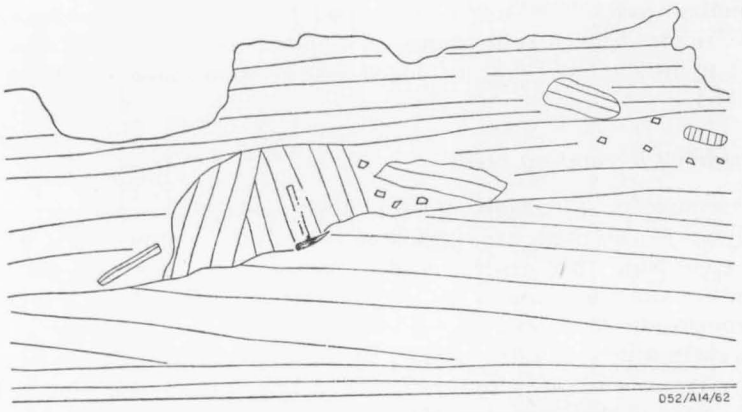

Figure 9. Intraformational breccia in the uppermost few feet of the Kellys Knob Member at locality 438, near Kununurra

Intraformational breccia was seen in the uppermost few feet of the Kellys Knob Sandstone Member at locality 438 (Fig. 9). The clasts consist of the same kind of laminated sandstone as that in which they are embedded, and they range in size from 1 inch to 3 feet across. The biggest clast that was seen is in the form of a faulted anticline. This breccia is interpreted as a recumbent fold which has broken up from the application of excessive lateral stress.

As already noted, intraformational breccia of siltstone clasts is common in parts of the Border Creek Formation (Pl. 1, fig. 2). The clasts commonly range in size from tiny flakes to plates 6 inches long. Blocks of siltstone up to 3 feet long and 1.5 feet wide were seen at locality 433/1, near Rocky Islet, in probable Border Creek Formation, and up to 6 feet long in the Border Creek Formation at Spirit Hill. Intraformational siltstone breccia is also common in the Permian Port Keats Group (Dickins et al., 1968).

Wedge-bedding is associated with lenses of conglomerate in sandstone. The conglomerate bed indicated by the hammer in Plate 8, figure 1 fills a trough eroded out of the underlying sandstone; its clasts 'dip' towards the right, indicating the effect of a current running from right to left. At this outcrop, this direction is north-northeastward, and corresponds with the current direction indicated by the cross-bedding in nearby outcrops of sandstone.

The Border Creek Formation contains several lenses of conglomerate which swell and pinch out in short distances; unlike the Upper Devonian conglomerates, those in the Border Creek Formation are distributed independently of the basin margin, in accordance with the view that they are terrestrial.

Though not a primary structure, jointing is mentioned here because it is diagnostic of the cross-bedded sandstone (Veevers & Roberts, 1968, pl. 32, fig. 2). Under repeated stress, the cross-bedded sandstone has broken into large joint-bounded blocks, whereas the flat-bedded sandstone has remained visibly unaffected. This different response to stress reflects an original depositional difference, probably chiefly in the kind of sand packing and bedding.

The restriction of large-scale joints to cross-bedded sandstone is seen in the Point Spring Sandstone, where jointed cross-bedded sandstone is associated with unjointed flat-bedded sandstone (Veevers & Roberts, 1968, pl. 33, fig. 2). Many of the smallest visible joints lie at right angles to each bed and cross-bed, and do not cross from one bed to the next; they probably originated from shrinkage during early diagenesis. Other small joints cross vertically through bedding and cross-bedding alike, and probably originated after lithification.

The patterns of large-scale joints in the cross-bedded sandstone are the subject of a separate report (Veevers & Maffi, 1968).

Analysis of Directional Structures

As mentioned already, cross-bedding is the only widespread directional structure in the cross-bedded sandstone. Ripple marks and parting lineation are locally important but regionally minor, and add little to a directional analysis. This analysis then is based on observations of cross-bedding, mainly of the omikron type, supplemented by a few observations of other directional structures, which include trough cross-beds, current lineations, ripple marks, and logs.

At large outcrops, a single observation of the direction and amount of the cross-dip was made from each accessible set; commonly as few as six observations were sufficient in visibly polarized cosets. At poorly exposed outcrops, all the few visible cross-beds were measured. Most measurements were made on omikron cross-beds, and the rest on trough-type cross-beds. At each outcrop, the secondary tilt was measured on the assumption that the bounding surfaces of sets were originally horizontal. According to this criterion, many outcrops are unaffected by tilting. The steepest tilt is 25°, and most outcrops are tilted less than 10°, and accordingly the effect of fold plunge was neglected.

The field data were processed on a CDC 3600 computer from a programme written by T. Quinlan. Computations were made in the following sequence: (a) the cross-dips were corrected for secondary tilt; (b) from the corrected cross-dips were derived the azimuth of the resultant vector (the vector mean), its magnitude, the (Raleigh) probability that the vector mean would be obtained by chance from a random distribution, and the standard deviation about the vector mean. This method was taken from Curray (1956). In assessing the results, a significance level of 5 percent ($P = 0.05$) was adopted.

Grand means and variances of cross-dips through entire formations, as described by Potter & Pettijohn (1963, pp. 86-9), were not computed because, in my opinion, such measures have little, if any, geological meaning. This view is based on the fact that whereas the mean cross-dip azimuth for each coset fairly closely indicates the direction of the principal bottom currents at one time and place, or in other words is homogeneous, the grand mean cross-dip azimuths and the variance of measurements from different stratigraphical and geographical positions within an entire formation are almost invariably heterogeneous measures of the variable directions of currents during the deposition of a single coset *and* of the different directions of currents during the deposition of cosets at widely different stratigraphical and geographical positions in an entire formation. Potter & Pettijohn (1963, p. 89) were aware of these difficulties and suggested that a qualitative appraisal of such data would be more appropriate than a more precise statistical evaluation.

TABLE 3: STATISTICS OF OBSERVATIONS OF DIRECTIONAL STRUCTURES

Locality	Vector Mean (degrees)	Standard Duration (degrees)	Magnitude (%)	n	P
		Ragged Range Conglomerate Member			
53-1	199	36.1	83	12	3x10-4
70-1	341	49.4	70	33	10-4
L14-55	277	47.8	71	12	2x10-3
411-2	277	17.9	96	6	4x10-3
426-1	230	26.7	91	6	7x10-3
426-2	257	29.3	89	6	8x10-3
464-4	176	56.6	70	8	2x10-2
		Kellys Knob Sandstone Member			
40-1	285	71.2	57	17	4x10-3
-5	316	67.7	60	12	10-2
43-6	285	55.5	66	16	10-3
42-2	317	35.1	85	6	10-2
44-3	275	19.9	95	8	10-3
49-2	283	15.2	97	7	10-3
49-3	269	25.5	92	15	10-4
75-6	352	34.6	84	13	10-4
76-3	302	32.4	87	10	6x10-4
77-3	322	51.9	71	12	2x10-3
81-3	215	39.3	80	24	10-4
87.3	302	44.5	75	12	10-3
87-5	281	39.7	81	6	2x10-2
123-22	332	19.9	96	4	3x10-2
404-2	301	18.2	96	6	4x10-3
404-3	290	26.5	91	6	7x10-3
404-4	307	14.6	97	6	3x10-3
404-5	263	53.3	70	6	5x10-2
405-1	291	29.8	90	6	8x10-3
407-1	255	35.7	85	6	10-2
411-1	296	23.3	93	6	5x10-3
411-3	319	18.3	96	7	10-3
411-4	331	44.0	77	6	3x10-2
414-1	255	36.3	83	11	5x10-4
417-1	3	37.1	85	6	10-2
		Cecil Sandstone Member			
36-2	88	51.1	71	9	10-2
36-3	75	50.2	70	10	7x10-3
36-6	35	19.4	96	4	3x10-2
45-1	59	32.6	86	10	6x10-4
46-3	47	68.6	50	12	0.048
46-4	52	60.8	71	11	4x10-3
47-3	66	31.6	87	12	10-4
80-1	24	63.7	60	12	10-2
266-1	7	16.1	97	5	10-2
405-2	119	22.9	94	5	10-2
415-320	56	39.9	82	6	2x10-2
415-515	16	35.5	85	6	10-2
415-590	55	50.6	71	6	5x10-2
		Border Creek Formation			
132-4	61	40.5	79	13	3x10-4
134-12	353	42.5	78	10	2x10-3
432-1	319	19.6	89	6	8x10-3
433-3	74	9.2	99	3	5x10-2
436-1280	311	22.3	94	6	5x10-3
436-1415	21	29.1	90	6	8x10-3
436-1460	353	24.7	92	6	6x10-3
452-450	32	24.5	93	6	6x10-3
		Point Spring Sandstone			
400-1	117	24.4	93	7	2x10-3
400-2	0	21.8	94	6	5x10-3
400-3	69	23.5	93	6	5x10-3
400-5	18	20.6	95	6	5x10-3
400-6	13	35.5	85	6	10-2
401-1	48	46.1	77	6	3x10-2
401-4	10	40.2	81	6	2x10-2
401-7	44	17.6	96	6	4x10-3
435-470	60	35.0	85	4	10-2
435-550	32	6.2	100	4	2x10-2
436-330	70	15.6	97	6	4x10-3
436-420	89	18.1	96	5	10-2
437-170	69	31.9	89	4	4x10-2
437-370	69	46.7	77	5	5x10-2
437-905	306	19.2	96	5	10-2
437-995	339	19.3	95	5	10-2
441-380	97	47.2	77	5	5x10-2
458-330	34	20.1	95	5	10-2
458-450	73	11.3	99	4	2x10-2

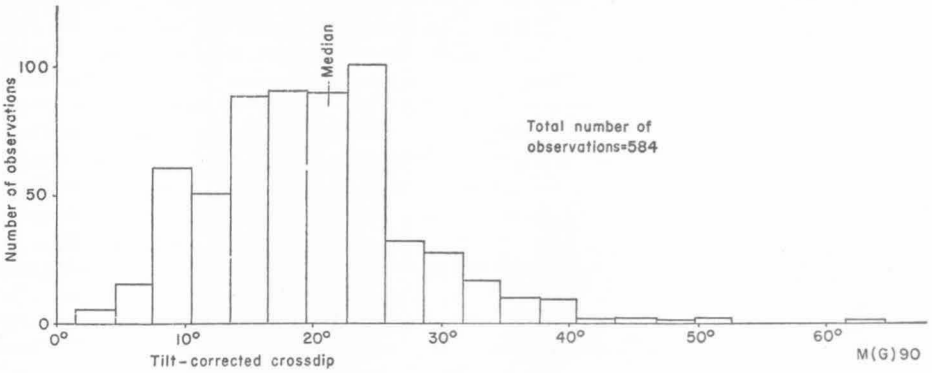

Figure 10. Frequency distribution of cross-dips

A total of 584 measurements from 72 localities have significant vector mean azimuths; their statistics are given in Table 3. The narrow scatter of most observations about their corresponding vector means is shown by the median standard deviation of 32.1° and median vector magnitude of 87 percent. The frequency distribution of cross-dips (Fig. 10) is skewed towards the right, and the large number of low dips possibly indicates that many measurements were made on the gently dipping flanks of only partly exposed large trough-type cross-beds, which in such situations simulate tabular cross-beds. The few dips greater than 40° were probably measured unwittingly from contorted cross-beds. The median dip of 20° lies within the range of 18° to 25° cited by Potter & Pettijohn (1963, p. 79) as the average dip of cross-beds. Further comments on these statistics will be made below in the section on interpretation.

As a check of the local scatter of current directions, observations were made at the same stratigraphical horizon and through several horizons in a small area of well exposed cross-bedded Point Spring Sandstone in the Weaber Range (Fig. 11). Eleven sets of observations were made in a distance of a little less than a mile, and through a stratigraphical interval of 150 feet. The vector means lie almost wholly within the northeast sector, and the extreme means come from a single section (400). All but two (those at 400/1 and 400/3) of the means lie within the interval 0° to 60°, indicating a strong general direction; the two means that lie outside this range indicate the variability of current directions through a vertical section. Between the sections, there seems to be a change from generally north-northeastward in section 400 to northeastward in sections 401 and 435. In as far as one can generalize from these results, the vector means of cross-bedded sandstone over a small area and stratigraphical interval are polarized; the means that deviate from the general direction indicate the need for caution in interpreting individual sets of observations. This set of observations and the others reported below agree with Potter & Pettijohn's (1963, p. 63) generalization that 'cross-bedding in a sand body, a formation, or even an entire basin, nearly always has well defined preferred orientation'. Exceptions, such as Wermund's (1965) Meridian Sand, must be expected, but they seem to be rare.

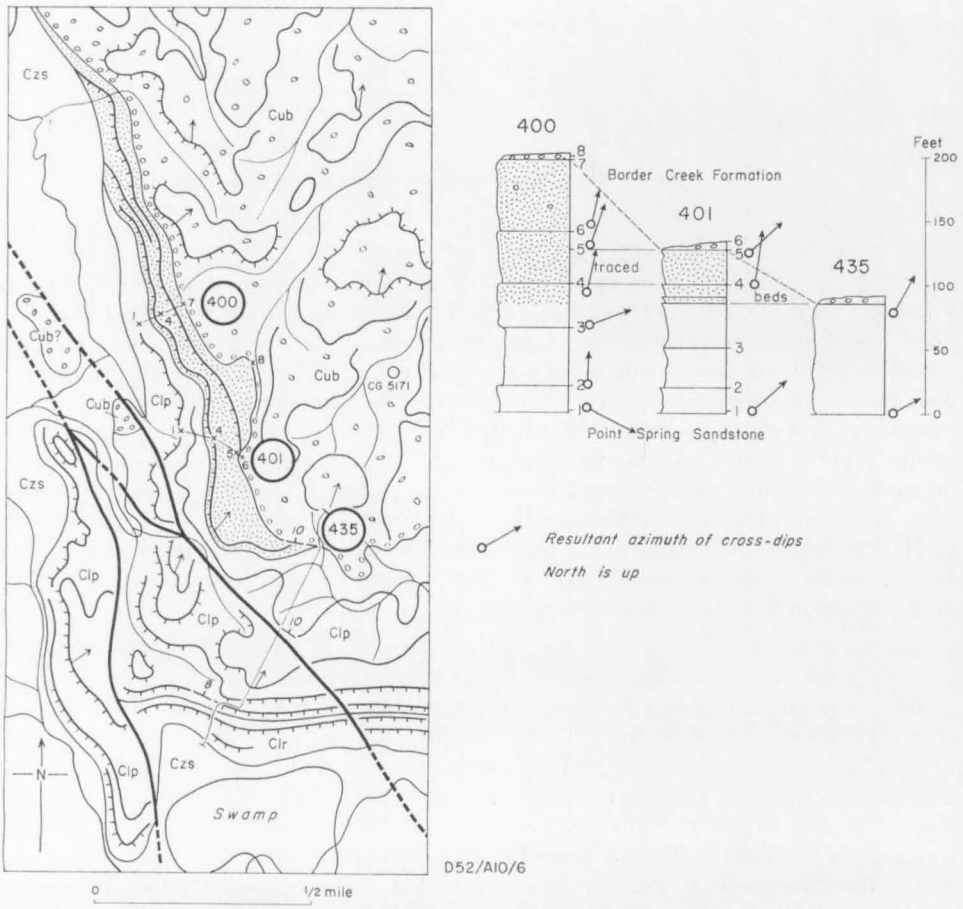

Figure 11. Geology and sections of part of the Weaber Range. (For location see Fig. 30.) (After Veevers & Roberts, 1968, fig. 61)

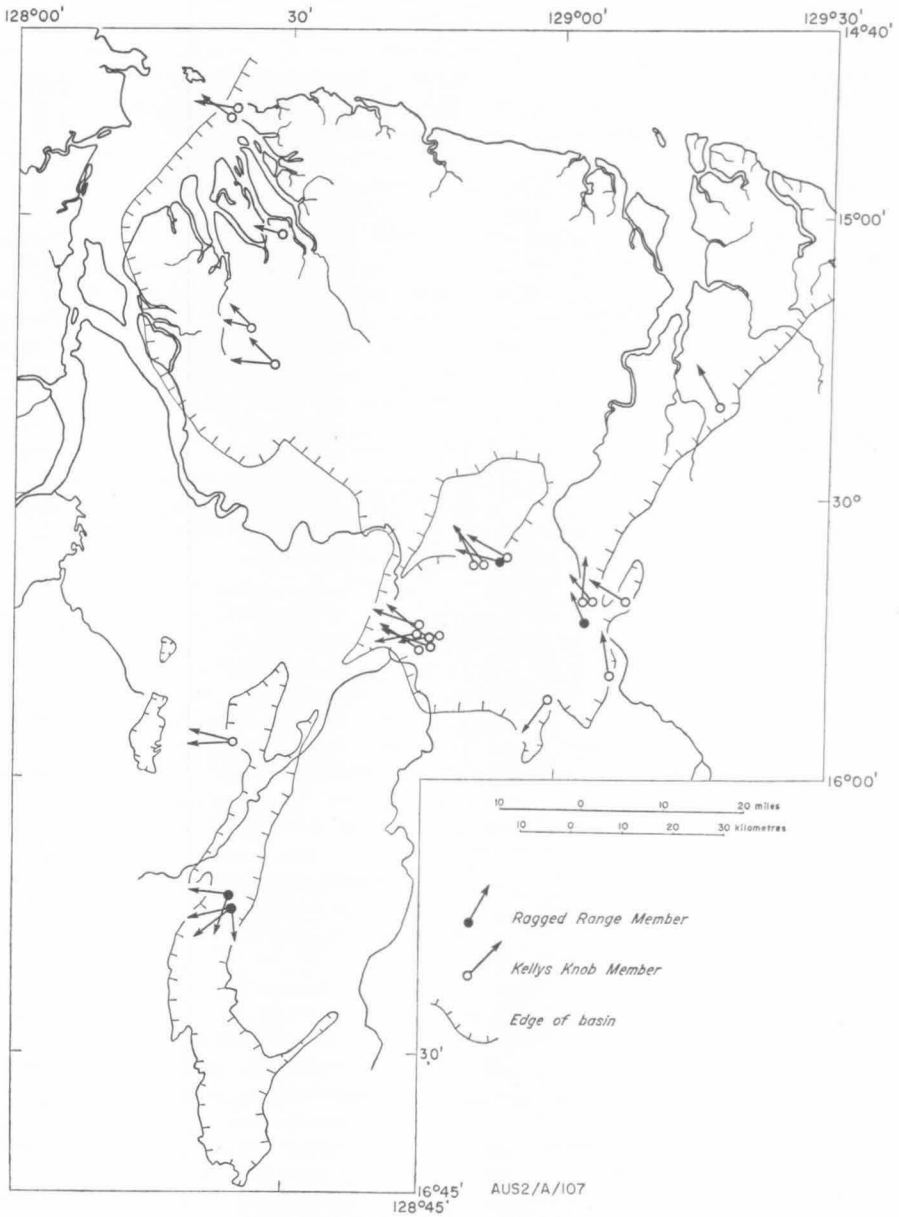

Figure 12. Resultant azimuths of cross-dips in the Ragged Range and Kellys Knob Members of the Cockatoo Formation

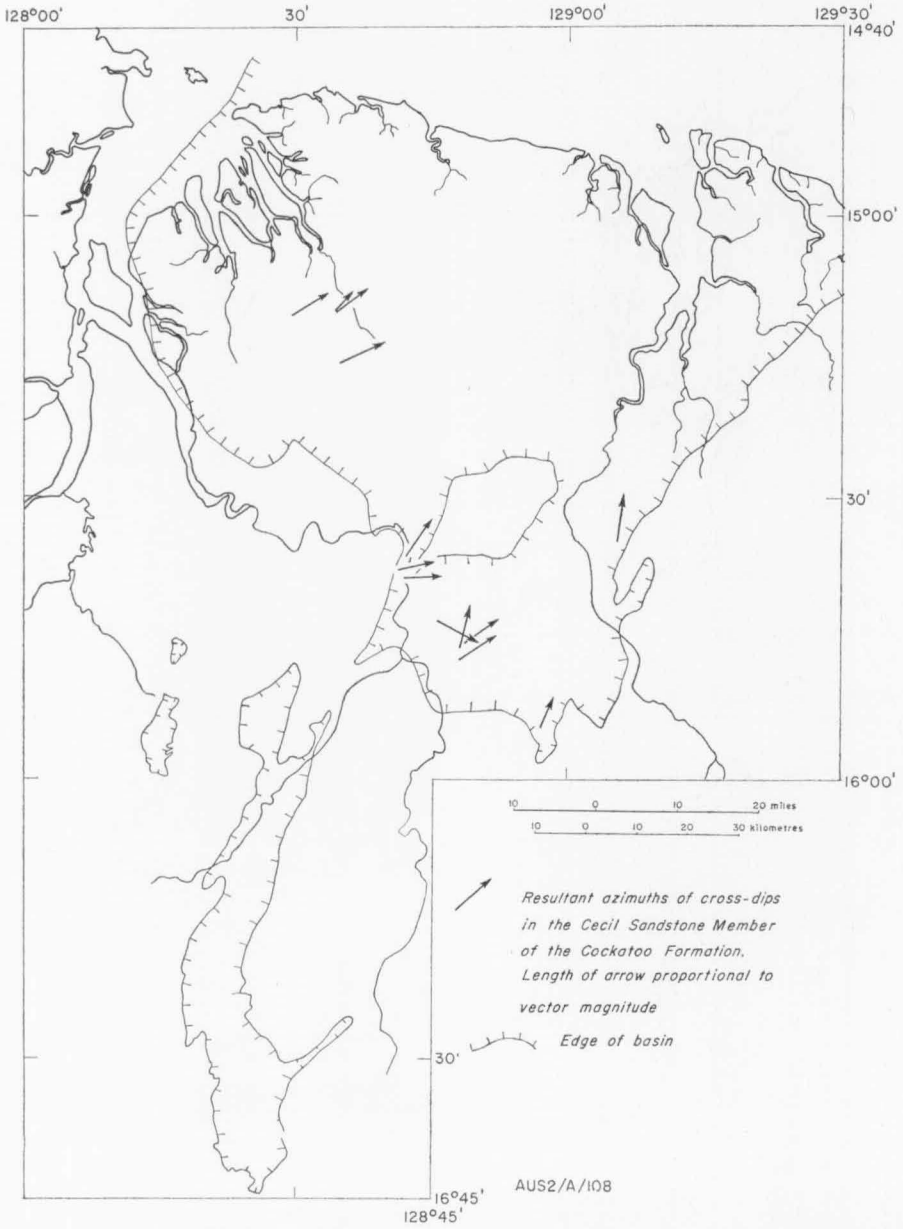

Figure 13. Resultant azimuths of cross-dips in the Cecil Member of the Cockatoo Formation

Cockatoo Formation

The resultant azimuths from 24 localities in the Kellys Knob Sandstone Member (Fig. 12) range from 255° to 3°; with a single exception (215° at loc. 81-3), all the azimuths lie generally within the northwest quadrant. The two azimuths of the Ragged Range Conglomerate Member outside the Ragged Range also lie in this quadrant. The five azimuths in the Ragged Range lie generally in the southwest quadrant. With a single exception (azimuth of 119° at loc. 405-2), the 13 azimuths of the Cecil Sandstone Member (Fig. 13) lie within the northeast quadrant, within the range of 7° to 88°.

Preliminary Interpretation. A valid interpretation of these directional structures hinges on the interpretation of the environment in which they were deposited. Veevers & Roberts (1968) argue that much, if not all, of the Cockatoo Formation is marine, but admit the possibility that some of the cross-bedded sandstone was deposited in fresh water, probably in rivers on a broad coastal plain.

If the Kellys Knob and Cecil Sandstone Members are fluvial, then the narrow range of cross-bedding azimuths in each of these members indicates the general direction of slope of the ancient depositional basin ('paleoslope' of Potter & Pettijohn, 1963, p. 82). An inferred northwest slope during the deposition of the Kellys Knob Sandstone Member would confirm the conclusion based on facies distribution that the southeast edge of the basin was the chief source area, or at least the chief area through which sediment from higher ground was funnelled (Veevers & Roberts, 1968). The northeast azimuths in the Cecil Sandstone Member would indicate the chief source to the southwest. This conflicts with the evidence from the distribution of facies that the southeast edge of the basin was also the chief source area during deposition of the Cecil Sandstone Member.

On the other hand, if, as we believe, both these members are marine, the uniform direction of azimuths in each member merely indicates that during the deposition of each member the directions of the depositing currents were uniform, but different between the Kellys Knob Member and the Cecil Member.

Whichever interpretation is true, the azimuths around the Pincombe Inlier are noteworthy because they point into the inlier, indicating that it had little or no effect on the direction of the currents; consequently doubt is cast on the existence of the inlier as land during the deposition of the Kellys Knob and Cecil Sandstone Members. The single azimuth of the Ragged Range Member in this area (loc. 411/2) also points into the inlier, and is anomalous in view of the conclusion from the facies distribution that the inlier was high ground during the deposition of the Ragged Range Member. McKee (1940, pp. 819-20, fig. 6) found the same kind of relationship in the marine Cambrian Tapeats Sandstone of the Grand Canyon of Arizona. During deposition, islands of Precambrian rocks studded the sea floor, but 'apparently these hills had little influence on the actual deposition at their bases, although erosion of their surface must have supplied some portion of the sediment involved. As a result, beds of the Cambrian sandstone slope away (mainly due to post-consolidation compaction over a hard centre) from the hills in all directions, yet the cross-laminae within them are constant in direction'. In the light of this occurrence, it is concluded that during the Frasnian the currents that shaped the sand into cross-beds swept past the emergent Pincombe inlier without sensible deviation.

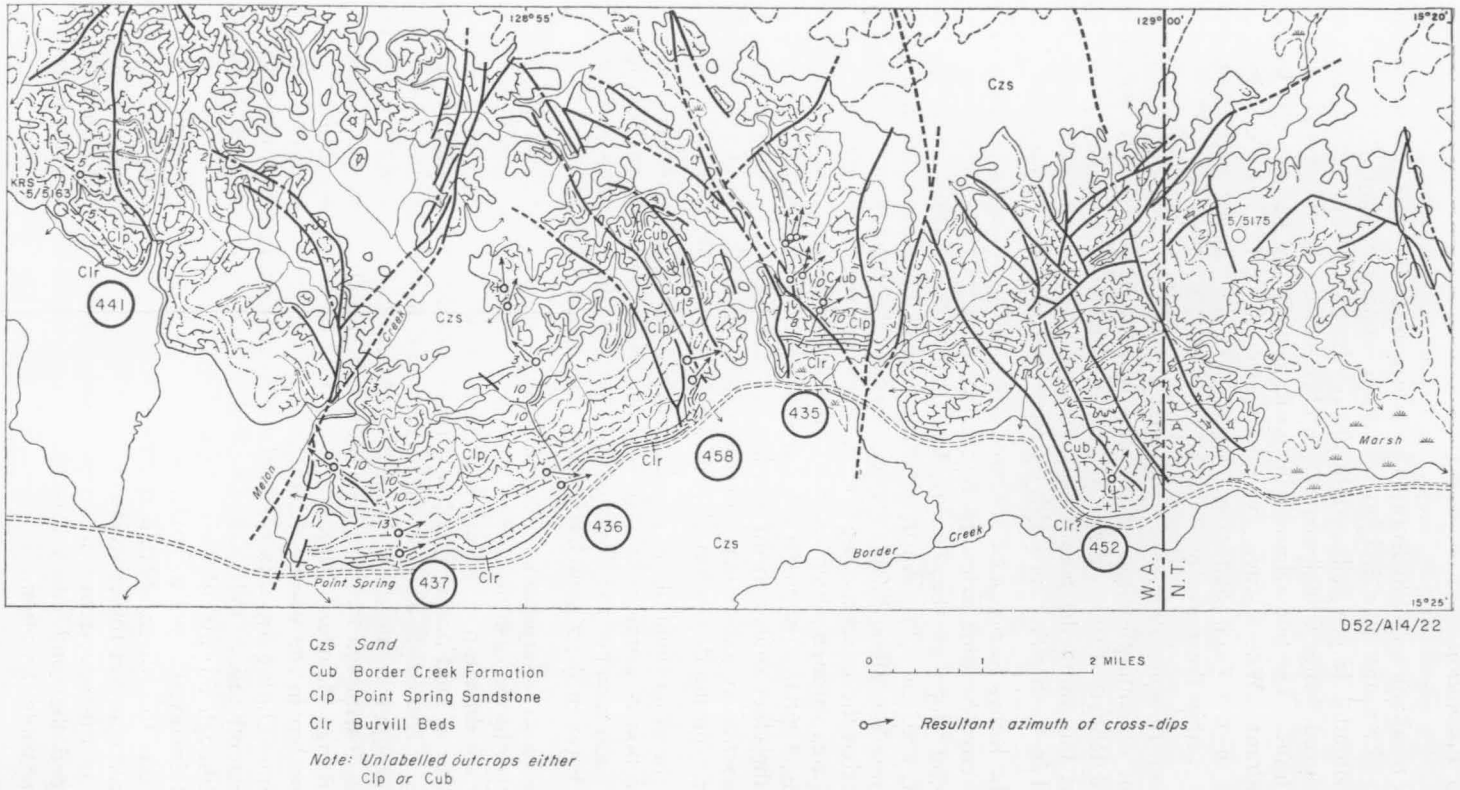

Figure 14. Geology of eastern part of the Weaber Range, and resultant cross-dip azimuths. (After Veevers & Roberts, 1968, fig. 60)

The southeast direction of azimuths in the Ragged Range Member of the Ragged Range also seems anomalous in view of the northward change from conglomerate to sandstone. This direction, however, is anomalous only if the Ragged Range Conglomerate is regarded as a fluvial deposit, whereby the cross-bedding azimuths are inferred to indicate the depositional slope. If, as indicated by the fossils in the Ragged Range Member, the conglomerate is marine, then the azimuths merely indicate the direction of marine bottom currents which here possibly ran parallel to the shore.

Point Spring Sandstone

Measurements. The resultant azimuths of cross-bedding dips in the Point Spring Sandstone of the Weaber Range (Figs 14, 15) lie within the range 306° to 177°. This total range is composite. In the basal 350 feet of the Point Spring Sandstone, all but one of the resultant azimuths lie within the northeast quadrant. The resultant azimuths in the basal 350 feet in the three sections of the western side of the area (sections 441, 437, and 436) lie within the narrower range of 69° to 97°, whereas in the four central sections (458, 400, 401, and 435—see Fig. 11 also), except for the resultant azimuths of 117° at locality 400-1, the range is 0° to 73°.

Only 3 resultant azimuths are available from the part of the Point Spring Sandstone above 350 feet, and they have a range of 306° to 356°.

Preliminary Interpretation. On the assumption that the cross-bedded quartz sandstone beds of the Point Spring Sandstone were deposited in rivers on a coastal plain, the resultant azimuths roughly indicate the local slope of the plain. Thus, during the deposition of the basal 350 feet of the Point Spring Sandstone, the coastal plain in the western part of the Range sloped eastward and in the central part of the Range northeastward. During the deposition of the upper half the slope was northwestward.

These inferred changes in direction of slope are possibly related to the interplay of earth movements in the west, south, and east. According to this view, the change in direction of slope during the deposition of the basal 350 feet of the Point Spring Sandstone from east to northeast reflects waning uplift in the west (Waggon Creek area) and new uplift in the south to southeast. During the deposition of the upper part of the Point Spring Sandstone the slope was northwest, indicating that uplift in the south and southeast was dominant. This interpretation accords with conclusions reached independently (Veevers & Roberts, 1968), viz., the waning uplift in the west during the late Lower Carboniferous compensated by uplift in the south and southeast.

On the other hand, if the cross-bedded sandstone is marine, the azimuths merely indicate the direction of bottom currents, which do not necessarily follow the slope of the sea floor.

Border Creek Formation (Fig. 16)

Measurements. Only six resultant cross-bedding azimuths are available from the Border Creek Formation; four are in the Weaber Range (Figs 14, 15), one is at locality 132/4, a few miles south of the eastern tip of the Weaber Range, and

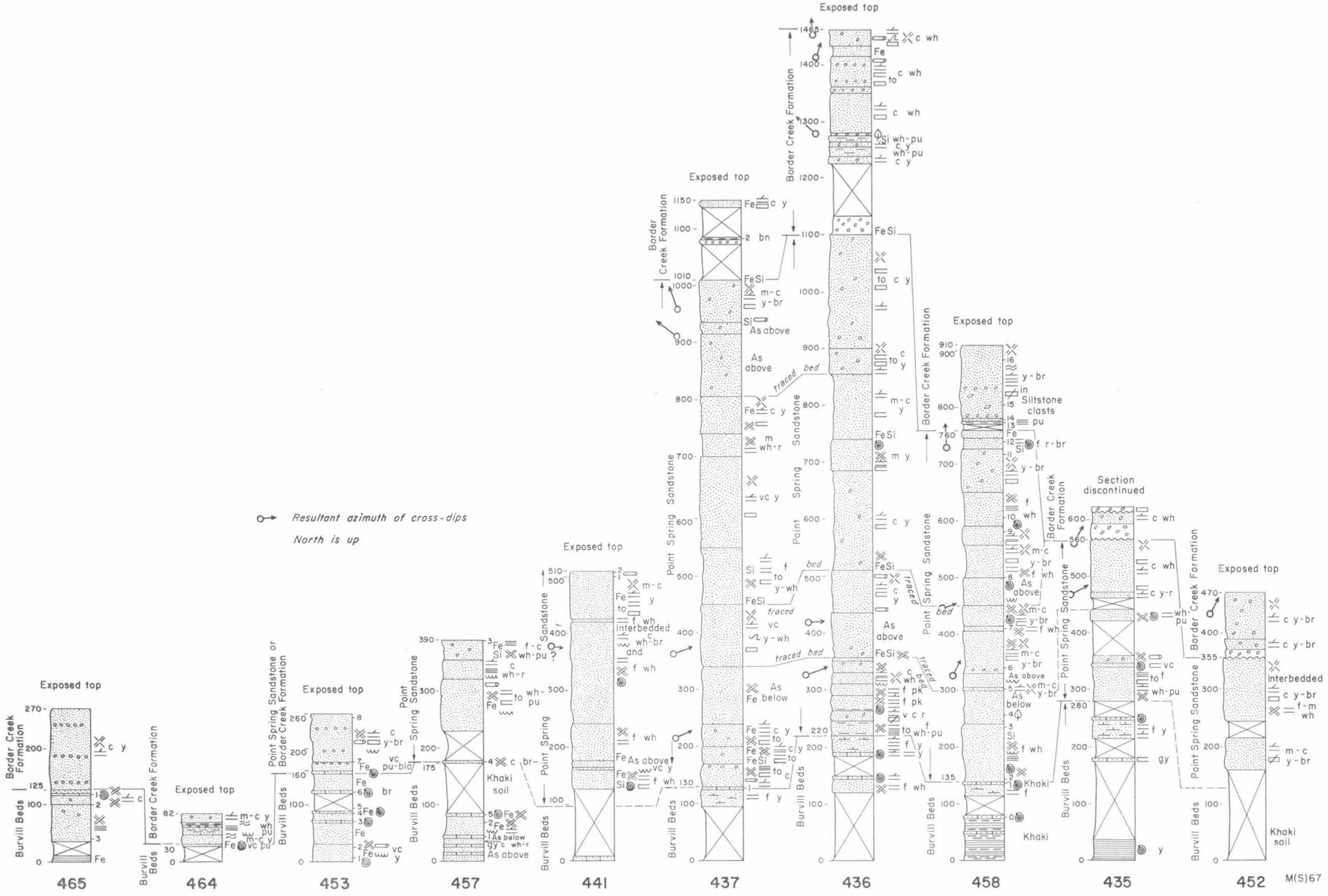

Figure 15. Columnar sections of the sequence in the Weaber Range, and resultant cross-dip azimuths. (After Veevers & Roberts, 1968, fig. 59)

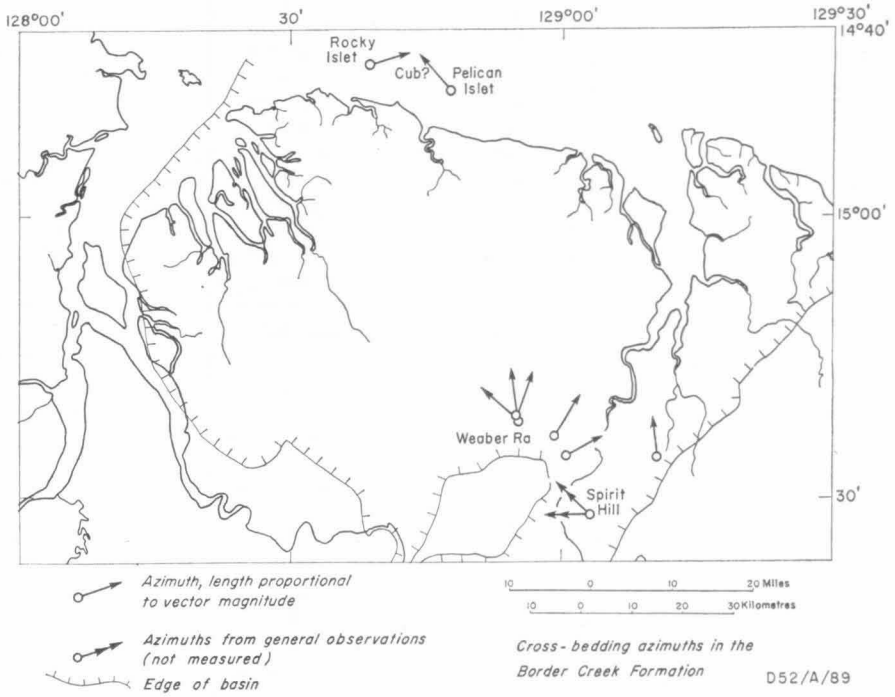

Figure 16. Resultant azimuths of cross-dips in the Border Creek Formation

another is at locality 134/12, near Alpha Hill. The range is 311° to 61°. General observations in the Border Creek Formation at Spirit Hill indicate that the cross-bedding generally dips westward to northwestward, and, in the probable Border Creek Formation of the offshore islets, the resultant azimuth is 319° at locality 431/2 on Pelican Islet and 74° at locality 433/3 on Rocky Islet. All told these azimuths encompass almost the entire northern semicircle.

Preliminary Interpretation. The Border Creek Formation is regarded as a fresh-water (fluvial) deposit so that cross-bedding azimuths are assumed to indicate the general direction of the depositional slope. The available azimuths are too few to indicate specific slopes. Lying wholly within the northern semicircle, they indicate a general northerly component of slope.

Preliminary Interpretation of Environment of Deposition of Cross-bedded Sandstone

The physical properties of the cross-bedded sandstone described above—the gross features of size and shape of the sandstone bodies, primary sedimentary structures, including directional structures, and petrology—show that this kind of sandstone is fairly uniform throughout all the units in which it is found. This, however, does not necessarily imply that all these units were deposited in the same kind of environment. What follows is an attempt to interpret these units in terms of their physical properties only; in this regard, the primary sedimentary structures are the most valuable, and will be treated first.

The almost ubiquitous cross-bedding indicates that most, if not all, of this kind of sandstone was deposited as long straight large-scale asymmetrical ripples in fairly shallow water. Very thick cross-beds, such as those at locality 239B, were possibly deposited by wind, but their association with the almost equally thick regular cross-beds at locality 239c, which were almost certainly deposited in water, shows that they are more likely to have been deposited in water. The strongest evidence of deposition in water is provided by the structures such as contorted bedding and recumbent folds, which could be formed only in water-saturated sediment, and the trough-type structures filled by conglomerate.

These conglomerate structures and the very thick cross-beds indicate the extremes in the depth of water. The erosion of a trough surface and its subsequent infilling with a boulder conglomerate seem to indicate the action of rapid currents found in very shallow water only. At the other extreme, the thickest known cross-bed (50 ft thick) was obviously deposited in water at least so deep, and according to the relationship between water depth and the height of straight large-scale asymmetrical ripple marks given by Allen (1963b, p. 212) probably at least as deep as 100 feet. Most of the omikron cross-beds have a median set thickness of about 1.5 feet, which corresponds to deposition in water 3 to 30 feet deep (these are the 95% confidence limits.).

The kind of ripples from which the omikron cross-bedding was derived are probably accounted for by the movement of trains of straight large-scale asymmetrical ripples. 'As the ripples are known from seas, estuaries and rivers, the cross-stratification cannot be taken as environmentally diagnostic' (Allen, 1963b, p. 211).

In summary the physical evidence indicates deposition in water ranging from a few feet deep in areas of conglomeratic troughs to at least 100 feet in areas with very thick cross-beds. None of this evidence has any bearing on the salinity of the water or other properties.

Marine Model

Other Evidence. As related elsewhere (Veevers & Roberts, 1968), the stratigraphical and palaeontological evidence points to the likelihood that the Cockatoo Formation and Point Spring Sandstone are wholly marine. If so, the widespread omikron cross-beds, including very thick ones, were deposited by marine currents, which kept a constant direction during the deposition of each body of sandstone. The only currents in present seas that have constant directions from the shore to the shelf edge and are capable of moving high sand waves or ripples are tidal currents; the sedimentary action of tidal currents is perhaps best known in the North Sea (Stride, 1963), where much of the sand floor has been shaped into large ripples (sand waves) lying roughly normal to the paths of the strongest tidal currents. It remains to be shown that the internal structure of these large ripples accords with their being able to generate tabular cross-bedding, though theoretically there seems to be no difficulty (Stride, 1965; Jordan, 1962; Off, 1963; Allen, 1966).

Smaller marine ripples certainly can. Asymmetrical ripples, with heights up to 60 cm., were observed by Salsman, Tolbert, & Villars (1966) to migrate in the direction of the predominant (flood) tidal current, and each ripple passing a given point left behind a layer of sand averaging 12 cm. thick. Ten such layers have accumulated in a short period.

The highest recorded sand wave is 26 m. (85 ft) quoted by Harvey (1966, p. 49). The lee-side slope of the sand waves ranges up to the angle of rest of the sediment, which is universally of sand grade (Stride, 1963). Thus, on the premise that the cross-bedded sandstone is marine, the omikron cross-bedding is attributable to the action of tidal currents over a shallow sand-covered sea floor.

As pointed out by Allen (1966, p. 175), these structures 'would seem to have a high preservation potential, especially under conditions of rising sea level, largely because of the enormous volumes of sediment involved'.

Interpretation of Cross-bedding Azimuths. In discussing bed forms and palaeocurrents, Allen (1966, p. 162) shows that of the four common types of large-scale asymmetrical ripple marks, 'only the straight form is an efficient indicator of the direction of general flow. Random sampling of lee-side azimuths or of cross-strata left behind following ripple migration must yield a sample of small variance and of vector mean close to the direction of general flow.' The omikron cross-beds correspond in form to cross-beds generated by the migration of straight large-scale asymmetrical ripple marks, and the low variance of azimuth of these cross-beds seems to confirm that the vector means of these azimuths lie close to the direction of general flow.

In the Kellys Knob Sandstone Member (Fig. 12), the vector means lie almost wholly within the northwest quadrant, and, following the marine model, indicate the general flow pattern of tidal currents. If the palaeogeographical deduction that the southeast edge of the basin was a shoreline is taken into account, the vector means seem to indicate the flow of tidal ebb currents, which flowed slightly swifter than the flood-tide, so the net movement of sand waves was in the direction of the ebb.

Finally, what, if any, inference can be drawn from the direction of ebb currents about the shape of the coast? The swiftest tidal currents at the present day flow longitudinally along funnel-shaped arms of the sea (Off, 1963). In most areas, sediment is deposited at the head of the inlet where rivers enter the sea. In these circumstances facies gradients and the direction of tidal currents are commonly parallel. Because the facies gradients and cross-bedding directions in the Kellys Knob Sandstone Member are parallel, this member was possibly deposited in a tidal inlet elongated in a northwesterly direction (Fig. 17a).

The same model may be applied to the deposition of the Cecil Sandstone Member of the Cockatoo Formation. The chief difference is that the vector means of cross-bedding in the Cecil Member lie almost wholly within the northeast quadrant, at right angles to those of the Kellys Knob Member. The facies gradient of the Cecil Member is observable in the Kununurra/Cockatoo Spring area only, where it is the same as that of the Kellys Knob Member. Elsewhere, the direction of its gradient is unknown. Thus, following the tidal inlet model, it is possible that the vector means of the cross-bedding in the Cecil Member indicate

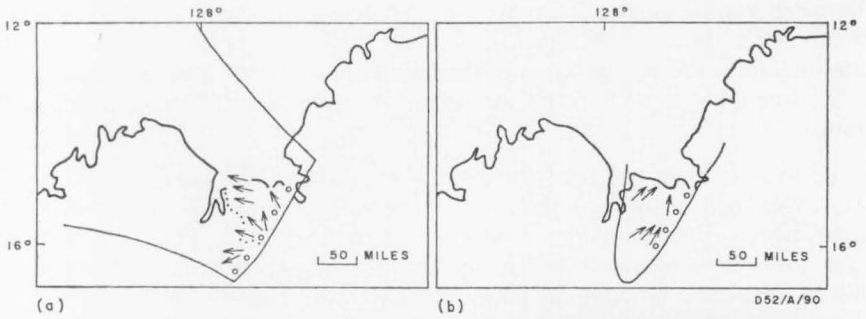

Figure 17. Cross-bedding azimuths (a) of the early Frasnian Ragged Range and Kellys Knob Members, and (b) of the later Frasnian Cecil Member, with distributions of conglomerate (circles), and postulated outlines of tidal inlet

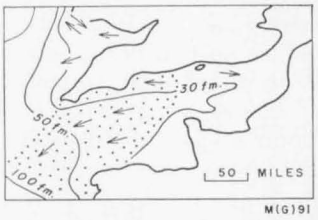

Figure 18. Continental shelf between Britain and France, showing bathymetry, area of sand waves (stipples), and direction of transport of sand inferred from the direction faced by the steep slopes of sand waves (after Stride, 1963)

the regional facies gradient towards the northeast, and the observed gradient in the Kununurra/Cockatoo Spring area is local only. This is an attractive possibility because in the western half of the basin the facies gradient of the overlying Famennian and Lower Carboniferous sequences is to the northeast, and the appearance of this direction in the Cecil Member probably indicates the first of a sequence of movements that radically changed the shape of the basin (Fig. 17b).

There is no other evidence to show that the sea covered the North Kimberleys during the early Frasnian. Certainly no Upper Devonian sediments have been found in this area. If, as implied in Figure 17a, the sea covered the North Kimberleys, then this was either a non-depositional area or any sediments deposited over this area during the early Frasnian were subsequently stripped off, probably during the rapid uplift of the southwestern part of the Bonaparte Gulf Basin in the mid-Tournaisian.

Fossils in the Kellys Knob and Cecil Members are rare, probably because, as Shepard (1963, p. 471) notes, 'tidally distributed sands are relatively free from marine organisms owing to the violent movement produced by the currents and waves operating over the shoals'.

A comparison of Figure 17 with Figure 18 (both at the same scale) shows that the postulated environment in the Bonaparte Gulf Basin resembles the existing situation in the English Channel. The chief factor determining the direction of

the tidal currents and hence the distribution of sand is not bathymetry, at least within the shelf, but the funnel-shaped coastlines. Furthermore, if uplift is intense, as it was in the Bonaparte Gulf Basin, then the direction of currents and the bottom slope will coincide.

In a study of the directional structures of the marine Lower Devonian Koblenzquartzit of Germany, Niehoff (1958) concludes that tidal currents were instrumental in shaping the sand into cross-beds. Like the currents that prevailed during the deposition of the Kellys Knob and Cecil Members, 'this direction changed in space and time . . . corresponding to the arrangement of basins and thresholds of the area of sedimentation' (p. 469).

Terrestrial Model

The independent evidence that the cross-bedded sandstone of the Cockatoo Formation and Point Spring Sandstone is marine is strong but not absolute, and the chief alternative, that these sandstones were deposited on land, cannot be wholly dismissed. The ramifications of this model will be examined mainly for comparison with these of the marine model. The difficulties in applying the model will be discussed first of all.

To recapitulate, the physical evidence of the cross-bedded sandstone itself indicates deposition in water ranging from a few feet to at least 100 feet deep. The action of swift currents in shaping the sand into cross-beds seems to rule out deposition in a lake or lakes, and to indicate deposition in river or delta channels. The few marine fossils found in the conglomerate and cross-bedded sandstone could have been introduced during brief marine incursions, and the intimate interbedding in the Point Spring Sandstone of cross-bedded sandstone (for the purpose of our argument assumed to be fluvial) and thin-bedded marine sandstone is interpreted as indicating cyclic marine and freshwater deposition.

If the deposits are fluvial it is difficult to explain the winnowing out of sediments finer than sand, because no fine overbank deposits were found, except in the Border Creek Formation, which is presumed to be terrestrial. These difficulties notwithstanding, what palaeogeographical deductions can be made from developing this model? The vector means specify the depositional slope with fairly high confidence; as indicated by the cross-bedding vector means or the facies gradient, the Kellys Knob Member was deposited on a surface sloping northwest. The main part of the Cecil Member was deposited on a northeasterly slope, as indicated by the cross-bedding vector means, and locally, in the Matheson Ridge area, on a northerly sloping surface, as indicated by the facies gradient. And the cross-bedded sandstone of the Point Spring Sandstone and the Border Creek Formation were deposited on a northerly sloping surface.

Petrography

Because no meaningful differences in petrography were found between the groups of cross-bedded sandstone and flat-bedded sandstone, both are dealt with here.

Constituents

Quartz. Quartz is the predominant constituent in all but a few sandstones of the Bonaparte Gulf Basin; most of it shows undulatory extinction. The quartz grains are cemented by quartz overgrowths, so that the sandstones are essentially granular aggregates of this single mineral. Other quartz types include polycrystalline quartz, present in varying amounts up to 8 percent, rare nonundulatory quartz, rare detrital euhedral quartz (Pl. 8, fig. 2), and microcrystalline quartz in aggregates of equidimensional grains about 10 microns across.

The predominant cement of overgrowth quartz is visible microscopically only on grains whose detrital nuclei are outlined by films of impurities such as clay (Pl. 9, figs 1 and 2) or by rows of vacuoles. In the 127 thin sections examined only 14 contain grains whose original detrital outlines are visible. In the rest, this boundary is not everywhere visible, and the presence of quartz overgrowths can be inferred from the interlocking of adjacent quartz grains. Two generations of overgrowths were seen in a few grains (Pl. 10, figs 1, 2; Pl. 11, fig. 1). The inner overgrowth is abraded, and is thus inherited from the source. Most overgrowths have irregularly shaped outlines, and only a few are euhedral or faceted (Pl. 11, fig. 2; Pl. 12). In the majority of specimens that are friable, the cement of overgrowth quartz is ineffective. In most sandstones, the grain boundaries are smooth; in only a few, exemplified by specimen L14-2 from the Ragged Range Member, were microstylolites found. And even here the rock remains crumbly. Specimen 40-2B (Pl. 13, fig. 2) is such a friable sandstone, but specimen 40-2A (Pl. 13, fig. 1), 20 feet away from it in the same bed, is firmly cemented. Microscopically this difference in cohesion is not obvious. In specimen 40-2B the sutures between grains are weak, and have spread during preparation of the thin section, but why they are weak is not apparent. The presence of rare firmly cemented sandstone (quartzite) in outcrop points to the possibility that beneath the weathered zone it is common, and that the predominant friable sandstone in outcrops is merely leached quartzite. Drillhole specimens from the platform province will be required to test this possibility.

Interstitial quartz cement was seen in a few thin sections only (Pl. 9, fig. 2).

Feldspar. Only twinned feldspar (Pl. 17, fig. 1) was identified in thin section. Untwinned feldspars, distinguishable from quartz by cloudy alteration products, are rare, and most are cloudy overgrowths on twinned feldspar.

The fine arkose conglomerate of the Ragged Range Member in the southern Ragged Range is the only rock in the basin known to have abundant (60%) feldspar. Only 4 of the 14 thin sections analysed contain measurable feldspar and it is less than 5 percent.

Other Constituents. Mica is rare; it is restricted to the conglomerate and conglomeratic sandstones, exemplified by specimen 415-3 (Pl. 15, fig. 2), which contains biotite. *Rock fragments* (Pl. 8, fig. 2; Pl. 14, fig. 2; Pl. 15, fig. 2) comprise micaceous quartz siltstone, quartz sandstone, microquartz, quartzite, vein quartz, and devitrified volcanic glass. *Hematitic clay,* as a film around detrital nuclei or as a matrix (Pl. 16, fig. 1), is an abundant constituent of all the red sandstones of the basin. It probably consists of varying proportions of hematite and kaolinite. Under the microscope, the dominant clay, determined as *kaolinite,* is pale brassy

yellow, fibrous, granular, or in accordion-like masses, with low double refraction; crystals are length slow. Some specimens contain illite. The *siltstone pellets* are intraformational and are therefore not classified as rock fragments. They are restricted to the Border Creek Formation. The siltstone consists of quartz grains of mean grainsize about 20 microns set in kaolinite, which is frequently in accordion-like masses. *Tourmaline* is the dominant heavy mineral, and the concentration probably nowhere exceeds 1 percent. An overgrown grain is shown in Plate 16, figure 2. Grains are well rounded. *Zircon* is rarer than tourmaline; the grains are rounded, and a few of the crystals are zoned. *Anatase* and *rutile* are the only other heavy minerals identified, and they are very rare. *Glauconite* (Pl. 17, fig. 1) is widespread, but in many slides it is represented by one or two grains only, which suggests that at least some of the glauconite is detrital. *Voids* constitute up to 20 percent of the slides analysed. Whether they are original or merely spaces left by leached-out clay or matrix is uncertain.

Modal Analysis

The outlines of original sand grains were visible microscopically in 14 thin sections (out of a total of 127), and these were the subject of a combined analysis for grainsize, grain-shape, and compositional mode (Veevers, 1967). The suite of specimens so analysed came from the Ragged Range Conglomerate Member (3 specimens), Kellys Knob Sandstone Member (4), Hargreaves Member (2), Enga Sandstone (2), Zimmerman Sandstone (1), Point Spring Sandstone (1), and Border Creek Sandstone (2). Not represented are the Westwood Member, Abney Sandstone Member, and Cecil Sandstone Member of the Cockatoo Formation. Seven specimens are from cross-bedded sandstone, 5 from flat-bedded sandstone, and 2 from cross-bedded sandstone with siltstone pellets.

A Swift point counter with a spacing of 0.33 mm. was used for the modal analysis.

The raw data are given in Table 4. The results were recalculated to remove the effect of secondary quartz and original voids (Table 5), and finally the modal analyses were calculated to give the composition of the original sand fraction (Table 6).

The recalculated data in Table 5 give the closest approximations to the originally deposited sediment. Eight of the 14 specimens contain 15 percent or more of clay matrix and are classified as argillaceous quartz sandstone; the rest are quartz sandstone.

No obvious difference in modal composition was found between the three sandstone groups, except for siltstone pellets in the third group. Both the cross-bedded and flat-bedded sandstone include specimens with as much as 40 percent of matrix (Table 5), and the original sand fraction of both groups is identical. Plotted on Folk's (1961) triangular diagram (Fig. 19), showing the proportion of quartz, feldspar, and rock fragments, 11 specimens fall in the orthoquartzite field, 2 in the subarkose field, and 1 in the subgreywacke field. The 11 specimens of orthoquartzite contain 98 percent or more of quartz.

TABLE 4: MODAL ANALYSES: RAW DATA

Type	Cross-bedded Sandstone							Thin-bedded Sandstone					Cross-bedded Sandstone with Siltstone Pellets	
Details \ Specimen	420-1	412-6	135-1	404-5	28-7	39-5	130-5	431-1	103-20	103-18	110A	400-3	458-16	104-21
Formation or member	Ragged Ra. Mbr	Ragged Ra. Mbr	Ragged Ra. Mbr	Kellys Knob Mbr	Kellys Knob Mbr	Kellys Knob Mbr	Kellys Knob Mbr	Hargreaves Mbr	Enga Ss.	Enga Ss.	Zimmerman Ss.	Pnt Spring Ss.	Border Cr. Fm.	Border Cr. Fm.
Locality	Nigli Gap	Church Steeple Pk	SW of Alpha H.	Kununurra	Matheson Ridge	Elephant H.	Shakespeare H.	Hargreaves Hills	Enga Ridge	Enga Ridge	Mt Zimmerman	Weaber R.	Weaber R.	Mt Septimus
MODAL ANALYSIS														
Number of counts	382	410	429	145	248	165	165	361	1,059	804	943	810	208	387
Percentage composition														
Quartz, total	75.4	73.5	67.8	87.0	83.9	97.6	89.7	80.3	77.0	84.4	63.8	79.0	78.8	64.3
Grains—														
undulatory	47.9	46.0	44.2	61.4	58.4	70.9	57.0	60.1	65.7	69.6	53.1	63.2	66.3	49.8
non-undulatory	—	—	0.5						0.1					0.3
polycrystalline	3.1	1.5	1.1		8.1	1.2		2.2	1.8	0.9	1.3	1.0	1.0	
Cement—														
overgrowth	22.8	23.6	14.0	24.1	16.2	25.5	30.3	17.7	9.2	13.8	9.2	13.3	10.1	13.9
interstitial	1.6	2.4	8.0	1.5	1.2		2.4	0.3	0.2	0.1	0.2	1.5	1.4	0.3
Feldspar				3.5			0.6	4.4					0.5	
Rock fragments	08	0.5		1.4	5.6			1.7	0.2	0.5	0.6	1.0		0.5
Hematitic clay	14.9	6.8	22.7		6.5				20.5		23.8	13.2	1.4	6.2
Clay matrix (unstained)	2.1	11.0	3.8	4.1	2.4	0.6	3.0			4.2	2.4	1.0	1.0	0.5
Siltstone pellets													16.9	8.3
Tourmaline										0.1				
Voids	6.8	8.2	5.7	4.1	1.6	1.8	6.7	13.6	2.3	10.8	9.4	5.8	1.4	20.2
Total	100.0	100.0	100.0	100.0	100.0	100.0	100.0	100.0	100.0	100.0	100.0	100.0	100.0	100.0

TABLE 5: MODAL ANALYSES

Recalculated to remove the effect of secondary quartz and original voids.

	Cross-bedded Sandstone							Thin-bedded Sandstone					Cross-bedded Sandstone with Siltstone Pellets	
Specimen No.	420-1	412-6	135.1	404-5	28-7	39-5	130-5	431-1	103-20	103-18	110A	400-3	458-16	104-21
Quartz	74.1	71.9	63.3	87.4	82.1	99.2	94.1	91.1	76.6	93.6	67.0	80.9	77.3	58.3
Undulatory	69.6	69.6	61.1	87.4	72.1	97.6	94.1	87.9	74.5	92.4	65.4	79.6	76.2	58.0
non-undulatory			0.7						0.1					0.3
polycrystalline	4.5	2.3	1.5		10.0	1.6		3.2	2.0	1.2	1.6	1.3	1.1	
Feldspar				4.8			0.9	6.4					0.6	
Rock fragments	1.2	0.8		2.0	6.9			2.5	0.2	0.7	0.7	1.3		0.6
Clay total	24.7	27.3	36.7	5.8	11.0	0.8	5.0		23.2	5.6	32.3	17.8	22.1	41.1
Hematitic clay	21.7	10.5	31.4		8.0				23.2		29.3	16.6	1.6	7.2
Clay	3.0	16.8	5.3	5.8	3.0	0.8	5.0			5.6	3.0	1.2	1.1	0.6
Siltstone pellets													19.4	33.3
Tourmaline										0.1				
Total	100.0	100.0	100.0	100.0	100.0	100.0	100.0	100.0	100.0	100.0	100.0	100.0	100.0	100.0

TABLE 6: MODAL ANALYSES

Recalculated in terms of original sand fraction (quartz, feldspar, metamorphic rock fragments)

	Cross-bedded Sandstone							Thin-bedded Sandstone					Cross-bedded Sandstone with Siltstone Pellets	
Specimen No.	420-1	412-6	135-1	404-5	28-7	39-5	130-5	431-1	103-20	103-18	110A	400-3	458-16	104-21
Quartz	98.4	98.9	100.0	92.8	92.2	100.0	99.1	91.1	99.7	99.3	99.0	98.4	99.2	99.0
undulatory	92.4	95.7	96.5	92.8	81.0	98.4	99.1	87.9	97.0	98.0	96.6	96.8	97.8	98.5
non-undulatory			1.1						0.1					0.5
polycrystalline	6.0	3.2	2.4		11.2	1.6		3.2	2.6	1.3	2.4	1.6	1.4	
Feldspar				5.1			0.9	6.4					0.8	
Rock fragments	1.6	1.1		2.1	7.8			2.5	0.3	0.7	1.0	1.6		1.0
Total	100.0	100.0	100.0	100.0	100.0	100.0	100.0	100.0	100.0	100.0	100.0	100.0	100.0	100.0

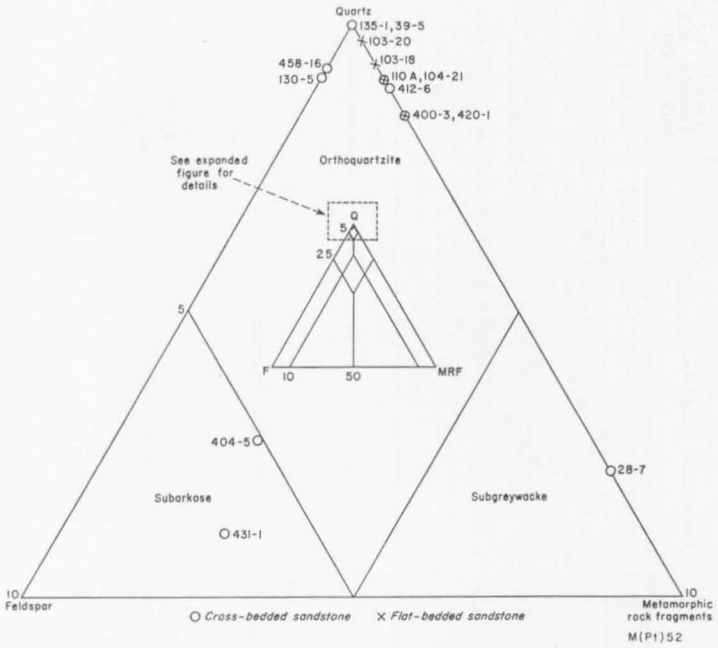

Figure 19. Composition of sand fraction

Granulometry

The size and shape of sand grains were determined concurrently with the modal analysis in the 14 thin sections with suitably preserved grains (Table 7). The method of combined analysis is described elsewhere (Veevers, 1967). In brief, it follows conventional modal analysis by point-counting, but additionally the length and width of each sand grain that falls beneath the cross-hairs were measured against a micrometer eyepiece, and the grain roundness estimated by visual comparison with a chart (Powers, 1953) with the rho scale of Folk (1955). The modal composition and any special features were also recorded. The analysis was stopped when 200 suitable sand grains were measured, or less if fewer suitable grains were available. Only 5 thin sections contained as many as 200 countable grains, and the rest less, down to as few as 95. These are obviously very small samples, and analyses of much larger samples would be required to detect subtle granulometric differences. These analyses are thus valuable only in establishing crude estimates of the more important granulometric parameters.

The data were recorded on a coding sheet and subsequently punched on to 80-column cards. The computations were done by a CDC 3600 Computer to a programme prepared by T. Quinlan.

The raw data of length (Lmts) and width (Wmts) are in millimetres and they are converted to phi units according to the relationship:

$$L\phi ts = -\log_2 Lmts = \frac{-\log_{10} Lmts}{0.69315}$$

Because the distribution of $L\phi$ and $W\phi$ are normal, the sieve equivalents of length ($L\phi se$) and width ($W\phi se$) are derived from the relationship (Friedman, 1958):

$$L\phi se = 0.3815 + 0.9027\ L\phi ts$$

The mean, standard deviation, skewness, kurtosis, and the critical ratio 't' $\left(\frac{\text{Skewness}}{\text{standard error}}\right)$ were computed for length, width, $\frac{\text{length}}{\text{width}}$ (elongation), and roundness (rho) by the method of moments. A matrix of correlation coefficients was computed. The frequency distribution of $L\phi se$ was computed, the values of various percentiles read off the curve, and the graphic parameters of Folk & Ward (1957), viz., M_z, δ_I, Sk_I, and K'_G, were computed. The moment values of skewness and kurtosis were found to be not significantly different from zero at the $p = 0.05$ level. The values of the parameters are given in Table 7. The mean grainsize ($L\phi se$) ranges from 3.26 ϕ (very fine) to 1.59 ϕ (medium), the standard deviation from 0.28 ϕ (very well sorted) to 0.64 ϕ (moderately well sorted), the skewness (SkI) from —0.117 (coarse skewed) to +0.184 (fine skewed), and kurtosis (K'_G) from 0.458 (platykurtic) to 0.557 (leptokurtic). Mean roundness (rho) ranges from 3.55 (subround) to 4.80 (round), and roundness sorting is good. Mean elongation ranges from 1.44 to 1.71. In brief, the sand fraction of these samples is fine and well sorted in a lognormal distribution. The grains are rounded, and their length is roughly one and a half times the width.

In terms of the granulometry of the sand fraction, these samples are homogeneous, and cannot be separated into the groups of cross-bedded sandstone, flat-bedded sandstone, and cross-bedded sandstone with siltstone pellets, that are distinguished by bed form and content of siltstone pellets.

In only four specimens were the correlation coefficients (r) between $L\phi se$ and rho statistically significant.

Specimen	404-5	420-1	431	458-16
Correlation				
$r_{L\phi se.rho}$	—0.23	—0.23	—0.26	—0.16
p	<0.05	<0.01	0.01	0.05

The negative correlation indicates that in these specimens roundness increases with length, in agreement with other studies (Pettijohn, 1957, p. 63).

All but two of the 14 specimens were measured for elongation, and all of these are correlated ($p<0.01$) with length:

Specimen	28-7	39-5	103-18	103-20	104-21	110A
$r_{L\phi se.\frac{L\phi se}{W\phi se}}$	0.62	0.55	0.57	0.51	0.60	0.60
Specimen	130-5	400-3	404-5	412-6	431-1	458-16
$r_{L\phi se.\frac{L\phi se}{W\phi se}}$	0.59	0.52	0.40	0.50	0.49	0.50

TABLE 7: GRANULOMETRY OF SAND FRACTION

Sample No.	Formation or Member and Locality	n	Mean Grainsize ϕ (moments)	Mean Grainsize ϕ (graphic) Mz	Grade	Standard Deviation (moments)	Standard Deviation (graphic 1)	Description	Skewness Sk 1	Skewness Description	Kurtosis K^1_G	Kurtosis Description	mean roundness ϕ (rho)	mean roundness Description	Sorting Value (SD rho)	Sorting Description	Mean Elongation Lm/Wm	Mean Elongation SD	Mean Elongation $L_\phi e / W_\phi e$	Mean Elongation SD
										Cross-bedded Sandstone										
420-1	Ragged Ra. Mbr, Nigli Gap	200	2.2859	2.270	fine	0.4856	0.492	well sorted	0.131	fine skewed	0.484	mesokurtic	3.69	subround	1.24	v. poor				
412-6	Ragged Ra. Mbr, Church Steeple Pk	200	2.1434	2.150	fine	0.5106	0.525	mod. well sorted	0.184 0.184	fine skewed	0.557	leptokurtic	4.27	round	0.99	moderate	1.67	0.52	0.78	0.11
135-1	Ragged Ra. Mbr. SW of Alpha H.	200	3.1428	3.140	v. fine	0.4431	0.420	well sorted	0.014	near symmetrical	0.523	mesokurtic	3.55	subround	1.02	poor				
404-5	Kellys Knob Mbr Kununurra	96	2.4012	2.367	fine	0.6240	0.628	mod. well sorted	—0.038 —0.038	near symmetrical	0.458	platykurtic	4.28	round	0.78	good	1.65	0.66	0.81	0.10
28-7	Kellys Knob Mbr. Matheson Ridge	168	1.5941	1.597	medium	0.6389	0.595	sorted sorted	0.003 0.003	near symmetrical	0.507	mesokurtic	4.24	round	1.14	poor	1.62	0.48	0.72	0.18
39-5	Kellys Knob Mbr, Elephant H.	120	2.0473	2.060	fine	0.4922	0.492	well sorted	0.000	symmetrical	0.502	mesokurtic	4.60	round	0.67	good	1.64	0.46	0.77	0.11
130-5	Kellys Knob Mbr, Shakespeare H.	96	2.1490	2.143	fine	0.4527	0.459	sorted	—0.038	coarse skewed	0.507	mesokurtic	4.52	round	0.99	moderate	1.53	0.42	0.81	0.11
										Thin-bedded Sandstone										
431-1	Hargreaves Mbr, Hargreaves Hs.	95	3.1939	3.200	v. fine	0.3490	0.325	v. well sorted	0.075	near symmetrical	0.522	mesokurtic	4.58	round	0.75	good	1.65	0.41	0.84	0.07
103-20	Enga Ss., Enga Ridge	179	1.9806	1.967	medium	0.2821	0.254	v. well sorted	0.007	near symmetrical	0.498	mesokurtic	4.80	round	0.71	good	1.44	0.30	0.82	0.09
108-18	Enga Ss., Enga Ridge	140	3.2565	3.237	fine	0.3439	0.330	v. well sorted	—0.036	near symmetrical	0.539	leptokurtic	4.36	round	0.80	good	1.67	0.59	0.84	0.08
110A	Zimmerman SS.. Mt Zimmerman	163	2.0873	2.087	fine	0.3796	0.375	well sorted	0.030	fine skewed	0.510	mesokurtic	4.51	round	0.80	good	1.58	0.46	0.79	0.11
400-3	Point Spring Ss., Weaber Ra.	200	2.4527	2.443	fine	0.6212	0.620	mod. well sorted	—0.117	coarse skewed	0.479	mesokurtic	4.09	round	0.96	moderate	1.71	0.54	0.79	0.11
										Cross-bedded Sandstone with Siltstone Pellets										
458-16	Border Cr Fm, Weaber Ra.	140	1.7432	1.730	medium	0.3979	0.378	well sorted	—0.064	near symmetrical	0.499	mesokurtic	4.64	round	0.87	moderate	1.53	0.39	0.77	0.12
104-21	Border Cr Fm, Mt Septimus	199	1.7470	1.717	medium	0.4625	0.400	well sorted	—0.108	coarse skewed	0.515	mesokurtic	4.58	round	0.79	good	1.62	0.43	0.75	0.13

NOTES: 1. The nearly identical value of means determined by the method of moments and by graphical methods, and of standard deviations determined by these methods, are a consequence of the lognormal distribution, independently indicated by the statistically insignificant differences from zero of skewness and kurtosis.

2. The terms describing the values of the grainsize mean (grade), grainsize standard deviation (sorting), skewness, kurtosis, mean roundness, and roundness standard deviation are defined in Folk (1961).

3. The formulae of M_Z, σ_1, Sk_1, and K^1_G are given by Folk & Ward (1957).

The use of the correlation coefficient between these variables is of doubtful validity because the distribution of elongation is not normal. On the face of it, the correlation coefficients indicate that with increasing length (decreasing Lϕse) the grains become more elongate (or less spherical). This disagrees with some studies (Pettijohn, 1957, p. 64), which find that sphericity increases with size, but agrees with others (Folk, 1961, p. 12). The well established correlation between roundness and sphericity (Pettijohn, 1957, p. 62) was not found in these specimens, the correlation coefficients between rho and $\frac{L\phi}{W\phi}$ being statistically not significant.

Environmental significance

The use of textural parameters for distinguishing the environment of deposition of sands has been promoted by Folk (1966) and Friedman (1967) among others. Friedman has sieved numerous specimens of Recent dune, beach, and river sands, and computed their textural parameters, mainly by the method of moments. Folk has relied on the use of graphic measures of sieved sands. The parameters of sieved equivalent length of Bonaparte Basin sandstones are thus compatible with Folk's and Friedman's work.

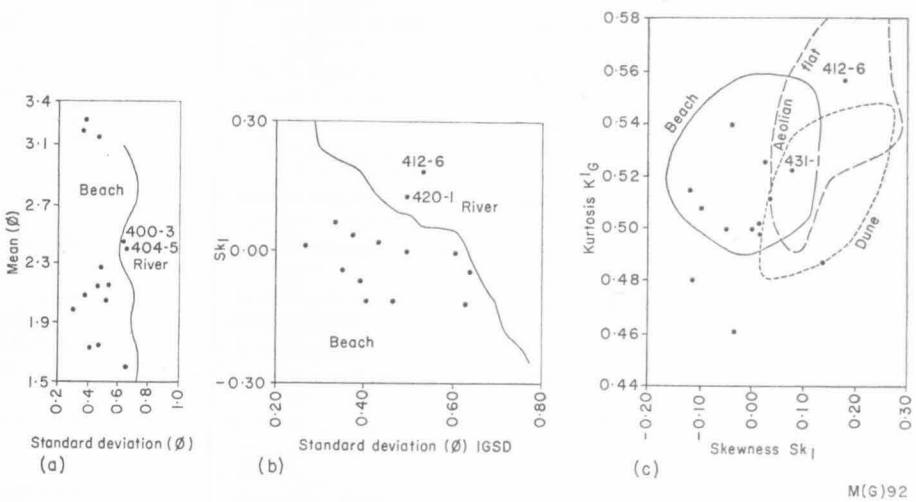

Figure 20. (a) Mean and standard deviation, (b) skewness and standard deviation, and (c) kurtosis and skewness

The values of mean and standard deviation of the 14 specimens and the fields characteristic of beach and river sands (Friedman, 1967, fig. 14) have been plotted on Figure 20a. Twelve specimens lie in the 'beach' fields, and 2 in the 'river' field. The plot (Fig. 20b) of σ I and Sk I and Friedman's (1967, fig. 15) fields contain 12 in the 'beach' field and 2 (not the 2 'river' sands of Fig. 20a) in the 'river' field. Finally, a plot (Fig. 20c) of Sk I and K'_G and Mason & Folk's (1958, fig. 9) field for Mustang Island sands has 8 in the 'beach' field, 1 in the 'dune' field, 2 in the area of overlap of the 3 fields, and 2 that lie altogether outside the fields.

In crude fashion, the bulk of the specimens analysed seem to be distinguishable as beach sands. This determination, however, contains three uncertainties:

(1) Friedman (1967) and Mason & Folk (1958) worked out empirically the fields of parameters of shallow-water (beach and river) and aeolian sands only, and their system therefore does not include sands deposited in other environments, such as sands deposited on shelves swept by tidal currents. Thus comparison is necessarily restricted to three kinds of sands.

(2) Friedman and Mason & Folk do not give estimates of the statistical significance of the parameters used, nor have they computed a statistically rigorous discriminant function between fields. In this study, the values of skewness and kurtosis obtained by the method of moments were found to be insignificant; that is, at the 5 percent level, the values do not differ significantly from zero, and hence they cannot even be classified into the crude divisions of positive or negative skewness and kurtosis. Until the statistical significance of Folk's and Friedman's parameters is determined, the statistical validity of their method remains in doubt.

Moss's (1962) method of analysing the elongation of grains is likewise entirely graphic and the statistical significance of the differences in elongation between various kinds of grains is untested.

(3) If abundant nuclei of reworked overgrown quartz grains were overlooked, and measurements of these grains were included with those of grains sized and sorted in the Upper Devonian and Carboniferous depositional environments, the granulometric data would be composite. This possibility is unlikely, however, because abraded overgrown quartz grains seem to be rare.

Flat-bedded Sandstone

Primary Structures

Flat-bedding in thin to laminate beds is the characteristic structure of this kind of sandstone. Cross-bedding is locally common, and is distinguished from that of the cross-bedded sandstone group by its low cross-dip ($<10°$) and less regular shape, whereby it merges into wedge-bedding (xi cross-bedding of Allen, 1963a). Biogenic structures, most commonly on a bedding surface but occasionally normal to it, are characteristic.

A structure of problematical origin (Pl. 17, fig. 2) was seen near the base of the Point Spring Sandstone in section 435, 5 miles northeast of Point Spring. The structure lies in a trough cut into otherwise unexceptional flat-bedded and cross-bedded laminated sandstone, and consists of sandstone in which the laminae are parallel to the steep sides of the trough. Dr R. L. Folk, University of Texas, who pointed out the structure in the field, suggested that it was probably a 'spring pit', as described by Quirke (1930) and Shrock (1948). Spring pits are produced on a sandy beach by ascending waters, and then filled in by later deposits of sand. The structure in the Point Spring Sandstone is deeper (2 ft) than those described by Quirke, and steeper sided (70°); indeed, to maintain this slope beneath water, the sand must have been somewhat consolidated. Then the pit had to be filled with sand whose laminae are parallel to the sides of the pit. How the laminae of water-saturated sand are stable on such slopes is unknown. Another possibility, suggested by Dr J. R. Conolly (pers. comm.), is that the trough was cut through a sand bar by a rip current.

The presence of abundant fossils indicates that the flat-bedded sandstone is marine. In marine deposits flat-bedding and xi cross-bedding are characteristic of littoral sands. A preliminary examination of the biogenic structures indicates shallow-marine deposition; and if the problematical structure in the Point Spring Sandstone is indeed a spring pit, then this too adds weight to the interpretation of the flat-bedded sandstone as a littoral or sublittoral sand.

Petrography and Granulometry

The petrography and granulometry of the flat-bedded sandstone, not being sensibly different from those of the cross-bedded sandstone, have been described above in the account of the cross-bedded sandstone. In summary, the flat-bedded sandstone is a quartz sandstone or argillaceous quartz sandstone, with an almost pure orthoquartzite sand fraction except for one specimen which is a subarkose. The sand fraction is fine and well sorted, and the grains are rounded.

SEDIMENT SOURCES AND ENVIRONMENTS OF DEPOSITION

Geological Setting

The present distribution of pre-Upper Devonian rocks in northwest Australia (Fig. 21) is the starting point for reconstructing the palaeogeology of the basal Upper Devonian surface. The Bonaparte Gulf Basin lies across the Halls Creek Mobile Zone between the Kimberley Block and the Sturt Block. The Halls Creek Mobile Zone contains Precambrian metamorphic and granite rocks, the Kimberley

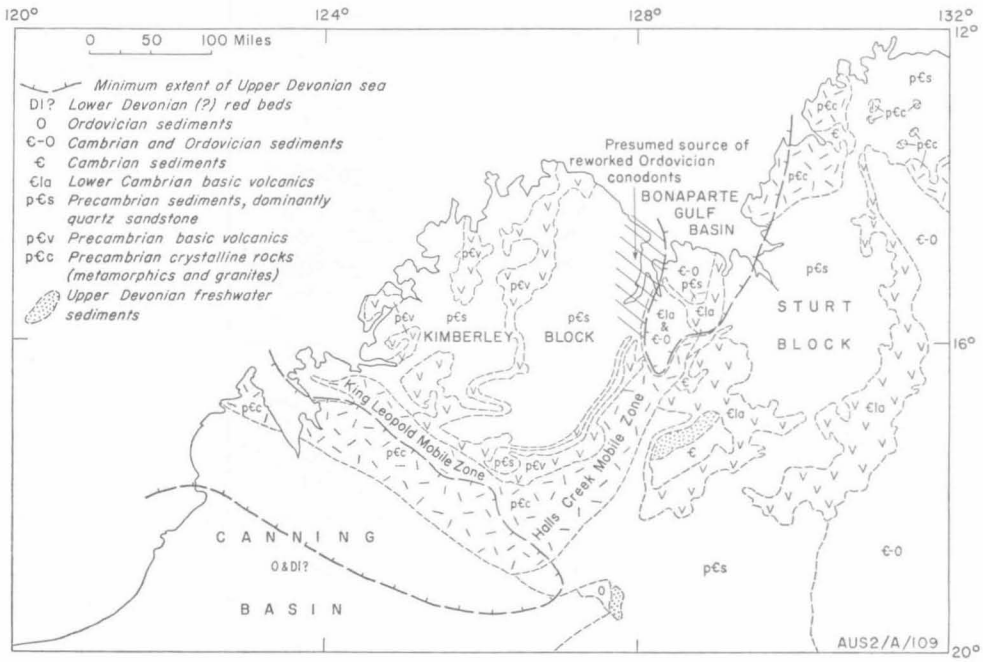

Figure 21. Present distribution of major pre-Upper Devonian lithostratigraphical units, minimum area of Upper Devonian marine deposition, and outcrops of Upper Devonian freshwater sediments in northwestern Australia. (After Geological Map of the World: Australia and Oceania, Sheet 6, 1965)

Block generally flatlying Precambrian sandstone and minor siltstone and shale, with interlayered basic volcanics, and the Sturt Block generally flatlying Precambrian sandstone, shale, and carbonate rocks, overlain by Lower Cambrian basic volcanics. The basal Upper Devonian sediments of the Bonaparte Gulf Basin overlie granite and metamorphics of the Halls Creek Mobile Zone, Precambrian sediments of the Kimberley and Sturt Blocks, Lower Cambrian volcanics, and Cambrian and Lower Ordovician sediments. The early Upper Devonian surface of the Bonaparte Basin thus had great structural relief. If, however, that part of the surface underlain by the Halls Creek Mobile Zone is disregarded, the greater part of the reconstructed early Upper Devonian surface is seen to consist of generally flatlying Precambrian sediments and interlayered basic volcanics, Lower Cambrian basic volcanics, and Cambrian and Lower Ordovician sediments. How far the upper part of the Lower Palaeozoic sequence extended across the blocks is not known. For considerations of Upper Devonian source material, this point is unimportant because whether the surface consisted of Precambrian or of Lower Palaeozoic sediments it would yield quartz sand as its chief coarse sediment. Only if the Lower Palaeozoic sediments were stripped back to expose a broad surface of Lower Cambrian basic volcanics would a markedly different sediment be supplied. From these considerations, the reconstructed early Upper Devonian surface is inferred to have been predominantly sandstone in the west, and sandstone, shale, and carbonate, and an unknown, probably small, area of basic volcanics in the east, and a small area of crystalline rocks to the south and southwest. The coarse conglomerate and its rapid wedging out in the Ragged Range Member indicate high relief along the southeast margin of the basin.

Source of Distinctive Fragments

In the Ragged Range Member, local accumulations of granite wash in the southern Ragged Range, of basalt wash and basalt boulders 3 feet across at Martin Bluff and Church Steeple Peak, and siltstone conglomerate between Nigli Gap and Legune indicate a nearby source of these materials. Farther from their source are the pebbles of porphyritic microgranite and porphyritic rhyolite in the Ragged Range Member at Church Steeple Peak, which probably came from the Halls Creek Mobile Zone 25 miles to the south. Grains of euhedral zoned quartz in the Kellys Knob Member (Pl. 8, fig. 2) were probably derived from vug infillings in the Lower Cambrian Antrim Plateau Volcanics.

The most firmly identified grains are the reworked Lower Ordovician conodonts found in the Westwood Member (E. C. Druce, BMR, pers. comm.). Druce has identified five species, at least two of which are also known in the Lower Ordovician Pander Greensand. The specimens are fragile and unabraded, and because no fragments larger than sand grains are known in the Westwood Member, these specimens must have been deposited not inside pebbles but as single sand grains. This implies a nearby source of Lower Ordovician sediments, either to the south or to the west (Fig. 21), which in the process were entirely stripped off. Because the Lower Ordovician and Cambrian sediments are coextensive in the Bonaparte Basin, the Cambrian sediments probably extended southwards and westwards too. Reworked Lower Ordovician conodonts were also found in the Upper Devonian Ningbing Limestone (E. C. Druce, pers. comm.) and in the Permian Keep Inlet beds (P. J. Jones, BMR, pers. comm.).

Source of Nondescript Grains

The grains of common quartz are nondescript, except the rare ones with double overgrowths (Pl. 10, figs 1, 2; Pl. 11, fig. 1), which testify to two episodes of detrital deposition. Any of the Precambrian or Lower Palaeozoic sandstones in the region could have provided these grains. Failure to detect abundant reworked grains with abraded overgrowths would have serious consequences to the granulometric study, because grains shaped during the Precambrian and Lower Palaeozoic would be mistaken for grains shaped in the Upper Devonian and Carboniferous.

The occurrence of reworked conodonts and sand grains prompts the question of whether the glauconite in the Upper Devonian and Lower Carboniferous sandstones is authigenic or detrital. The likely source of the conodonts is the Pander Greensand, and glauconite-bearing rocks are common in the Precambrian sequences of the Kimberley and Sturt Blocks. Abundant glauconite associated with layers of shelly fossils in the Upper Devonian and Lower Carboniferous sediments is unquestionably authigenic, and hence an indication of deposition in normal sea water; but rare grains of glauconite dotted throughout a cross-bedded sandstone are obviously suspect, as, for example, the glauconite in the base of the Cockatoo Formation unconformably above the Pander Greensand at locality 275-6 at Gap Point. Whether the glauconites in other sandstones are detrital grains from pre-existing sandstone or merely authigenic grains that have been rolled around before being finally deposited cannot be established.

The ultra-stable heavy mineral suite of tourmaline and zircon has probably been reworked from older sediments rather than derived from the intense chemical weathering of crystalline rocks because these minerals coexist with feldspar. At the present day, the crystalline rocks of the Halls Creek Mobile Zone yield unstable heavy minerals to the Ord River (Carroll, 1947), and thence to the sea (von der Borch, 1965). The lack of unstable heavy minerals in the Upper Devonian and Carboniferous sandstones probably indicates that the Halls Creek Mobile Zone contributed little sediment to the Upper Devonian and Carboniferous deposits, except, as noted above, locally, as in the southern Ragged Range. Elsewhere, the small contribution of sand grains from the Halls Creek Mobile Zone was diluted to vanishing point by a preponderant volume of sand from reworked sandstone. Weathering products of the Halls Creek Mobile Zone may be represented by the kaolinite matrix of some sandstones.

The origin of the red pigment, mainly hematite, in the sandstones is obscure. As is common in red sandstones (Walker, 1967), the hematite stains both the matrix and the quartz grains, so that the date of staining of the grains, either before (detrital) or after (authigenic) they were deposited, is unknown. Walker (1967) points out the risk of error in interpreting the occurrence of hematite exclusively in terms of the source area.

The clay minerals in the sandstones, chiefly kaolinite, were derived either from the weathering in situ of feldspar, by diagenetic growths, or, if they are detrital, from deeply weathered crystalline rock in the Halls Creek Mobile Zone. The clay minerals that form the bulk of the basinal shale facies were probably

derived from the Sturt Block, Halls Creek Mobile Zone, and Antrim Plateau Volcanics, with minor amounts from the Kimberley Block. Most of the clay minerals were separated from the sand by waves and currents on the marine platform to be finally deposited in the calm deeper water of the basinal province.

Environments of Deposition

1. Contained fossils, facies relationships, and granulometry indicate that the whole sequence of sandstone and conglomerate, except the Border Creek Formation, is marine.

2. The cross-bedding in the cross-bedded sandstone dips generally away from the shoreline, indicating the seaward migration of straight large-scale asymmetrical sand waves. Tidal (ebb) currents were probably the principal agents responsible for this, because they are the only marine currents considered capable of transporting sand in waves from the shore across a broad shallow shelf. The other kinds of marine currents that can transport fine sand in shallow water lack this unique feature of ebb-tidal currents—their seaward flow from the very shore.

3. Structures and trace fossils in the flat-bedded sandstone indicate deposition in very shallow water, probably close inshore (sublittoral). Repeated advance and retreat of the shore led to some 500 feet of these sediments accumulating in the one place.

4. The alternation of cross-bedded and flat-bedded sandstone in the Point Spring Sandstone indicates cyclic changes: (a) deposition of cross-bedded sandstone in water flowing in tidal currents, which shaped the sand into long asymmetrical waves; and (b) deposition of flat-bedded sandstone in shallower water, in which tidal and other currents were damped out.

5. The Border Creek Formation, which is the first unit in an Upper Carboniferous to Lower Triassic paralic sequence, resembles the cross-bedded sandstone in petrography and structures, but differs in containing siltstone in beds and in intraformational pellets and blocks. It lacks marine fossils, and it was deposited disconformably on a fairly deeply dissected surface. The Border Creek Formation is interpreted as a fluvial deposit, the cross-bedded sandstone, conglomerate, and intraformational siltstone breccia being channel deposits and the bedded siltstone an overbank deposit.

Conclusions

In the Upper Devonian and Lower Carboniferous, during episodes of uplift of the land and subsidence of the sea floor, the land behind the Bonaparte Gulf Basin shed sand, predominantly quartz, and mud on to a marine shelf, part of which was shallow (a platform), part deeper (a basin). Conglomerate accumulated at the foot of upthrown fault blocks along the southeastern shore. The sediment was separated in beaches into sand and mud, and was kept separated on the rest of the platform by waves and currents. The mud finally settled in the deeper calm water of the basin, and the sand was driven by tidal currents across the platform in long asymmetrical sand waves. Continued supply of sediment and subsidence of the sea floor led to the accumulation of thick bodies of cross-bedded sandstone. With slower subsidence of the sea floor, the water shallowed, and tidal currents waned. As before, the sediment shed from the land continued to be separated into sand and mud along beaches, and the mud finally lodged in the basin, but the sand

remained close inshore because the tidal currents were too weak to carry it seaward. With a continued supply of sand, the shore advanced across the platform, leaving behind a layer of flat-bedded sandstone. The Point Spring Sandstone was laid down during short cycles of deposition of cross-bedded and flat-bedded sandstone. Individually thicker bodies of cross-bedded and flat-bedded sandstone were deposited during longer cycles, the thicker bodies of flat-bedded sandstone accumulating during repeated advance and retreat of the shore with different rates of sea-floor subsidence. Carbonate sediments, the subject of the rest of this Bulletin, were deposited on the platform during episodes of reduced supply of terrigenous sediments.

After the sea floor was uplifted at the end of the Lower Carboniferous, the sediments previously deposited were dissected by rivers, whose valleys were later filled with the fluvial sediments of the Border Creek Formation.

This study is a reconnaissance, and accordingly the conclusions reached are probably oversimplifications. The next step is to seek more definite evidence in the field for reconstructing the depositional environment. Detailed field studies of the trace fossils of the flat-bedded sandstone and of the relationships between the cross-bedded and flat-bedded sandstones that are interbedded in the well exposed Point Spring Sandstone would be two lines of fruitful enquiry.

CARBONATE ROCKS

INTRODUCTION

Geological Setting

Together with quartz sandstone and conglomerate, carbonate rocks make up the bulk of the Upper Devonian and Lower Carboniferous platform sequence: carbonate rocks aggregate about 4,500 feet, sandstone and conglomerate about 6,000 feet. Of the carbonates, limestone predominates, and only a few hundred feet—the Jeremiah Member—consists of dolomite. Most of the limestone is concentrated in an almost unbroken sequence through the Famennian to the early Tournaisian, with minor amounts in the Frasnian, late Tournaisian, and Visean.

The lateral sequence of Famennian platform carbonate rocks is fairly complete, and comprises reef, inter-reef, fore-reef, and back-reef, all called the Ningbing Limestone, and inshore and offshore lagoonal carbonate rocks and sandstone called the Buttons Beds. Part of the subsurface siltstone and shale of the Bonaparte Beds is the basinal equivalent of this sequence. The lateral carbonate sequences of other ages are less varied or incomplete owing to denudation. The carbonate rocks in the Frasnian Kununurra, Hargreaves, and Westwood Members become progressively purer and thicker with increasing distance from the southeast margin of the basin, culminating in reefal* limestone at Westwood Creek, at the northwest

* 'Reefal' is used here as a collective term for all the facies associated with reef development. 'Reef' is restricted to the facies of the reef wall. Terms for the other facies are described by Nelson, Brown, & Brinehan (1962, pp. 249-50). In correspondence, Dr P. E. Playford points out that our use of the term inter-reef differs from that applied in the Canning Basin (Playford & Lowry, 1967). From its poor outcrop and obscure field relations, the inter-reef facies of the Bonaparte Gulf Basin is regarded as a deposit in narrow channels through the reef. In the Canning Basin, the term is applied to the deposits of the broad basins that lay between various complexes.

limit of outcrop. The lateral sequence of early Tournaisian carbonates includes calcareous quartz sandstone along the southeast margin, passing in a short distance into fairly pure skeletal lump limestone, the Burt Range Formation. The only known equivalent limestone elsewhere is the reef limestone 32 miles northwestward at locality 7-1, in the Ningbing Range. In the late Tournaisian and Visean, the limestones vary laterally and vertically only in their content of quartz and dolomite. For the late Tournaisian Septimus Limestone and early Visean Utting Calcarenite, the small variation may be explained by their narrow known distribution, but the equally small variation in the widely distributed late Visean Burvill Beds seems to indicate a radical change in the depositional regime starting at least in the late Visean and, as indicated by the Septimus Limestone and Utting Calcarenite, possibly as early as mid-Tournaisian. The remaining late Lower Carboniferous carbonate rocks are two dolomite breccias, the Waggon Creek Breccia and an unnamed one at locality 210-6, each known from one outcrop only.

Outline of Methods of Study

Little attention was given to the study of the finer details of the carbonate rocks. Most of the carbonates are limestones which are fairly simple and only slightly recrystallized, so that the interpretation of diagenetic changes was of secondary importance. Rather it was felt that the time available would best be spent gathering information in a broad survey of all the material, including some 500 thin sections, and concentrating this into a synthesis. After a review of all the material, 103 representative specimens were chosen for detailed study by modal and chemical analysis. Altogether 47 modal and chemical constituents were determined for each specimen, and this information was processed on a computer with a programme of numerical classification and Q-factor analysis.

Field Occurrence and Structure

The field occurrence of the carbonate rocks is described and illustrated by Veevers & Roberts (1968, pls 10-13, 16-19, 21, 24-25). The Famennian Ningbing Limestone is the only carbonate formation that is well and extensively exposed. The other carbonate formations are well exposed in one or two areas, and poorly exposed elsewhere. The Famennian carbonate sequence is consequently the best known, and it serves as a reference for the others.

Except in massive reef carbonates, flat-bedding is the commonest structure. Unlike the coarse terrigenous sediments described above, the carbonate rocks visibly lack cross-bedding. Suitable fossils indicate ancient current directions, such as the oriented nautiloids illustrated by Veevers & Roberts (1968, pl. 22, fig. 2), and others, notably brachiopods, serve as geopetal structures.

A few specimens showing special features are illustrated here. *Stromatactis* (Pl. 42, fig. 1), a problematical structure (Bathurst, 1964; Playford & Lowry, 1967), is common in the reef and near-reef limestones. Limestone conglomerate (Pl. 42, fig. 2), was found in fore-reef limestone, and a breccia of siltstone clasts cemented by carbonates was found at the base of the Buttons Beds in the Sorby Hills.

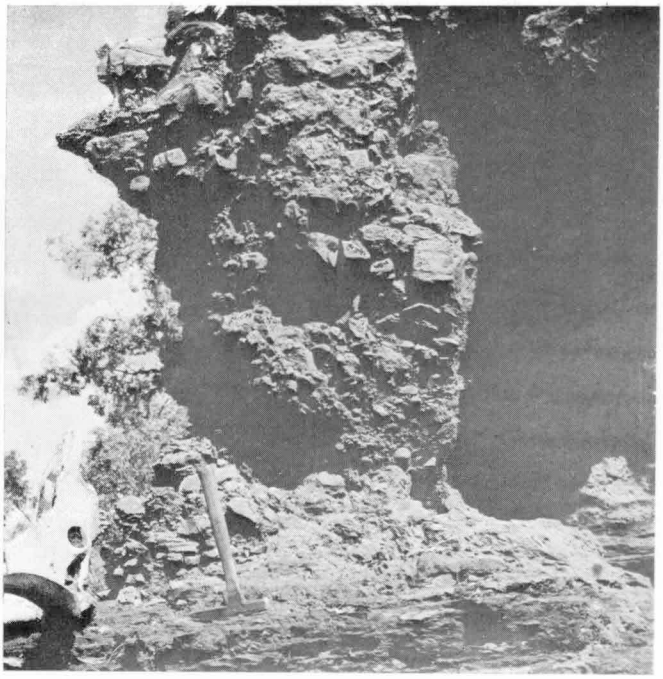

Plate 1, Figure 1. Poorly rounded and poorly sorted metaquartzite conglomerate in the Ragged Range Member, northwest of Policeman Waterhole (loc. 417-1). Bedding is roughly indicated by subparallel plates of metaquartzite

Plate 1, Figure 2. Siltstone breccia in probable Border Creek Formation, rock stack off eastern tip of Rocky Islet (loc. 433-1)

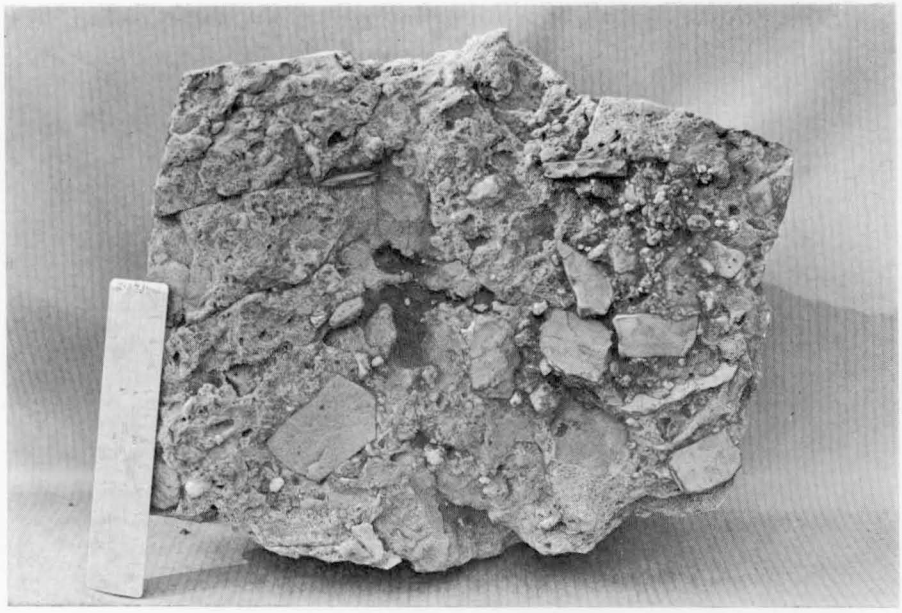

Plate 2, Figure 1. Crudely bedded surface of basal breccia of Buttons Beds at Sorby Hills (loc. 402). The scale is 6 inches long. Photo by J. Zawartko

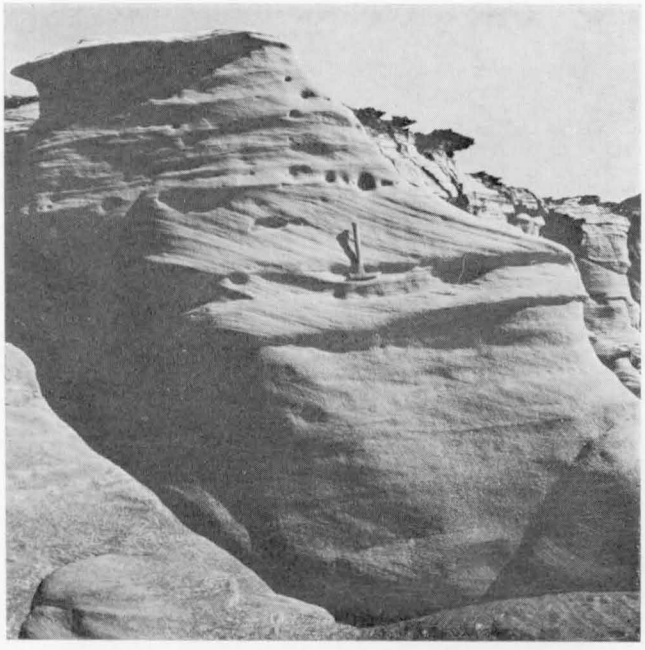

Plate 2, Figure 2. Looking west at omikron cross-bedded sandstone of probable Border Creek Formation on the northern cliff face of Pelican Islet (loc. 432-1). At least 17 sets with the same cross-dip are visible

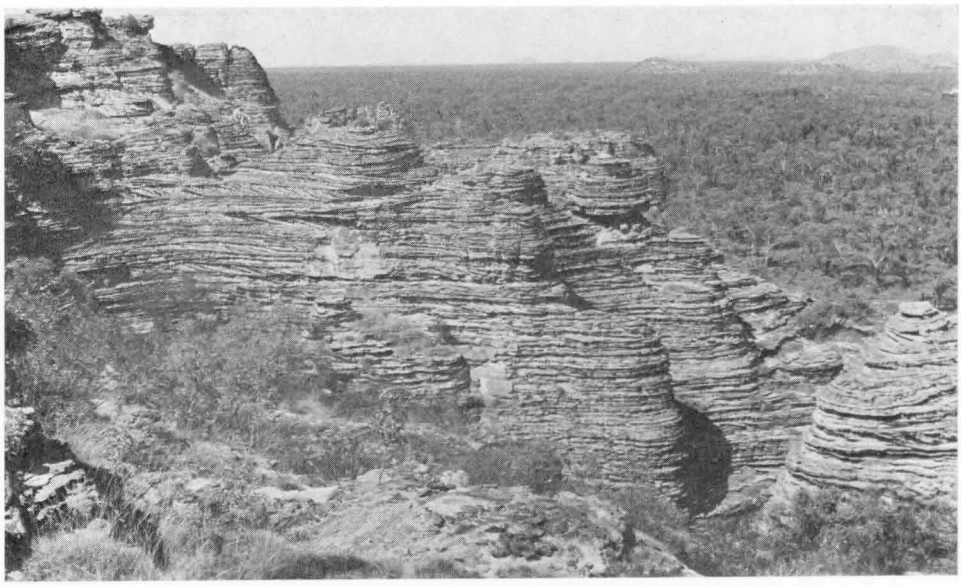

Plate 3, Figure 1. Looking south at a thick composite coset of cross-bedded sandstone of the Kellys Knob Member near Elephant Hill (loc. 40-3). Most of the sets are about 1.5 feet thick, and the cross-dip is uniformly to the right (westward)

Plate 3, Figure 2. Cross-bedded sandstone of the Kellys Knob Member north of Onslow Hills (loc. 43-7). Typical composite cosets of omikron sets and flat-bedded sandstone in upper part of picture overlying steeply dipping set at least 25 feet thick. Note contorted bedding on left-hand side. Scale indicated by seated figure at bottom left centre.

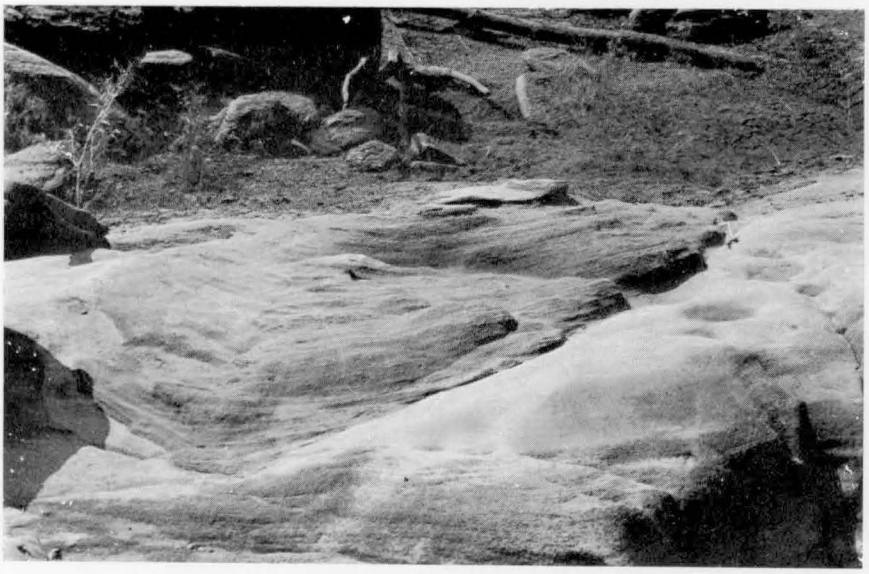

Plate 4, Figure 1. Looking down the axis of zeta cross-beds in Cecil Member at locality 36

Plate 4, Figure 2. Iota cross-bed in Cecil Member at locality 36. Pebbles and boulders are Recent alluvium

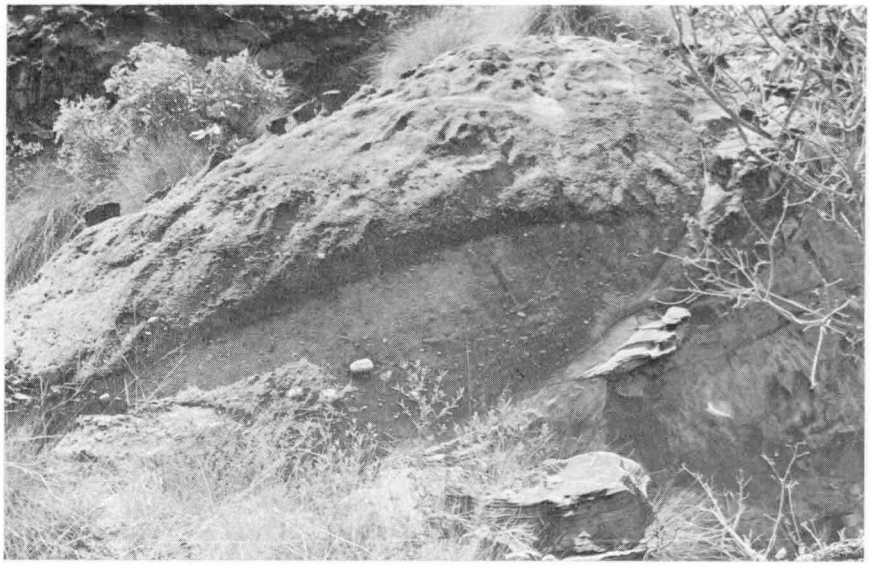

Plate 5, Figure 1. Trough in Border Creek Formation near top of section 25 in the Weaber Range. Note contrast between coarse poorly defined bedding in trough and lamination in underlying sandstone.

Plate 5, Figure 2. Troughs filled with siltstone fragments below and with quartzite cobbles and boulders above. Note imbrication in siltstone fragments, down to right. Ragged Range Member, west of Nigli Gap (loc. 70-3)

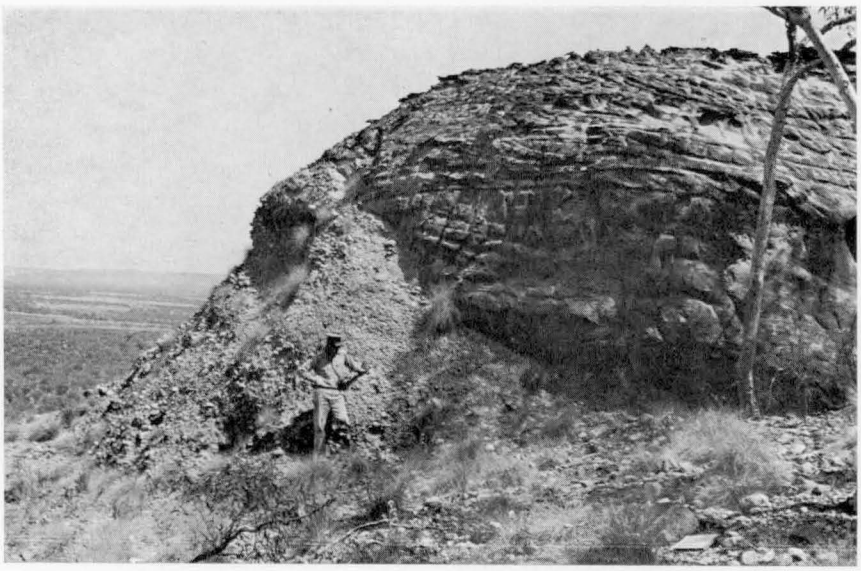

Plate 6, Figure 1. Jointed and cross-bedded sandstone filling a trough in conglomerate in Border Creek Formation at Spirit Hill (loc. 73-4)

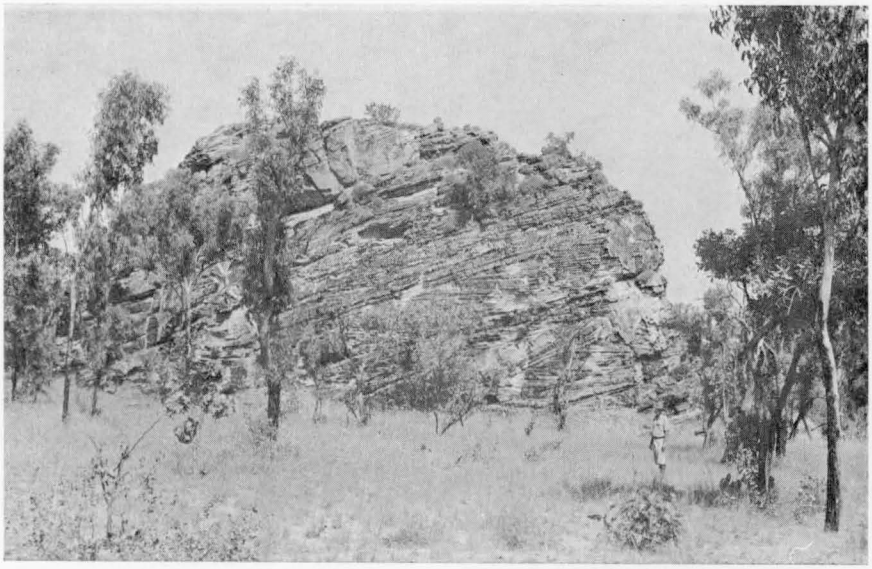

Plate 6, Figure 2. Looking southwest at cross-bedded Kellys Knob Member in isolated hillock half a mile northwest of locality 239B

Plate 7, Figure 1. Looking west at the trace of an S-shaped fold in a hardened joint surface in Kellys Knob Member north of Nigli Gap (loc. 76-3). The scale is 6 inches long

Plate 7, Figure 2. Flat beds between cross-bedded sets in Kellys Knob Member at locality 43-6, north of the Onslow Hills. Most sets are 1 to 2 feet thick

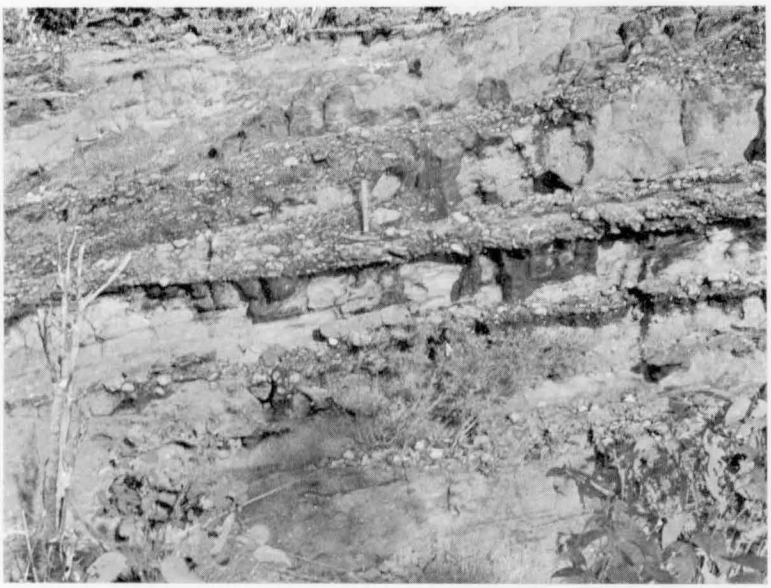

Plate 8, Figure 1. Wedges of imbricated conglomerate in Cecil Member north of Matheson Ridge (loc. 29-4)

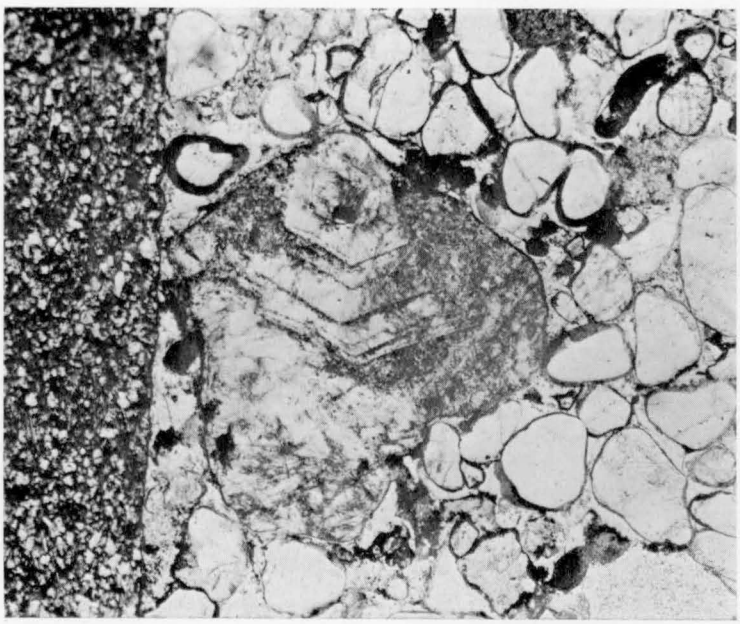

Plate 8, Figure 2. Large composite grain of euhedral quartz (centre), pebble of micaceous siltstone (left), and rounded quartz grains coated with hematite, in turn overgrown by secondary quartz. The euhedral quartz was probably derived from a vug infilling in the Lower Cambrian Antrim Plateau Volcanics, and the siltstone from Precambrian siltstone. Kellys Knob Member, Matheson Ridge (loc. 28-7). Ordinary light, × 35.

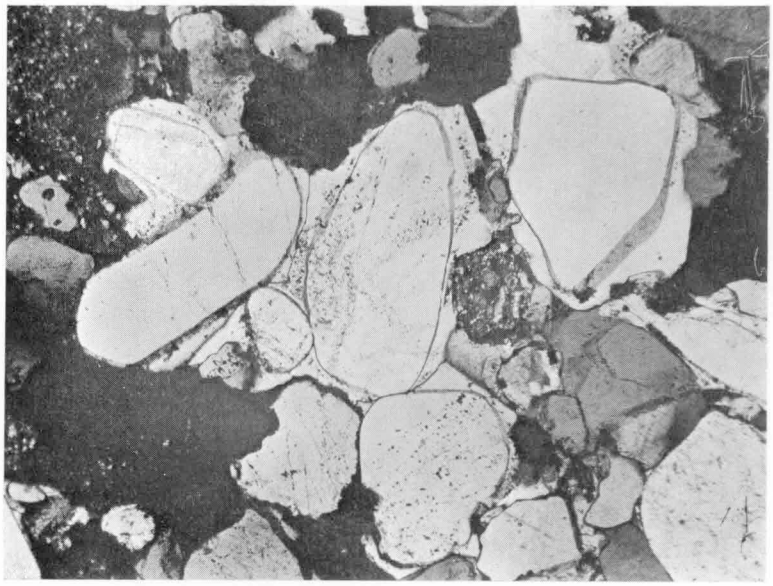

Plate 9, Figure 1. Another view of the previously illustrated slide, showing rounded quartz grains coated with hematite and quartz overgrowths. Crossed nicols, x 80

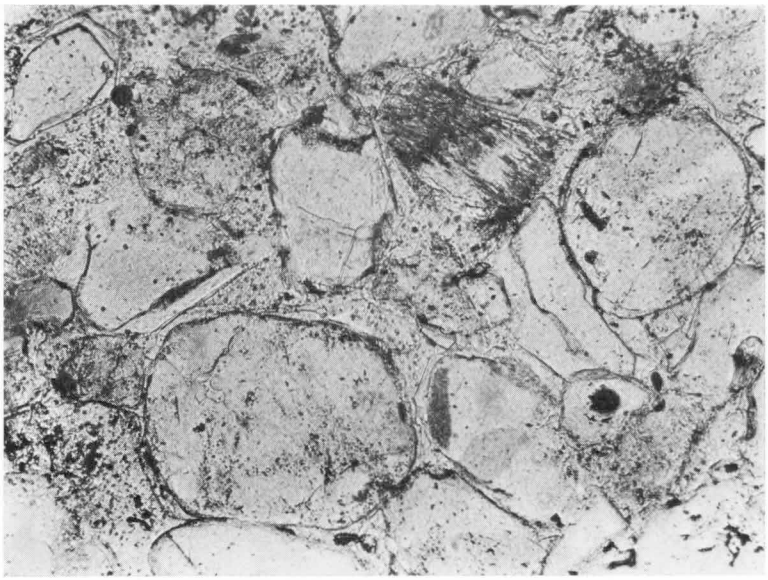

Plate 9, Figure 2. Quartz grains with hematite coatings and faceted overgrowths. Note euhedral overgrowths in top left-hand corner. The cloudy grain centre right is weathered untwinned feldspar. Note interstitial quartz cement in centre. Kellys Knob Member, Kununurra (loc. 404-5). Ordinary light, x 70

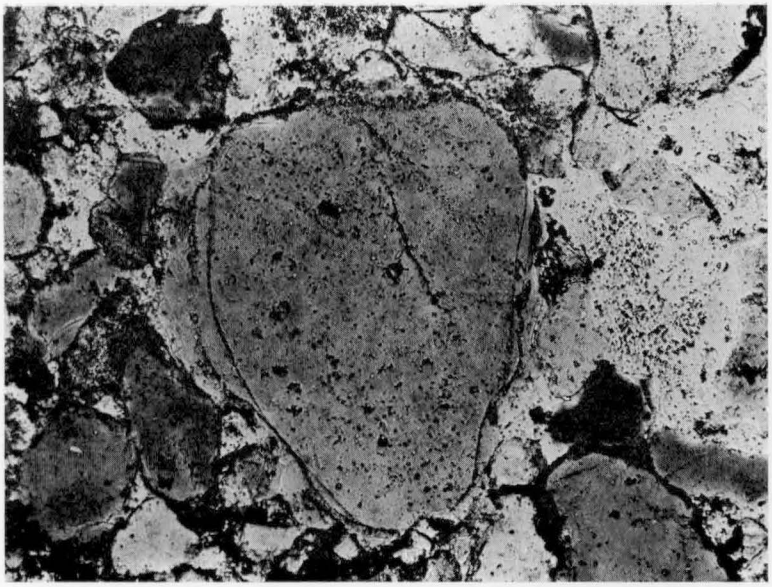

Plate 10, Figure 1. Quartz nucleus with abundant vacuoles, and two generations of overgrowths: an abraded inner overgrowth and an incomplete outer one. Ragged Range Member, Cockatoo Spring (loc. 81-1A). Crossed nicols, x 70

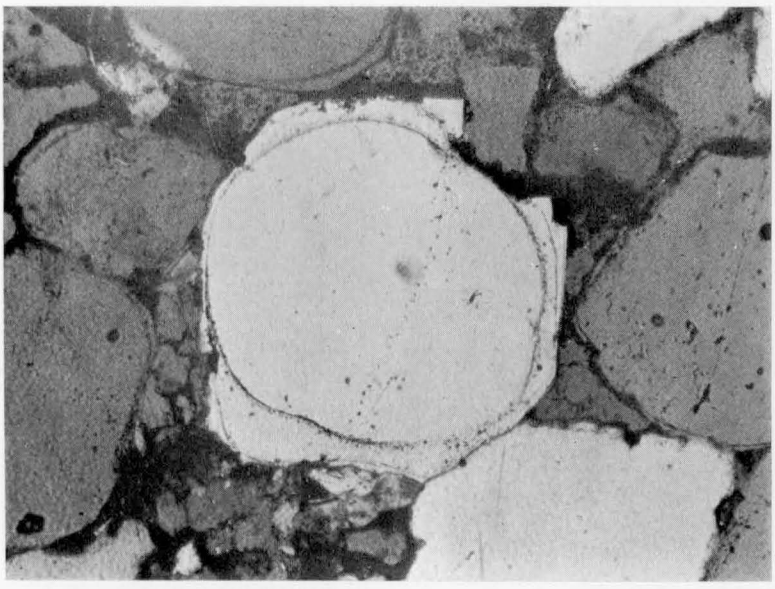

Plate 10, Figure 2. Quartz nucleus crossed by a string of vacuoles, enclosed by two generations of overgrowths, the outer one faceted. Intergranular spaces filled with hematite. Border Creek Formation, Mount Septimus (loc. 104-21). Crossed nicols, x 70

Plate 11, Figure 1. Quartz nucleus outlined by zone of vacuoles; inner overgrowth abraded and rounded, outer one faceted. Locality 104-21. Crossed nicols, x 70

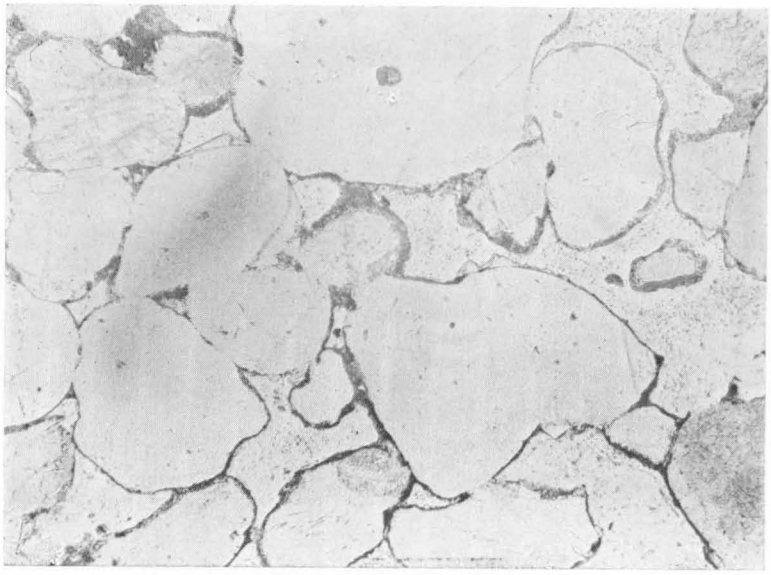

Plate 11, Figure 2. Faceted overgrowths protruding into space between grains. Border Creek Formation, Mount Septimus (loc. 104-18c). Ordinary light, x 70

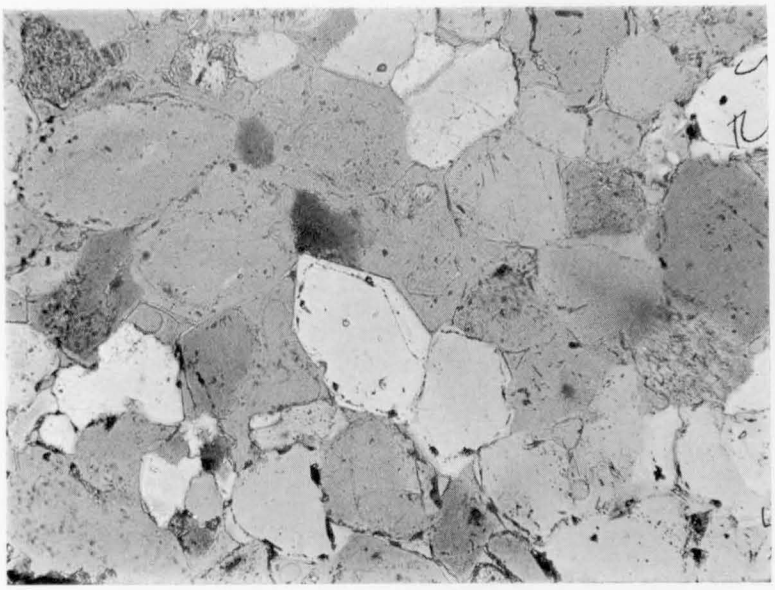

Plate 12, Figure 1. Mosaic of euhedral overgrown quartz grains. Cockatoo Formation, west of Burt Range (loc. 100-2). Crossed nicols, x 70

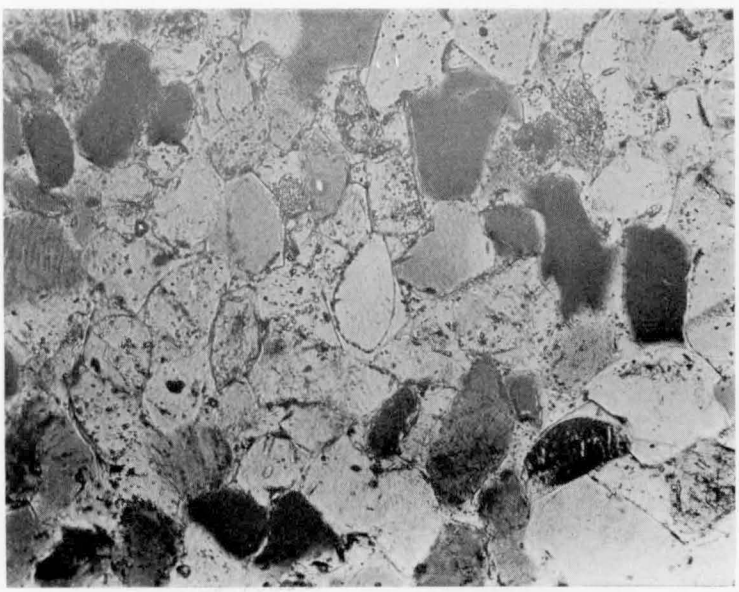

Plate 12, Figure 2. Mosaic of euhedral overgrown quartz grains, and a single feldspar nucleus (cloudy, bottom right-hand corner) with a clear faceted overgrowth. Hargreaves Member, Hargreaves Hills (loc. 431-1). Crossed nicols, x 70

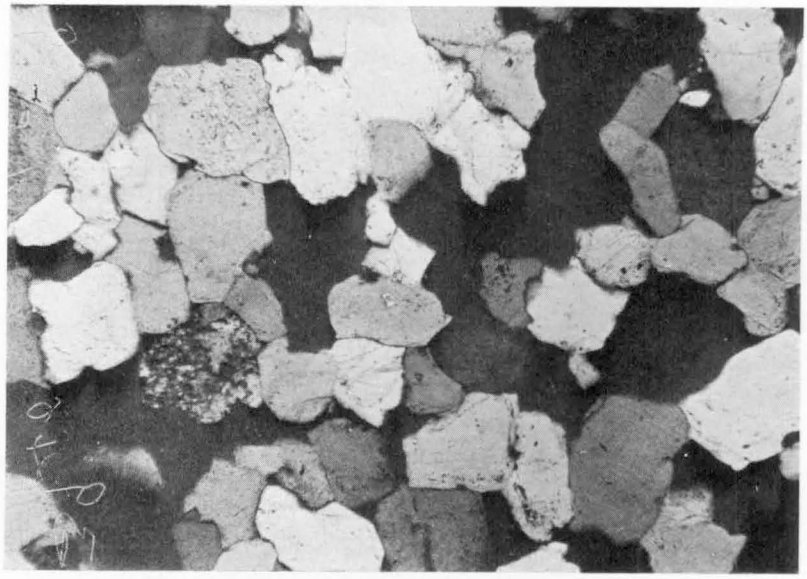

Plate 13, Figure 1. Mosaic of overgrown quartz grains in a firmly cemented sandstone. Cockatoo Formation, west of Elephant Hill (loc. 40-2A). Crossed nicols, x 35

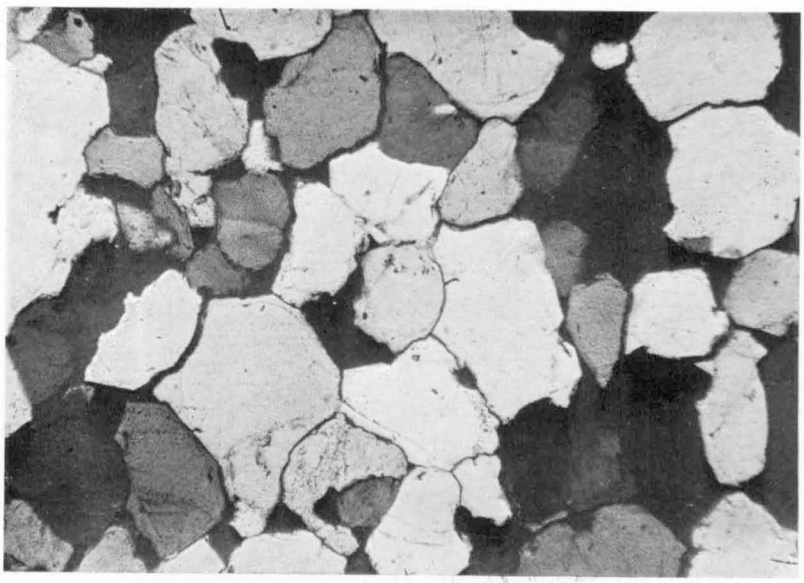

Plate 13, Figure 2. Crumbly sandstone from the same bed as in Figure 1. Weak sutures between grains have opened during preparation of the slide. Locality 40-2B. Crossed nicols, x 35

Plate 14, Figure 2. Rounded pebbles of poorly sorted sandstone and sand grains of quartz, set in matrix of hematite. Border Creek Formation, Mount Septimus (loc. 104-22A). Crossed nicols, x 20

Plate 14, Figure 1. Rock fragments and quartz grains. Micaceous quartz siltstone (top and bottom) and vein quartz (middle left). Kellys Knob Member, Matheson Ridge (loc. 28-7). Crossed nicols, x 20

Plate 15, Figure 2. Grains of quartz, microcrystalline quartz, feldspar, and biotite, cemented by overgrowth quartz. Cecil Member, Kununurra (loc. 415-3). Crossed nicols, x 20

Plate 15, Figure 1. Granules of quartz, quartz sandstone, and microcrystalline quartz, and sand grains of quartz set in a matrix of hematite. Border Creek Formation, Mt Septimus (loc. 104-22A). Crossed nicols, x 20

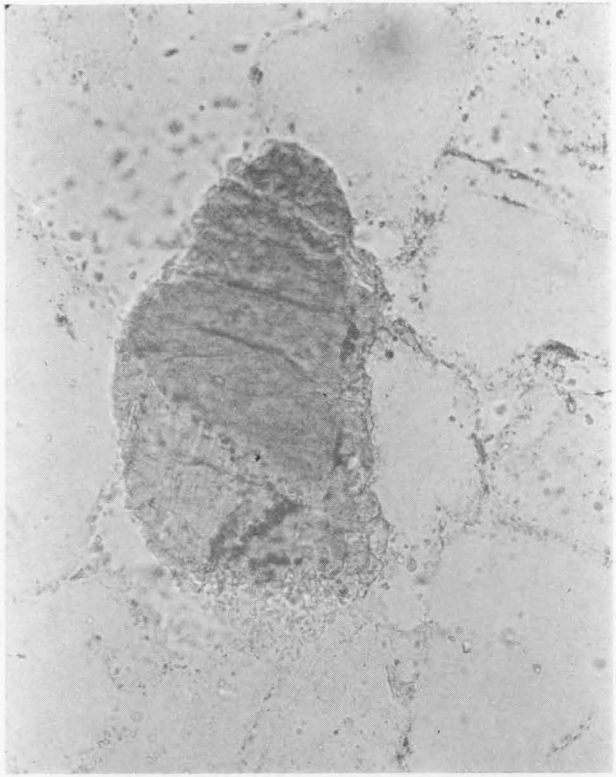

Plate 16, Figure 2. Grain of tourmaline with overgrowth in quartz sandstone. Kellys Knob Member, Matheson Ridge (loc. 58-3). Crossed nicols, x 170

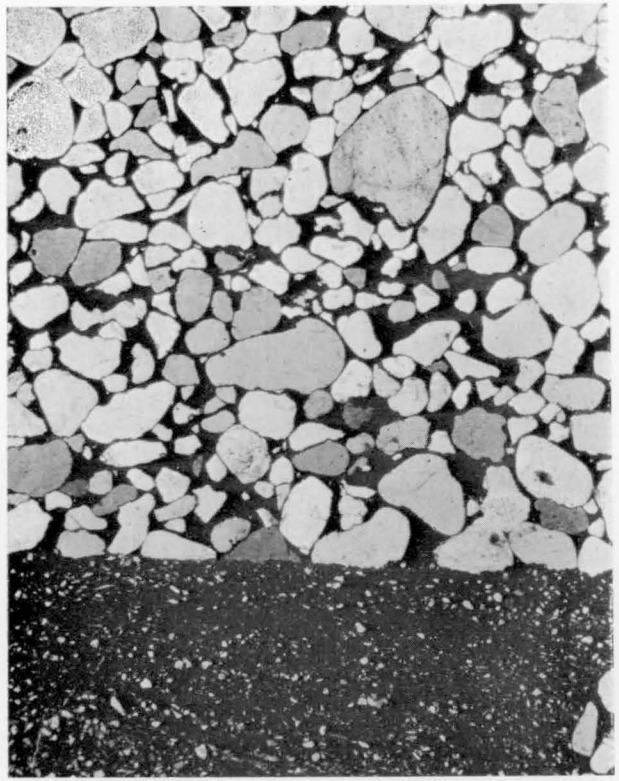

Plate 16, Figure 1. Quartz sand grains without overgrowths embedded in a matrix of hematite. Ragged Range Member, Policeman Waterhole (loc. 70-2). Crossed nicols, x 20

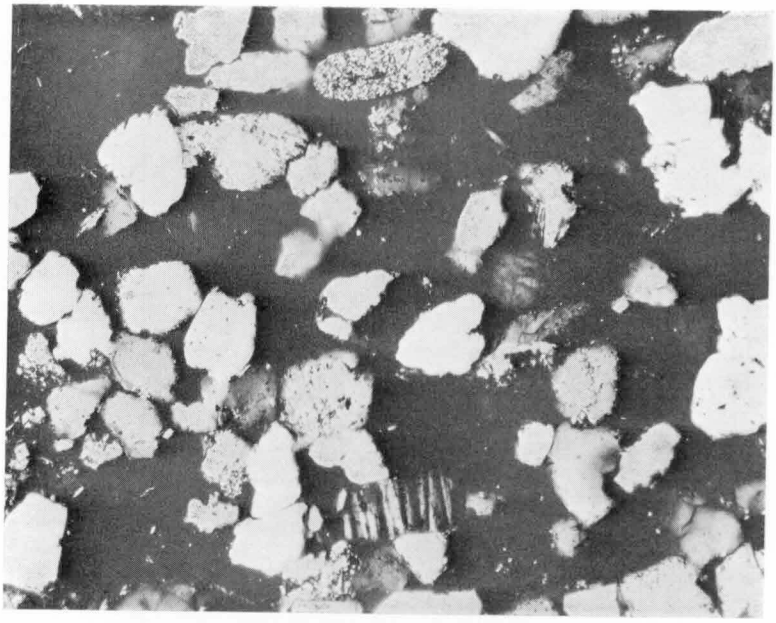

Plate 17, Figure 1. Feldspar (left) and glauconite (right) in quartz sandstone. Hargreaves Member, Hargreaves Hills (loc. 437-3). Crossed nicols, x 90

Plate 17, Figure 2. Possible spring pit near base of Point Spring Sandstone in section 435, 5 miles northeast of Point Spring

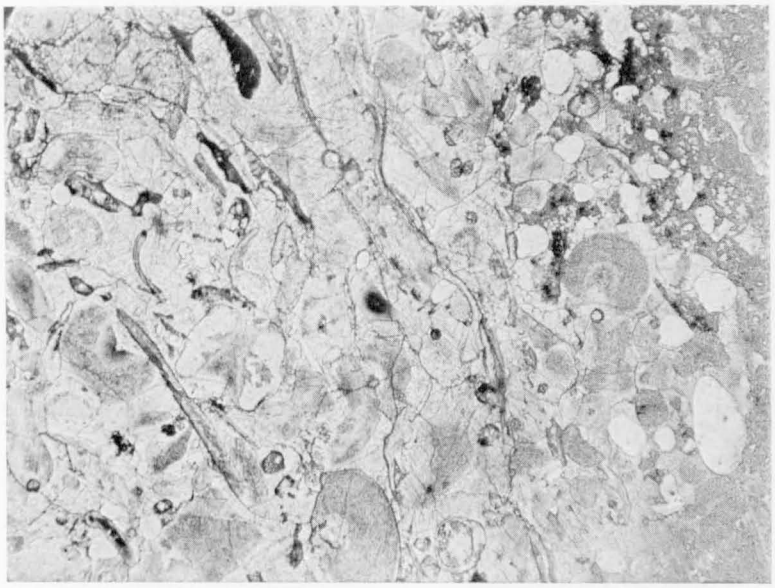

Plate 18, Figure 1. Crinoid ossicles (columnals) with circular central cavity (lumen) and fine microstructure, with clear overgrowth calcite. Totally clear grains are quartz. Septimus Limestone, Mount Septimus. x 20

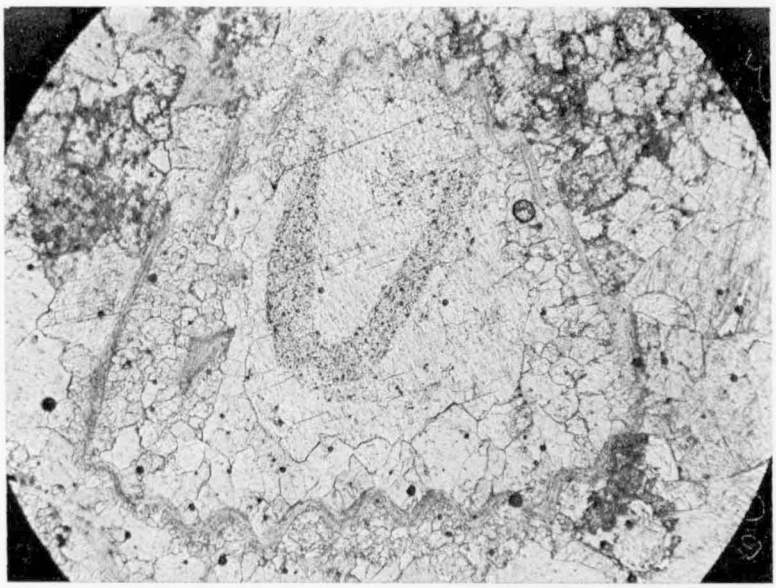

Plate 18, Figure 2. Cross-section of brachiopod shell with cavity filled with crinoid ossicle and secondary calcite. Septimus Limestone, Mount Septimus (loc. 104-10-1). x 80

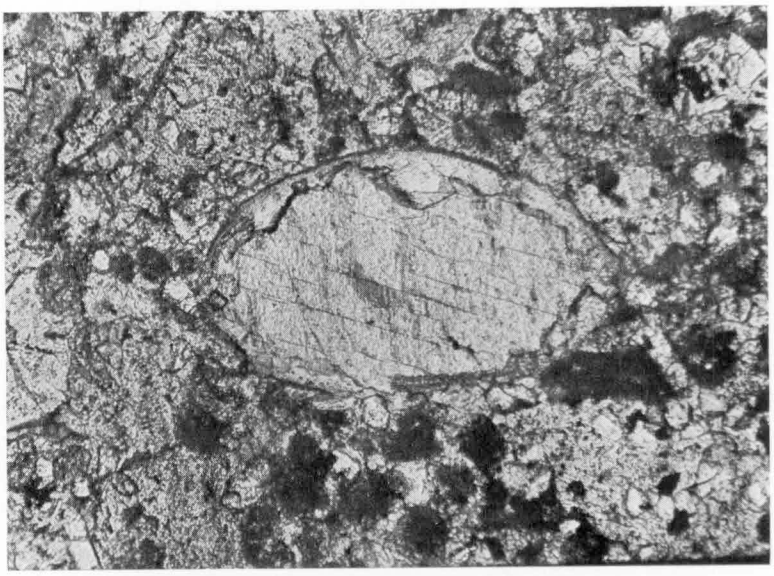

Plate 19, Figure 1. Ostracod shell filled with single crystal of calcite that has replaced part of shell wall. Burt Range Formation, type area (loc. 101-10-2). x 130

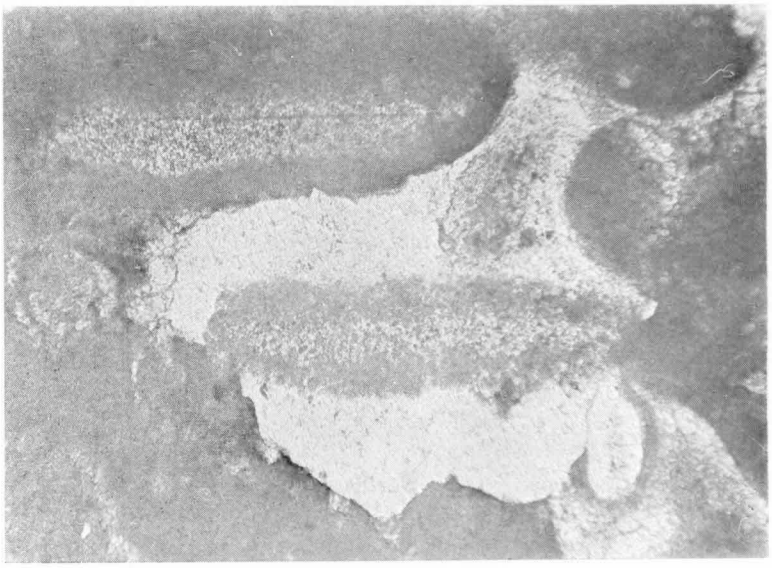

Plate 19, Figure 2. Degradation of crinoid ossicle to micrite. Ningbing Limestone, near Ningbing homestead (loc. 18-1). x 120

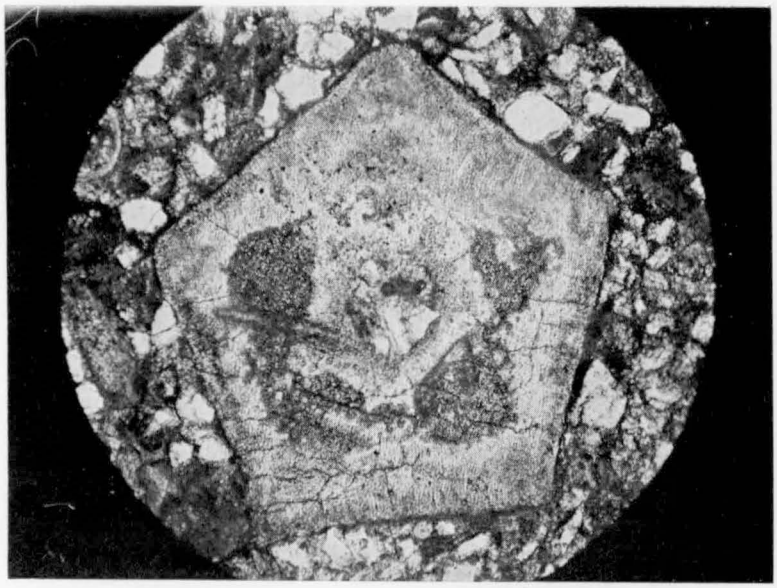

Plate 20, Figure 1. Almost entirely silicified crinoid ossicle, with microstructure preserved. Septimus Limestone, Mount Septimus (loc. 104-2). x 60

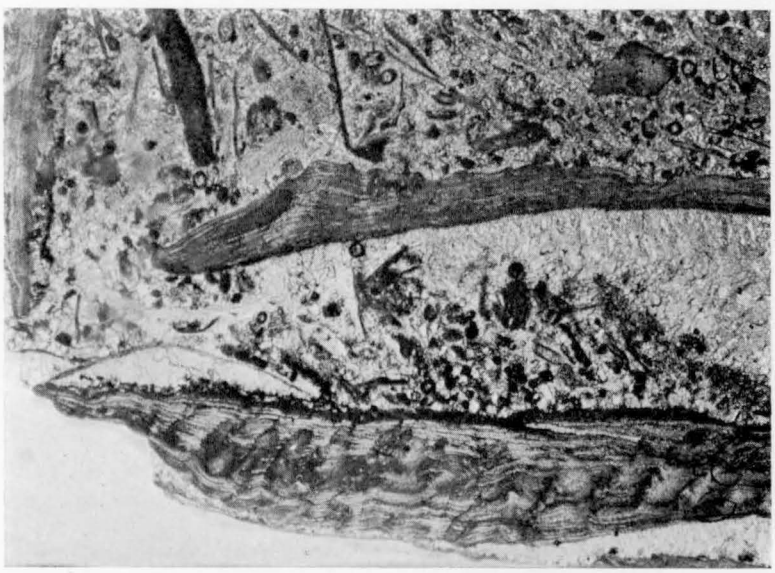

Plate 20, Figure 2. Section through open valves of a finely fibrous pseudopunctate brachiopod shell with cavity filled with sediment, mainly micrite lumps, below and drusy mosaic above, forming a geopetal structure. Note the same situation at a smaller scale beneath the canopy of an unidentified shell on the left-hand side of the lower valve of the brachiopod. Burt Range Formation, type area (loc. 100-13-1). x 20

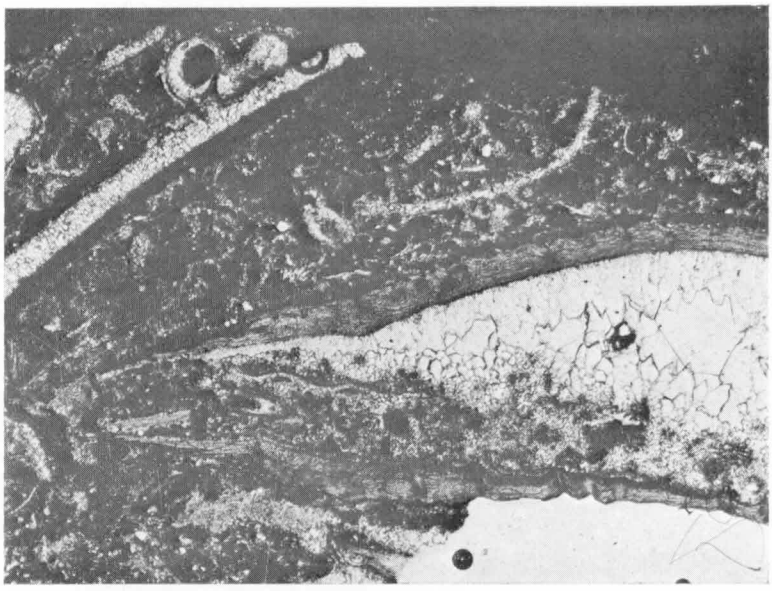

Plate 21, Figure 1. Another view of slide shown in Plate 20, figure 2, showing more clearly the structure of the drusy mosaic. x 20

Plate 21, Figure 2. Geopetal structure of brachiopod spiralia trapping fine sediment, with drusy mosaic above. Buttons Beds in type area (loc. 105-735-3). x 95

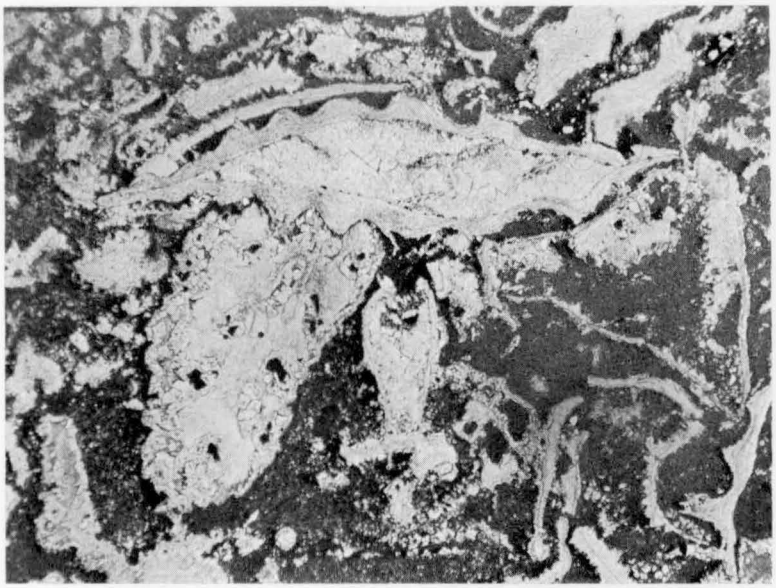

Plate 22, Figure 1. Brachiopod with cavity filled with drusy mosaic, and corals with dolorhomb replacement around internal pores and periphery. Westwood Member, type area (loc. 12-2A-1-2). x 10

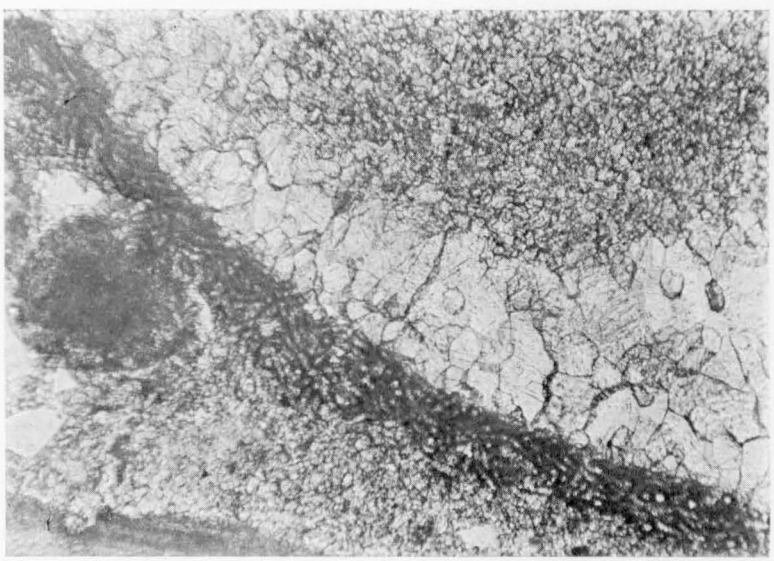

Plate 22, Figure 2. Boring blue-green alga *(Girvanella)* on surface of a recrystallized spiriferid brachiopod shell. Matrix and brachiopod infilling consists of calcisilt. Burt Range Formation, type area (loc. 101-13-3). x 130

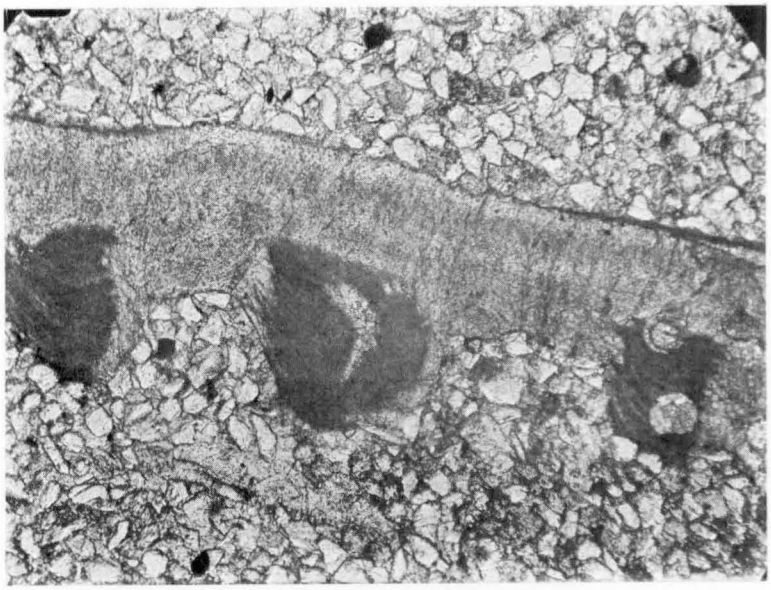

Plate 23, Figure 1. Almost entirely recrystallized brachiopod shell in quartzose limestone. Only parts of the costae have their original microstructure, wisps of which extend into the recrystallized part of the shell. Burt Range Formation, type area (loc. 101-20-1). x 90

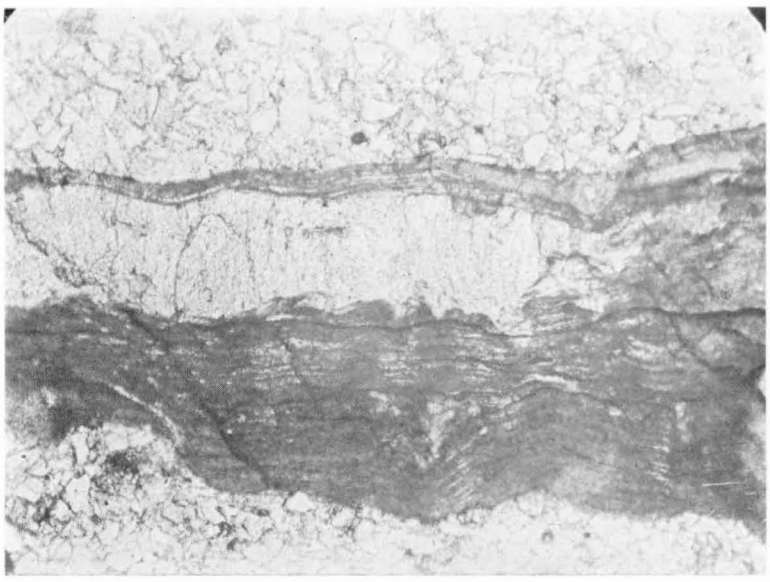

Plate 23, Figure 2. Another view of slide shown in Figure 1. The structure of the replacing calcite is that of drusy mosaic. x 90

Plate 24, Figure 1. Partly recrystallized brachiopod shell, with a wispy contact between original and replacing calcite. Again, the replacing calcite has the structure of drusy mosaic. The circles are cross-sections of productid brachiopod spines. Burt Range Formation, type area (loc. 101-13-4). x 100

Plate 24, Figure 2. Partly recrystallized brachiopod valve, but with replacing granular calcite which has a sharp boundary against original shell. Note totally recrystallized upper valve of brachiopod, enclosing a geopetal structure with micrite lumps and quartz grains at bottom, and the ostracod shell, itself another geopetal structure. Note also micrite rim at bottom of recrystallized valve. Burt Range Formation, type area (loc. 101-11-2). x 100

Plate 25, Figure 1. View continuing to right from that shown in Plate 24, figure 2, showing vague boundary between original and replacing calcite. Note discontinuous rim of micrite. x 100.

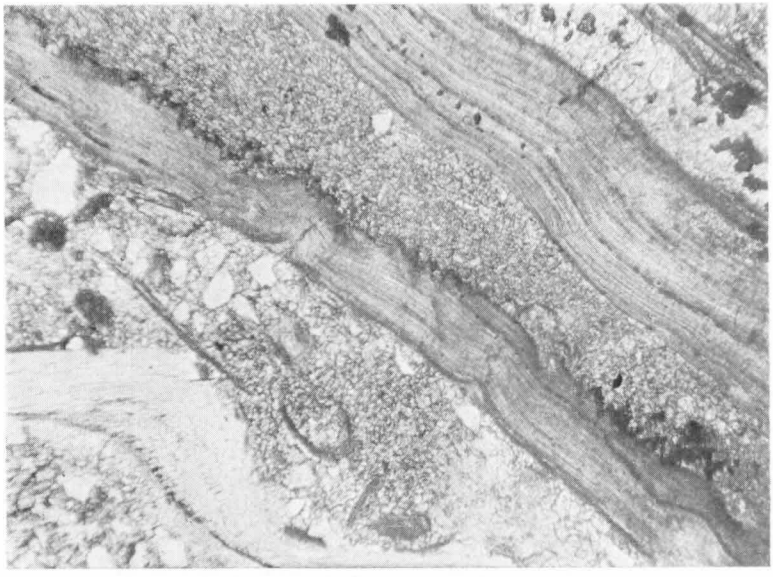

Plate 25, Figure 2. Microstylolite along most of length of inner part of lower brachiopod valve. Burt Range Formation, type area (loc. 101-13-1). x 100

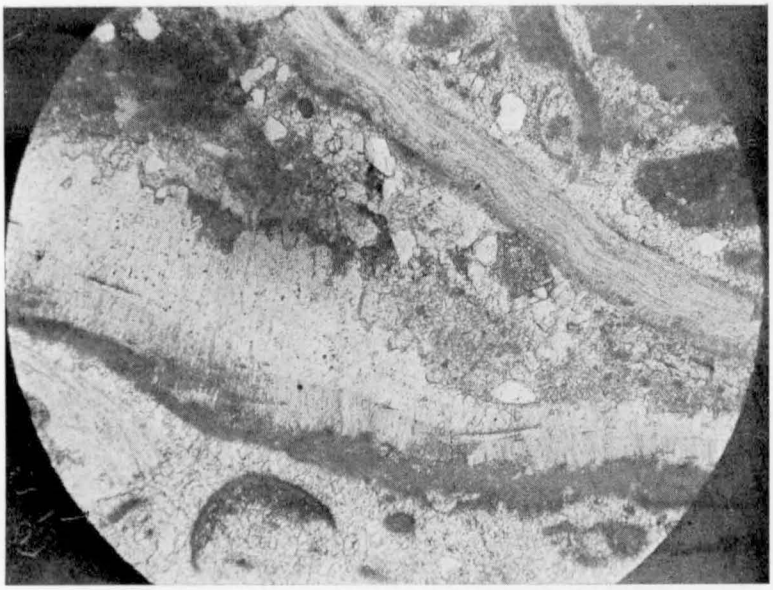

Plate 26, Figure 1. Microstylolite along interior of recrystallized lower valve of a brachiopod rimmed with micrite. The lower part of the recrystallized valve contains ghosts of the original microstructure. Westwood Member, type area (loc. 12-12A). x 70

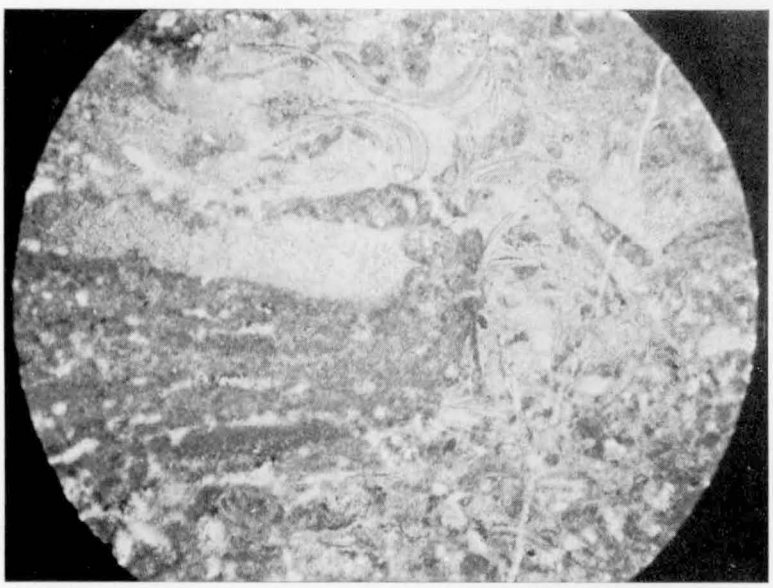

Plate 26, Figure 2. Grumose structure in micrite of stromatolite, granular calcite between micrite layers, and cross-sections of valves of the ostracod *Cryptophyllus* showing overlapping plates. Burt Range Formation, type area (loc. 100-9). x 30

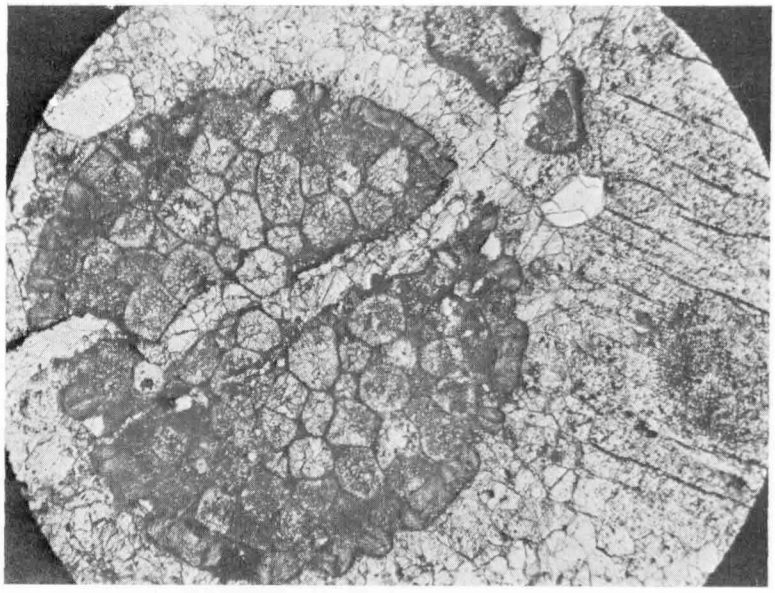

Plate 27, Figure 1. Cross-section of bryozoan, crossed by a calcite vein, and a crinoid ossicle (left-hand side). Septimus Limestone, type area (loc. 104-4-2). x 80

Plate 27, Figure 2. Mash of corals, crinoid ossicles, brachiopods, and quartz grains. The large grain near the centre is the coral *Syringopora*.. Burvill Beds, near Ningbing homestead (loc. 5-2). x 20

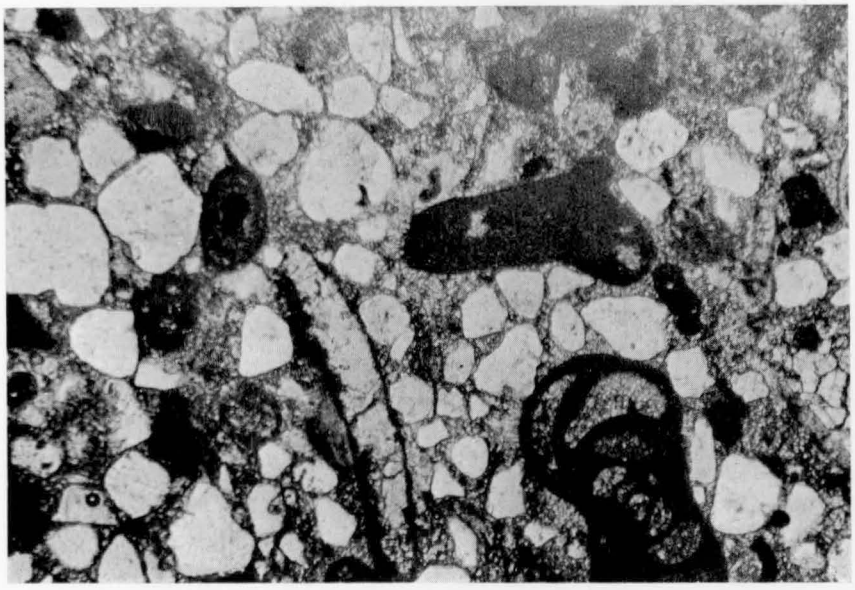

Plate 28, Figure 1. Endothyrid foraminifers in a quartzose limestone. Utting Calcarenite (loc. 107-5B). x 20

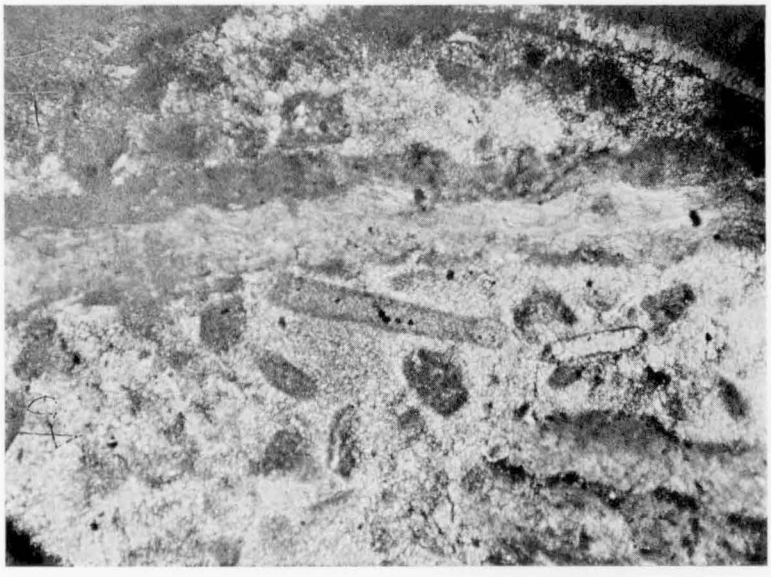

Plate 28, Figure 2. Partly recrystallized brachiopod with geopetal structure, overlying a hyperamminid foraminifer (tube with small bulbous tip). Burt Range Formation, type area (loc. 100-13-5). x 130

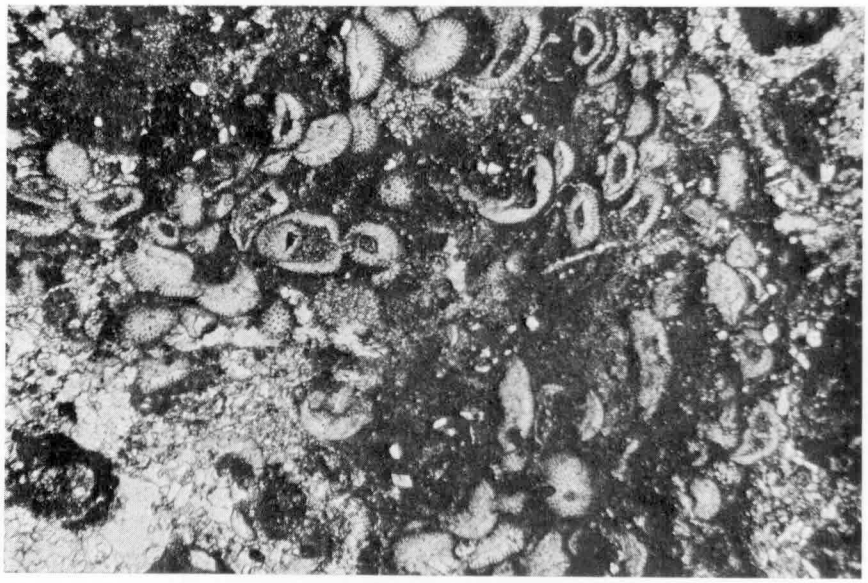

Plate 29, Figure 1. The encrusting foraminifer (?) *Wetheredella*. Ningbing Limestone (back-reef), Jeremiah Hills (loc. 447-12F4). x 20

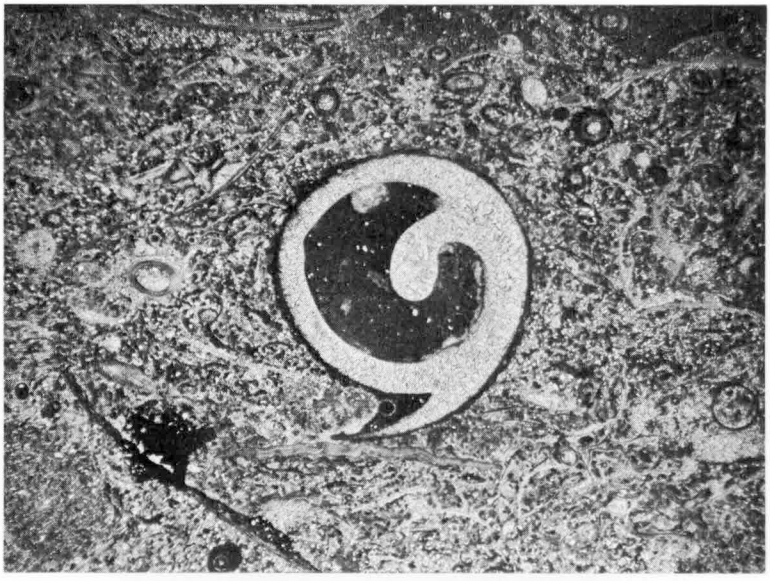

Plate 29, Figure 2. Cross-section of recrystallized gastropod rimmed and filled with micrite, in matrix of brachiopod debris cemented with sparry calcite. Westwood Member, type area (loc. 13-6). x 10

Plate 30, Figure 1. Red (solenopore) alga, probably *Parachaetetes*. Buttons Beds, type area (loc. 105-400A). x 30

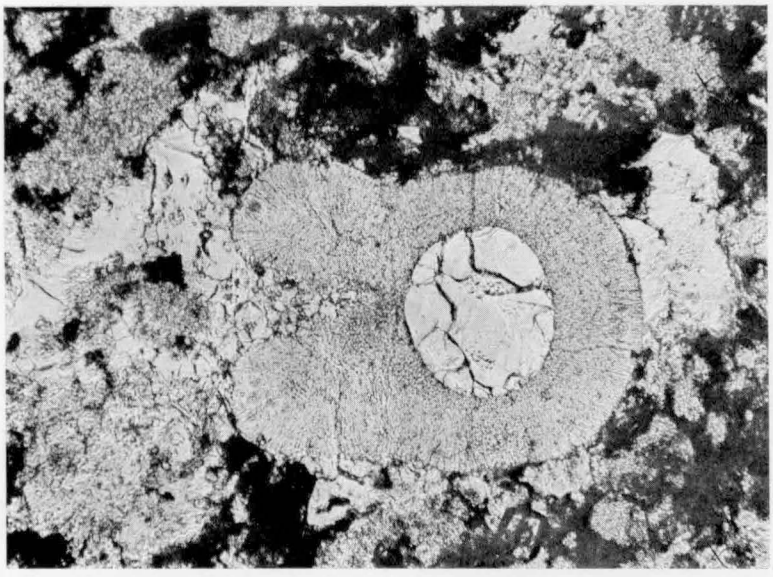

Plate 30, Figure 2. The alga (?) *Umbella*. Ningbing Limestone (back-reef), southwest Ningbing Range (loc. 21-20B). x 220

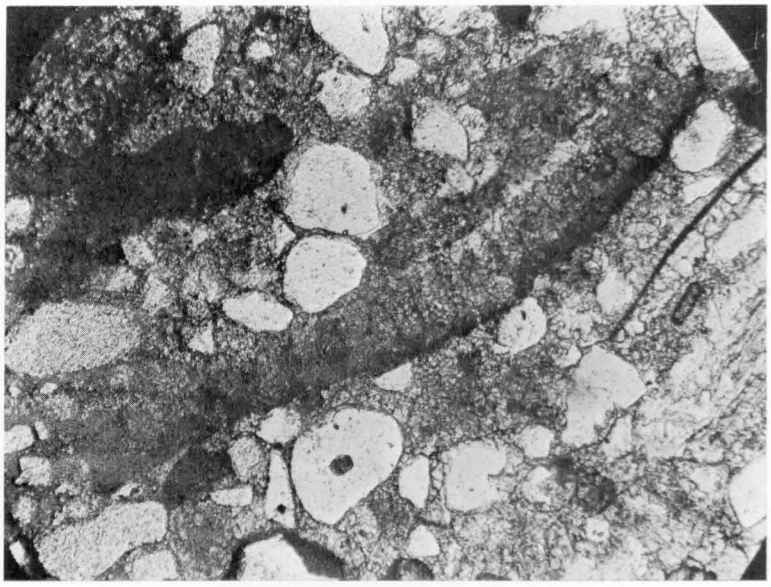

Plate 31, Figure 1. The alga (?) *Koninckopora* in a quartzose limestone. Utting Calcarenite, near Utting Gap (loc. 107-5B). x 90

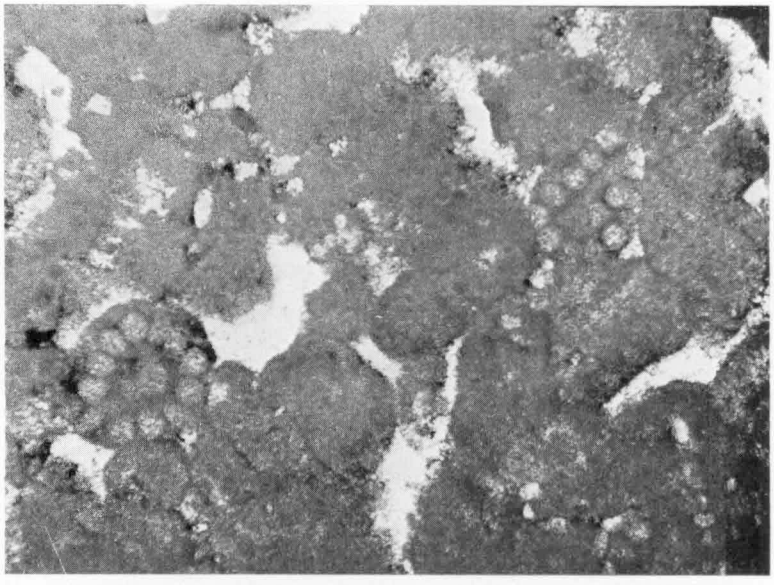

Plate 31, Figure 2. Problematical bodies, possibly the dasycladacean alga *Atractyliopsis,* in a birdseye limestone. Ningbing Limestone (back-reef), southwest Ningbing Range (loc. 21-16D). x 100

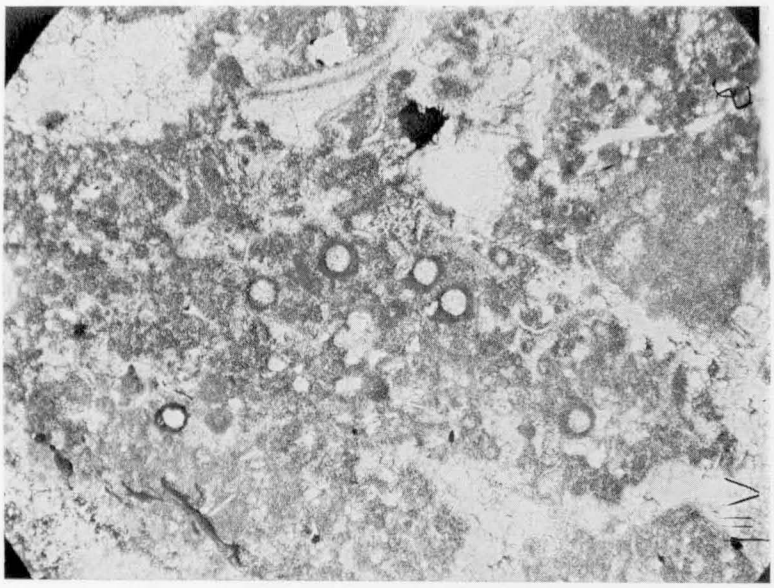

Plate 32, Figure 1. Problematical algal fragments, possibly of the bodies shown in plate 31, figure 2 in lump limestone. Ningbing Limestone (back-reef), southwest Ningbing Range (loc. 21-23D). x 90

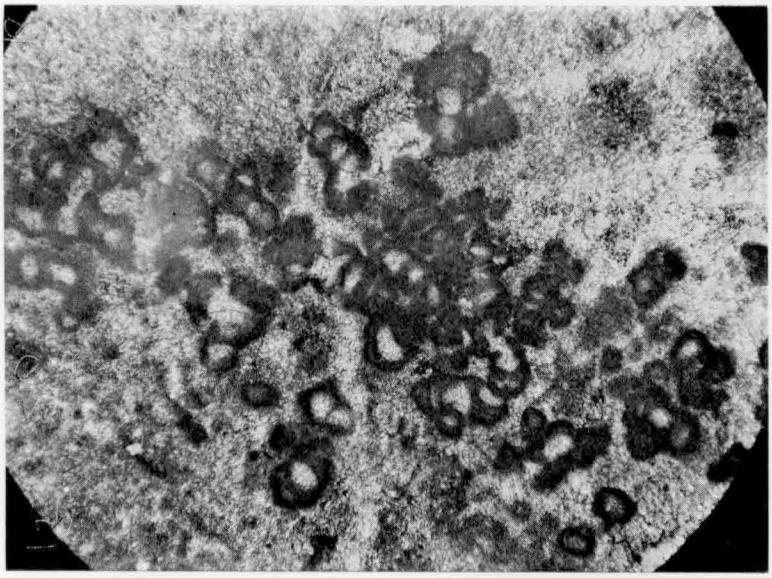

Plate 32, Figure 2. The schizophyte alga *Renalcis*. Westwood Member type area (loc. 12-3). x 90

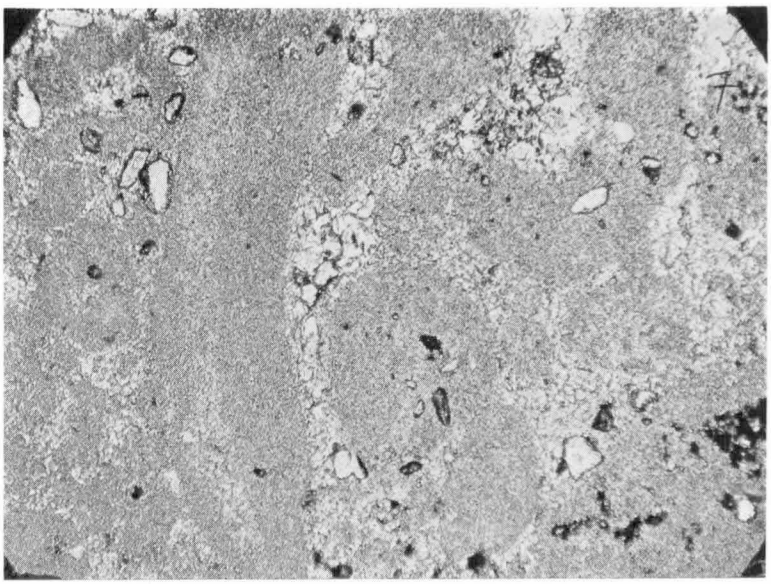

Plate 33, Figure 1. Micrite lumps cemented by sparry calcite. Ningbing Limestone (back-reef), southwest Ningbing Range (loc. 21-16E). x 90

Plate 33, Figure 2. Dolorhombs preferentially replacing micrite in a lump limestone. Jeremiah Member, Jeremiah Hills (loc. 442-12). x 20

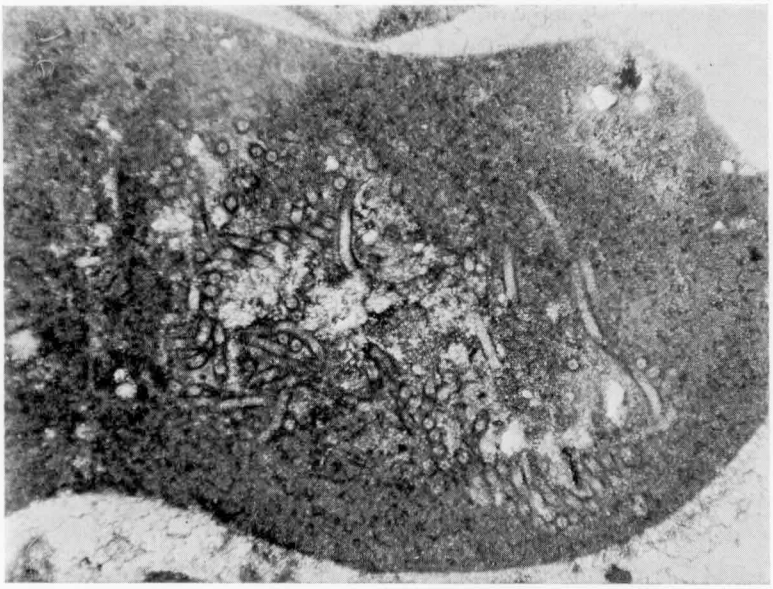

Plate 34, Figure 1. Lump of algal micrite riddled with filaments of the blue-green alga *Girvanella*. Ningbing Limestone (back-reef), Jeremiah Hills (loc. 88-8A). x 95

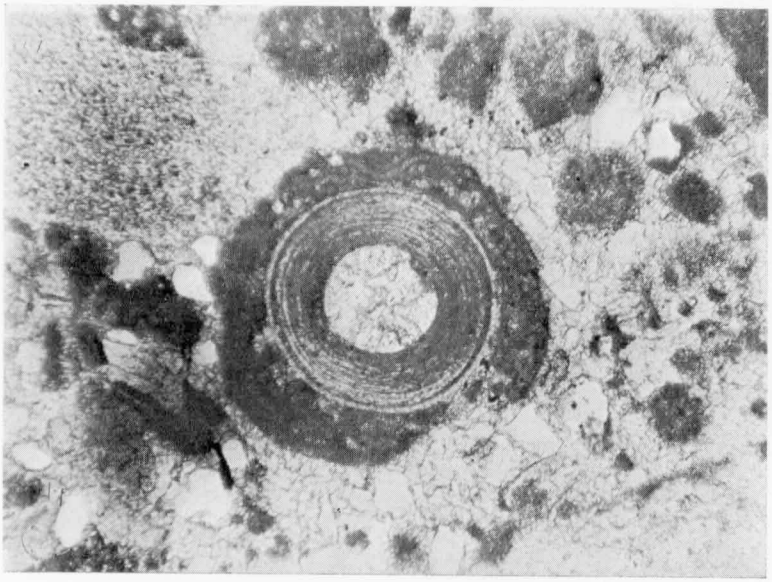

Plate 34, Figure 2. Brachiopod spine coated by algal micrite. Westwood Member, type area (loc. 12-2A). x 130

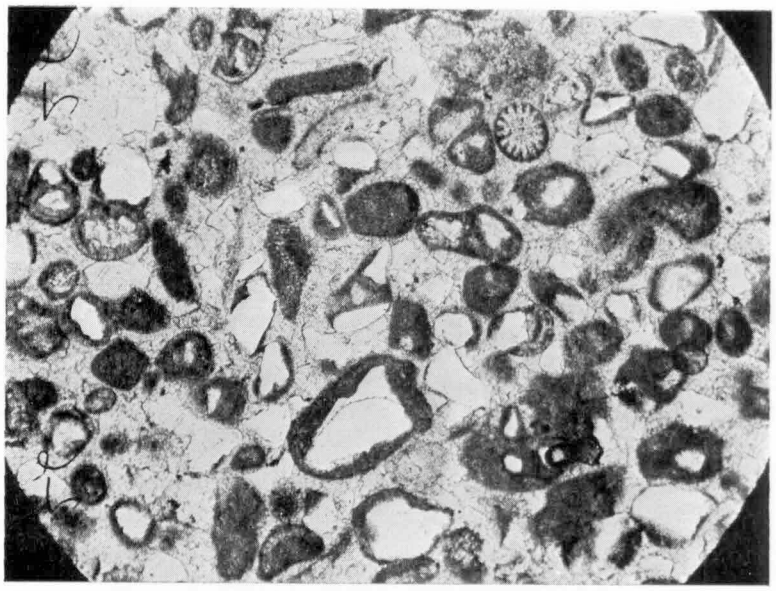

Plate 35, Figure 1. Grains, mainly quartz, coated with structureless micrite. Burt Range Formation, type area (loc. 100-10a). x 30

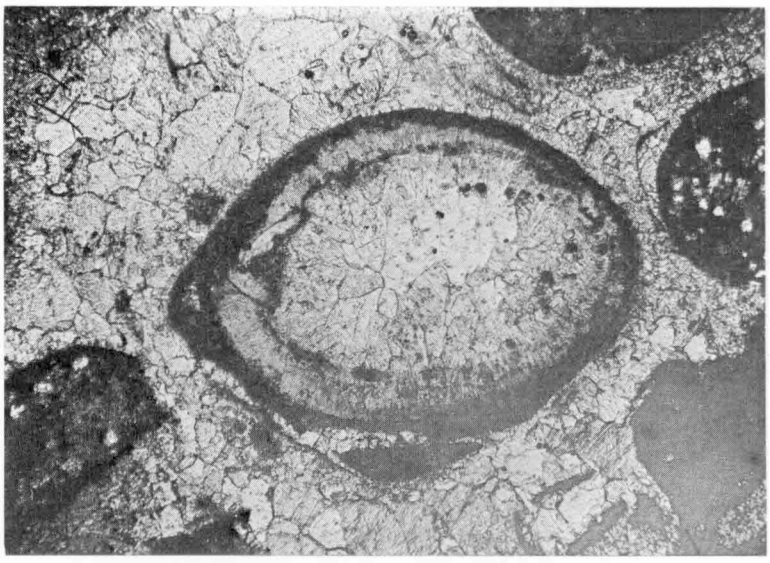

Plate 35, Figure 2. Recrystallized ostracod shell filled with drusy mosaic and rimmed with micrite in a calcarenite cemented by granular calcite. Ningbing Limestone, Jeremiah Hills (loc. 88-8A). x 60

Plate 36, Figure 1. Oncolith of algal micrite *(Girvanella)* **in crudely overlapping skins on nucleus of unidentified shell. Burt Range Formation, type area (loc. 100-6). x 80**

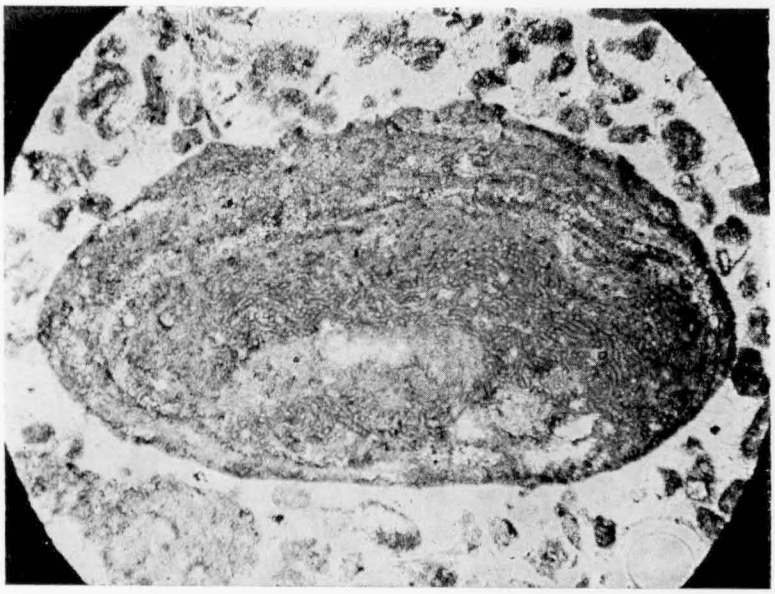

Plate 36, Figure 2. Oncolith of algal micrite *(Girvanella)*. **Ningbing Limestone (back-reef), southwest Ningbing Range (loc. 21-20). x 70**

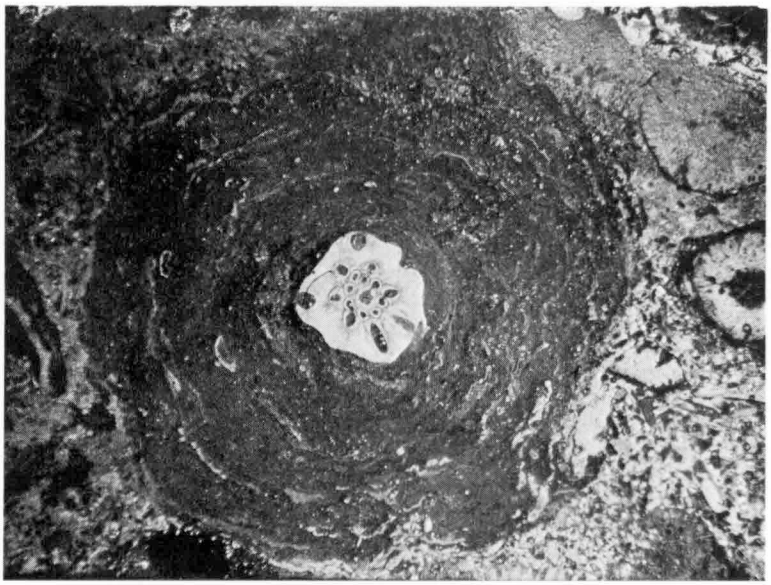

Plate 37, Figure 1. Oncolith of *Sphaerocodium* in micrite, on a nucleus of a crinoid ossicle. Westwood Member, type area (loc. 12-2A). x 12

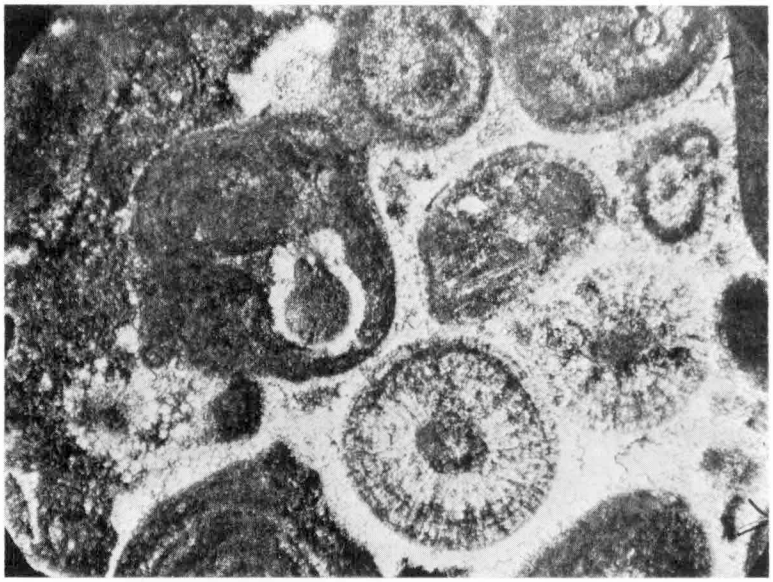

Plate 37, Figure 2. Ooliths and oncoliths (one a composite one incorporating an *Umbella*) cemented by granular calcite. Ningbing Limestone (back-reef), southwest Ningbing Range (loc. 21-21). x 90

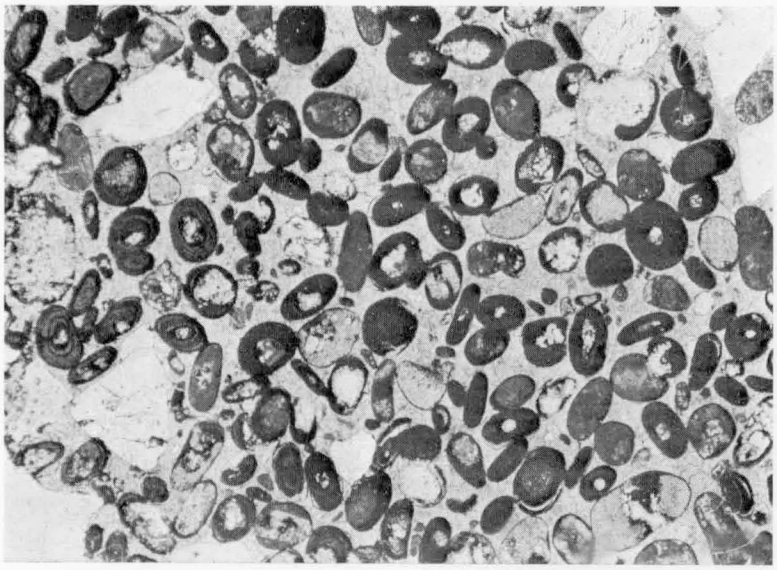

Plate 38, Figure 1. Ferruginous ooliths and large quartz grains cemented by granular calcite. Burvill Beds, Milligans Hills (loc. 301C). x 10

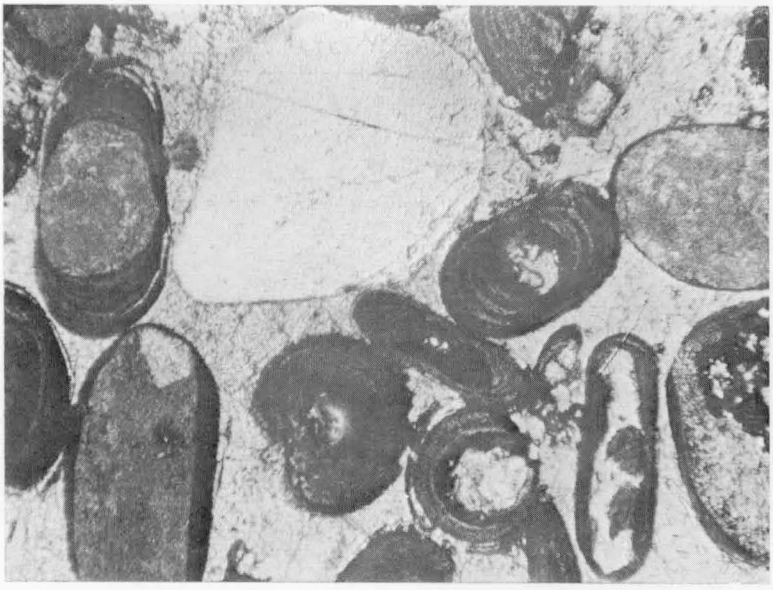

Plate 38, Figure 2. Enlarged view of ferruginous ooliths in Figure 1. x 100

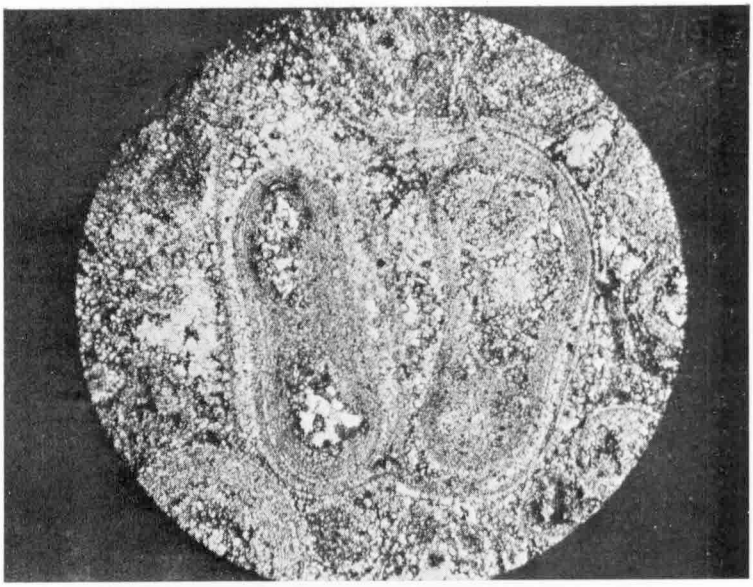

Plate 39, Figure 1. Dolomitized composite oolith. Ningbing Limestone (back-reef), southwest Ningbing Range (loc. 21-15F). x 55

Plate 39, Figure 2. Zoned dolorhombs and quartz grains. Septimus Limestone, type area (loc. 104-13A). x 130

Plate 40, Figure 1. Ostracod involved in recrystallization of micrite to calcisilt. The upper part of the ostracod, above the calcisilt, is virtually unaffected by recrystallization. Burt Range Formation, type area (loc. 100-6). x 100

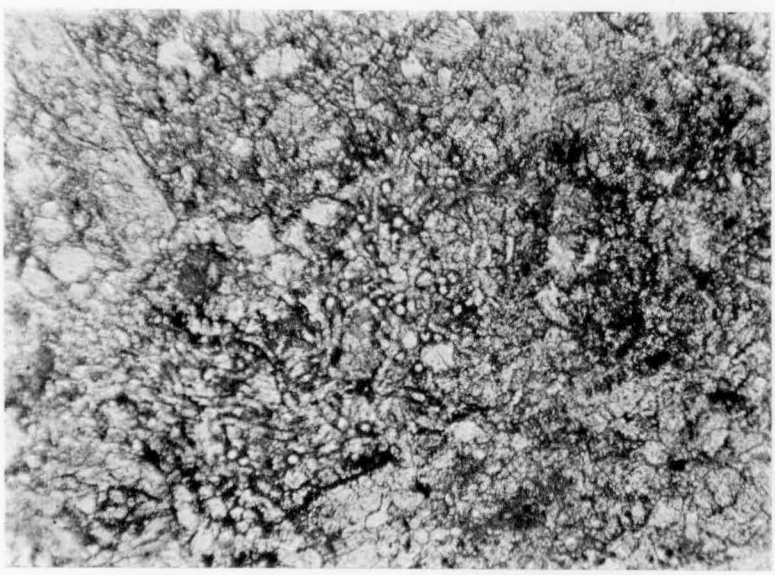

Plate 40, Figure 2. Collapse of *Girvanella* filaments to form calcisilt. Burt Range Formation, type area (loc. 101-21)

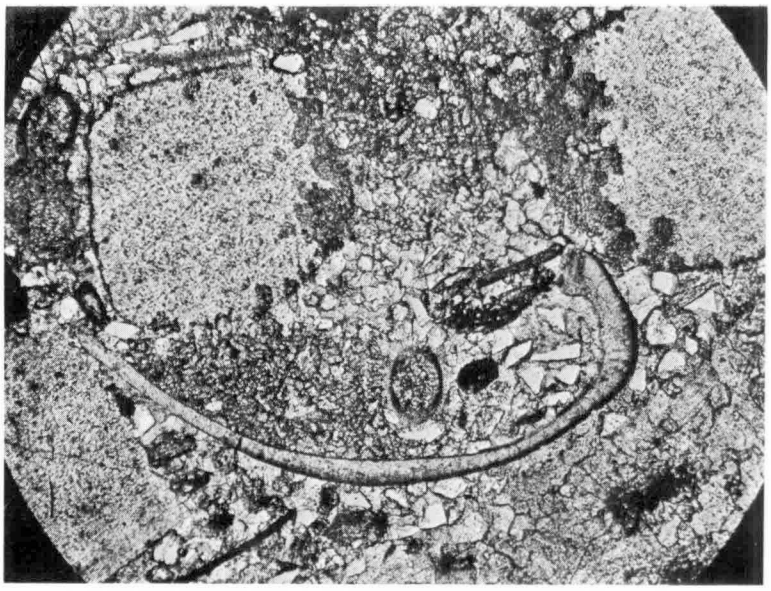

Plate 41, Figure 1. Degradation of edges of crinoid ossicles to calcisilt. Note calcisilt also at left bottom of micrite-rimmed ostracod valve. Burt Range Formation, type area (loc. 101-16). x 75

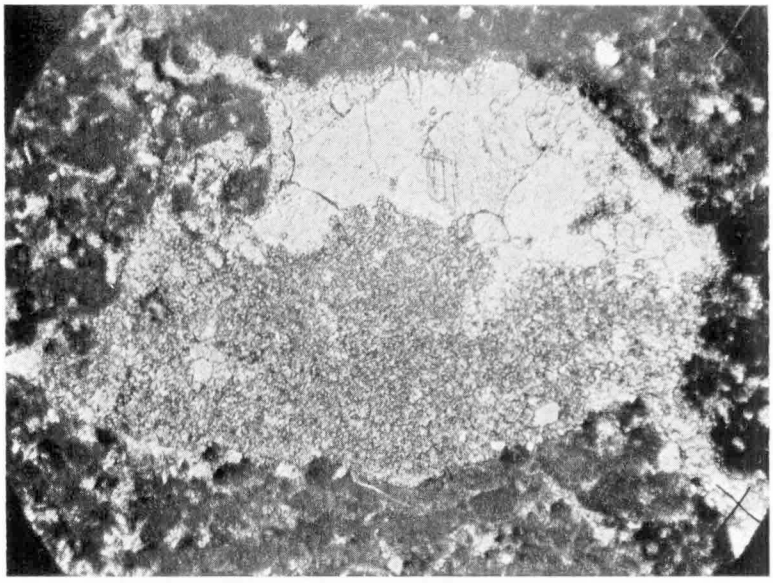

Plate 41, Figure 2. Birdseye of calcisilt below and drusy mosaic above in lump limestone. Ningbing Limestone (back-reef), southwest Ningbing Range (loc. 21-23D)

Plate 42, Figure 1. *Stromatactis* **in Ningbing Limestone (reef). Ningbing Range (loc. 454). The scale is 6 inches long.**

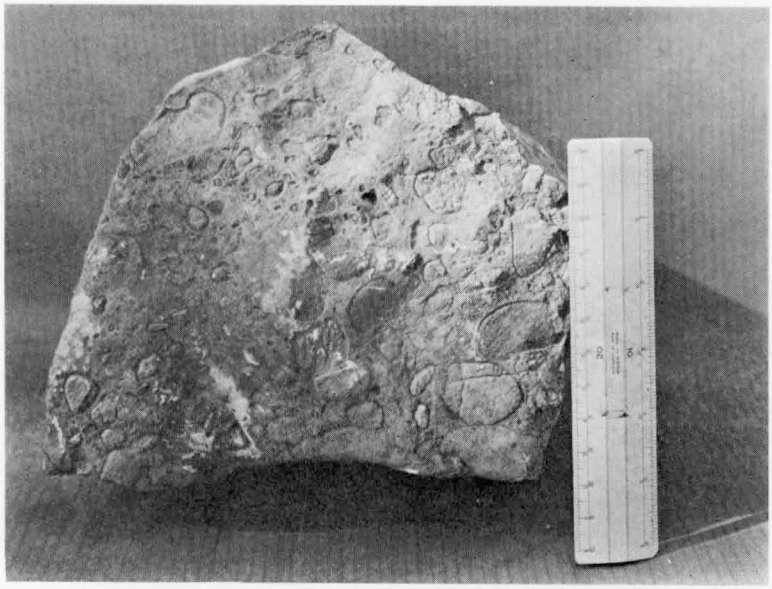

Plate 42, Figure 2. Limestone conglomerate. Ningbing Limestone (fore-reef), Ningbing Range (loc. 17-4)

CONSTITUENTS

The carbonate rocks studied consist of various combinations of the following thirty modal constituents:

Carbonate Grains

Skeletal invertebrates

Crinoid ossicle
Crinoid ossicle, silicified
Brachiopod
Ostracod
Bryozoan or coral
Foraminiferan
Gastropod
Unidentified shell

Algae

Red alga
Umbella
Renalcis
Calcisphere

Grains deposited through algal activity

Micrite lump
Micrite lump dolomite
Algal micrite
Coated grain
Oncolith
Oolith, calcite
Oolith, dolomite
Grapestone

Terrigenous Grains

Quartz
Feldspar
Rock fragments

Matrix

Microspar or calcisilt

Cement

Granular calcite

Fillings

Drusy mosaic
Birdseye
Dolomite infillings

Diagenetic Minerals

Glauconite
Undifferentiated dolomite

Skeletal Invertebrates

Crinoid Ossicles. Disarticulated and broken crinoidal debris is the dominant constituent of many limestones. Parts of the column (columnals, pinnules) are the commonest recognizable ossicles; ossicles from the crinoid crown were found at only one locality. Entire articulated crinoids are unknown.

The ossicles are 2 cm or less across, and are easily recognized in thin section because they consist of single large calcite crystals penetrated by a distinctive internal network. Most ossicles are rimmed by optically continuous overgrowth calcite, which is commonly marked off from the ossicle by a film of impurities or by lack of internal structure; where there are no impurities, or where the ossicle itself lacks internal structure, the distinction cannot be made. A mosaic of overgrown crinoid ossicles in an orthomarble (Pettijohn, 1957, p. 652) is shown in Plate 18, figure 1. The characteristic internal structure is shown by the ossicle lodged in the cavity of a brachiopod (Pl. 18, fig. 2). Also in the cavity of a fossil, the single calcite crystal shown in Plate 19, figure 1 simulates a crinoid ossicle but lacks internal structure, and for reasons of space must have grown inorganically in situ.

Parts of some ossicles are degraded to micrite and calcisilt (Pl. 19, fig. 2). In contradistinction to Banner & Woods' (1964, p. 27) observations in Tertiary limestones, the crinoid ossicles of the Bonaparte specimens are one of the last types of calcite grains in dolomitic limestone to be dolomitized. They are, however, preferentially silicified.

Silicified Crinoid Ossicles. The pentagonal ossicle shown in Plate 20, figure 1 is almost completely replaced by silica. The replacement is preferential as the sparry calcite cement of the rock is unaffected.

Brachiopods, like crinoid ossicles, are abundant constituents of many limestones. Well preserved brachiopod material is readily identified by its finely fibrous structure (Pl. 20, fig. 2). With their large cavities, brachiopod shells are excellent geopetal structures (Pl. 21, fig. 1), sediment lodging in the bottom and drusy mosaic filling the top. The spiralia of spiriferid brachiopods (Pl. 21, fig. 2) may act as sets of baffles that catch sediment. Many brachiopod shells lack sediments and are filled with drusy mosaic (Pl. 22, fig. 1). Brachiopods seem to be the favourite material for boring by blue-green algae (Pl. 22, fig. 2).

Parts of some brachiopods are recrystallized. Plate 23, figures 1 and 2 and Plate 24, figure 1 show originally finely fibrous calcite passing into coarsely fibrous calcite, with 'rafts' of unaltered material floating in the recrystallized calcite (Pl. 23, fig. 2). Another kind of recrystallized calcite is shown in Plate 24, figure 2 and Plate 25, figure 1. What is surprising in these last two figures is the sharp contrast between the original and the recrystallized structure. Stylolites may develop at the edge of a brachiopod valve (Pl. 25, fig. 2) and in the specimen shown in Plate 26, figure 1, the stylolite develops at the edge of a valve partly recrystallized as coarsely fibrous calcite.

Ostracods appear in thin section as oval bodies with a thin shell commonly of recrystallized calcite, and with a cavity generally filled with sparry calcite (Pl. 19, fig. 1). Occasional shells contain sediment and drusy mosaic (Pl. 24, fig. 2) and are thus useful as geopetal structures. Disarticulated valves are uncommon, except of *Cryptophyllus* (Pl. 26, fig. 2), an eridostracan (Jones, 1962, 1968). *Cryptophyllus* is distinguished by a well preserved wall structure of overlapping plates.

Bryozoans seen in thin section are compact zoaria with zooecia filled with sparry calcite (Pl. 27, fig. 1).

Few *corals* were seen in thin section; the commonest coral is the tabulate colonial *Syringopora* (Pl. 27, fig. 2).

Foraminiferans. Endothyrids (Pl. 28, fig. 1) are the commonest group recognized in thin section. Hyperamminids (Pl. 28, fig. 2) and the encrusting *Wetheredella* (Pl. 29, fig. 1) are locally common.

Gastropods are invariably recrystallized. The one shown in Plate 29, figure 2 was probably first enclosed in a micrite envelope, then the shell was dissolved, and the cavity later filled with sparry calcite by the process described by Bathurst (1966).

Unidentified shelly material consists of shell fragments whose form and structure are too poorly preserved to be identified.

Algae

Red (solenopore) algae have a distinctively fine structure (Pl. 30, fig. 1). Except in or near the reef itself or in a few localities in the lagoonal Buttons Beds, the solenopore algae are abraded fragments. Other calcareous algae are problematical.

Umbella (Pl. 30, fig. 2) is one of these. As *Umbellina* Loeblich & Tappan, 1964, it is classified as a foraminiferan; and as *Umbella* Maslov, 1955, it is regarded by the Russians Poyarkov (1966), Reitlinger (1966), and Maslov (1966) as a charophyte alga, and this interpretation is followed here.

Koninckopora, first described by Lee (1912) as a bryozoan, was later assigned to the dasycladacean algae by Wood (1943). The specimen shown in Plate 31, figure 1, is tentatively identified as *Koninckopora.*

More problematical still are the bodies shown in Plate 31, figure 2, which probably disintegrate into the fragments shown in Plate 32, figure 1. These forms are possibly the dasycladacean *Atractyliopsis* Pia, 1937. These and the other problematical algae will be described in detail in my forthcoming paper on Upper Devonian and Lower Carboniferous calcareous algae from the Bonaparte Gulf Basin.*

Renalcis. The systematic position of *Renalcis* (Pl. 32, fig. 2) among the algae is also uncertain (Wray, 1967, pp. 44-5), and I follow Wray in regarding it as a schizophyte (blue-green) alga. *Renalcis* is a ubiquitous component of the reef limestone of the Ningbing Limestone and it occurs also in the reefal limestone of the Westwood Member.

* In *Bur. Miner. Resour. Aust. Bull.* 116, Palaeontological Papers 1968, in press.

Grains Deposited Through Algal Activity

The grains described under this heading consist of micrite deposited chiefly through the activity of porostrome algae.

Micrite Lumps (Pl. 33, fig. 1). This name refers to 'irregular well-cemented forms that show no outstanding feature to label them' (Thomas, 1962). Micrite lumps have a wide range in diameter up to 5 cm. with a mode at about 1 mm. Lumps are the most abundant type of grain in the limestones studied.

Micrite Lump Dolomite. Dolorhombs preferentially replace lumps in some specimens (Pl. 33, fig. 2).

Algal Micrite. Micrite enclosing threads of porostrome algae, such as *Girvanella* (Pl. 34, fig. 1), is another abundant constituent. Probably many if not most of the micrite lumps were originaly algal micrite from which all traces of threads were subsequently lost. The environment equally favoured porostrome algae regardless of whether the micrite was deposited on mats of sticky porostrome algae or the micrite lumps were bored by algae after deposition.

Coated Grains. Coats of algal micrite (Pl. 34, fig. 2) and structureless micrite (Pl. 35, fig. 1) on grains are locally common. The original outline of recrystallized skeletons would be lost but for this micrite coat (Pl. 35, fig. 2), as observed in Recent limestone by Bathurst (1966).

Oncoliths or algal balls (Pl. 36, fig. 1) consist of concentric shells of micrite around porostrome algae, such as *Girvanella* (Pl. 36, figs 1, 2) or *Sphaerocodium* (Pl. 37, fig. 1). The nucleus is frequently a shell or algal grain such as the unidentified shell in Plate 36, figure 1 or the echinoderm ossicle in Plate 37, figure 1. With decreasing size, the oncoliths merge into ooliths.

Ooliths. The common association of ooliths (Pl. 37, fig. 2) with oncoliths and other bodies of algal origin suggests that many if not most ooliths in the Bonaparte limestones are algal. Rare ferruginous ooliths (Pl. 38, figs 1, 2) are not associated with algae and probably have another, unknown, origin.

Dolomitic Ooliths. Ooliths are entirely dolomitic only where they occur in a dolomite (Pl. 39, fig. 1). Occasionally, as in specimen 443-11, they are partly replaced by dolomite in preference to sparry calcite.

Grapestone. Lumps, algal micrite, and ooliths clustered in grapestones were seen in only one of the analysed specimens, 443-11.

With their wealth of algal sedimentary grains, the Bonaparte specimens resemble those of the Lower Devonian Nubrigyn reef complex of central New South Wales (Wolf, 1965).

Terrigenous Grains

Quartz, feldspar, and *rock fragments* (mainly cryptocrystalline quartz and quartzite), all described in the first half of this Bulletin, constitute almost the entire sand fraction of the insoluble residue. Some quartz grains are partly replaced by dolorhombs (Pl. 39, fig. 2). Glover (1963, pp. 40-1) described the diagenesis of a quartzose dolomite from the Septimus Limestone, similar to that illustrated

in Plate 39, figure 2, and concluded that the dolorhombs formed before the quartz grains were enlarged by overgrowths because the dolomite 'never penetrates clastic quartz grains when it abuts them'. This conclusion seems to be contradicted by Walker's (1957) observations in similar rocks. With a convincing series of illustrations, Walker (1957, pl. 1, figs 5A-C) demonstrated the preferential replacement of quartz overgrowths by dolomite and the virtual lack of replacement of the nucleus. Glover was conscious of the complex relationship between dolomite and quartz in the Septimus Limestone, and as Dr R. L. Folk (pers. comm.) commented, the dolomite and secondary quartz may have grown simultaneously. Walker's work, however, shows that Glover's criterion for judging the relative age of growth of dolomite and secondary quartz (Glover, 1963, fig. 5e) is false.

Matrix

Calcisilt. The only fine-grained matrix in these limestones is calcisilt, which consists of grains of calcite 10 to 50 μ across. Its origin is composite. Much calcisilt is microspar or recrystallized micrite, as indicated by its occurrence in patches of even-sized grains (Pl. 40, fig. 1), but some is produced by the collapse of algal threads (Pl. 40, fig. 2) which enclose grains of calcisilt, and other calcisilt arises in the degradation of skeletons (Pl. 41, fig. 1). Virtually lacking matrix, the Bonaparte skeletal and lump limestones are described as submature to mature grainstones (Folk, 1962; Dunham, 1962), and the birdseye limestone, stromatolites, and oncolites as boundstones.

Cement

Granular or sparry caclite is the common clear pore-filling cement that is an abundant constituent of almost all the limestones studied.

Fillings

Drusy mosaic calcite is the clear calcite that grows in shell cavities (Bathurst, 1958). Crystals commonly grow normal to the surface of the cavity (Pl. 21, fig. 1) but exceptionally, as shown in Plate 19, figure 1, a single crystal occupies the entire cavity.

Birdseyes are internal sediments and fillings of drusy mosaic that occupy cavities in fine-grained lump or algal micrite limestones (Pl. 41, fig. 2). Internal sediments serve crudely as geopetal structures. Birdseye limestone is commonly thought to be an algal-mat deposit, the birdseyes themselves being early diagenetic infillings of cavities left by decomposing algae.

Diagenetic Minerals

Glauconite occurs as pellets and is a rare constituent of a few limestones, never exceeding 1 percent. This is similar to its occurrence in associated quartz sandstones.

Undifferentiated dolomite is the term given to any dolomite not already classified as replacing micrite lumps, ooliths, or occupying fillings. In thin section it was distinguishable from calcite by not being stained by Alizarin Red S (Warne, 1962).

METHODS

Modal Analysis

The constituents described above were determined by modal analysis in 103 thin sections of representative specimens. Three hundred counts were made of each thin section except in very simple slides of say, sparry oolite, for which 200 counts sufficed. A spacing of 0.33 mm. was used.

Chemical Analysis

The same 103 specimens were chemically analysed to the following scheme:

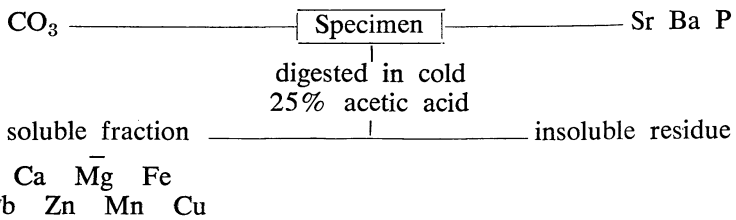

Ca, Mg, CO_3 and insoluble residue were required for the basic mineralogy of the specimens, and to serve as a check on the modal analyses. The major elements Ca, Mg, and Fe and the trace elements Pb, Zn, Mn, and Cu were determined on the acetic acid soluble fraction to avoid contamination from the insoluble residue. Such determinations are interpreted as showing the concentration of these elements in calcite, and there is little or no contamination from clay minerals or other insolubles when the whole sample is digested in cold 25 percent acetic acid (Hirst & Nicholls, 1958). Sr, Ba, and P, on the other hand, were determined on the whole sample to avoid missing any occurrences of these elements outside calcite.

The analyses were carried out under contract by P. J. Busby of Australian Mineral Development Laboratories in South Australia. The following analytical methods were used:

Strontium and *barium* were determined by X-ray fluorescence using a lithium fluoride crystal and scintillation counter on the pulverized sample held in a Philips container with a Mylar window. Barium was read at 10.97° and strontium at 25.09°. Background corrections were read at 0.5° either side of the peak angle and mass absorbance was read also at the peak angles for barium and strontium.

Phosphorus was determined by an initial digestion of the sample with perchloric acid followed by water dilution to a fixed volume. A clear aliquot was taken, ammonium molybdate solution added, and the phosphomolybdate complex reduced with ascorbic-sulphuric acid mixture overnight at 40°C to give a molybdenum blue colour which was then read spectrophotometrically.

Carbonate (CO_3) was determined by evolution in special apparatus using dilute perchloric acid. The sample was digested in an electrically heated flask connected to a reflux condenser. The carbon dioxide was purified by passing first through concentrated sulphuric acid then pumice impregnated with copper sulphate, and finally dried and absorbed on soda-asbestos in a weighed Fleming tube.

Insoluble residue. 1 gram of sample was digested with 20 ml. of 25 percent acetic acid overnight for approximately 16 hours, filtered and washed, the filtrate being made up to 100 ml. The insoluble residue was then ignited and weighed.

Calcium was determined on an aliquot from the acid digestion by titration with E.D.T.A. after complexing interfering ions with triethanolamine and potassium cyanide. Magnesium was determined by atomic absorption spectrometry using standards containing acetic acid and the equivalent of 90 percent calcium carbonate. The higher *magnesium* figures were determined by E.D.T.A. titration after complexing interfering ions with triethanolamine and potassium cyanide.

Iron was determined on a further aliquot by reduction with hydroxylamine hydrochloride, the addition of o-phenanthroline, pH adjustment, and spectrophotometric readings of the colour with a Beckman spectrophotometer at 510 mμ.

Lead, zinc, manganese, and *copper* were all determined by atomic absorption spectrometry using standards prepared similar to the assays and containing the equivalent of 90 percent calcium carbonate in a dilute acetic acid solution.

One standard of known analysis was included in the analysis for every 20 samples, and every tenth sample was replicated. The precision, as indicated by twice the standard deviation from the mean (95 percent confidence) is as follows:

$\leqslant 1\%$	2%	6%	10%
CO_3	Fe	Zn	Sr
Ca		Mn	Ba
Mg		P	insoluble
Pb			residue

The concentration of copper in all the samples was below the level of detection (<10 ppm).

COMPUTER CLASSIFICATION

Introduction

With the advent of electronic computers, multivariate analysis has been increasingly applied to the classification of carbonate rocks and to the identification of carbonate facies. Carbonates, because of their wide range of easily recognized grain types, are ideal subjects for multivariate analysis, as instanced by the analyses of modern carbonates by Imbrie & Purdy (1962) and van Andel & Veevers (1967), and of ancient carbonates by Harbaugh & Demirmen (1964) and Bonham-Carter (1965), to mention only a few of the many authors who have contributed to this field. Factor analysis has been the principal method used by authors, and as well as using this method the present contribution shows the calibre of a newly developed hierarchical agglomerative programme using an information statistic for the classification of mixed data.

The most coherent lateral sequence of carbonate facies was found in the Famennian Ningbing Limestone and Buttons Beds (Playford et al., 1966), and is shown diagrammatically in Figure 24b. From the ancient shore to the open sea, the facies sequence is inshore lagoon, offshore lagoon, back-reef, barrier reef and inter-reef, and fore-reef, which is replaced seaward by a basinal facies of shale

and siltstone. This follows the sequence well known from modern and ancient barrier-reef complexes and associated facies (Dunbar & Rodgers, 1957, pp. 92-4).

Veevers & Roberts (1968) suspected the existence of Frasnian (early Upper Devonian) reefs from an isolated occurrence of inferred fore-reef breccia, and of Tournaisian (early Lower Carboniferous) reefs from a reef limestone of probable Tournaisian age in the same area as the Famennian reefs. The numerical classification of the Famennian reefal carbonates was attempted in the hope of sufficiently refining knowledge of reefal facies that the facies of the fragmentary Frasnian and early Tournaisian limestones could be rigorously identified.

Method

Each of 103 specimens from representative carbonate facies was modally analysed in thin section for 30 attributes: 8 skeletal types, 4 algae, 8 varieties of pellets and ooliths, 5 of matrix and cement, 3 of terrigenous grains, and 2 diagenetic minerals. Each specimen was chemically analysed for CO_3, Ca, Mg, insoluble residue, Fe, Pb, Zn, Mn, P, Sr, and Ba. Cu was also determined but the results could not be used because its concentration fell below the limit of detection. The final numerical attribute determined was the estimated distance of the specimen from the shore of the depositional basin. This, incidentally, is the only attribute with any appreciable subjective component. Six attributes were determined qualitatively, i.e. as present, absent, or not known: they are red (solenopore) alga, a problematical alga(?) called *Umbella,* conodont, ostracod, bryozoan, and glauconite. All but the conodont are duplicated as numerical attributes. E. C. Druce supplied the information about the conodonts, and P. J. Jones about ostracods.

All this information on 103 specimens, each with 48 attributes, was processed on a Control Data 3600 computer using Lance & Williams' (1967) hierarchical agglomerative programme with an information statistic for the classification of mixed data (MULTBET), supplemented by an ordination programme (MAXGOWER), adapted by Lance & Williams (1967) from a suggestion by Gower (1966) which carries out a principal co-ordinate (or Q-factor) analysis. The results of the Gower analysis are given on page 62 and following.

No further mention of the numerical method is made here because I am not qualified to discuss the details, which in any case the interested reader will find in Lance & Williams' paper. I have approached this problem as a pragmatic geologist; as will be seen below, the classification 'works'.

Figure 22. Upper part of hierarchical classification. The following abbreviations are used:

alg.-micr.	**algal micrite**	**oncol.**	**oncolitic**
calcis.	**calcisiltite**	**qtz.**	**quartzose**
crin.	**crinoidal**	**skel.**	**skeletal**
dol.	**dolomitic**	**solen.**	**solenopore alga**
LS	**limestone**	**sp.**	**sparry**
ool.	**oolitic**	**SS**	**sandstone**

qtz dol lump sp skel (crin) Lst
ool skel alg-micr sp lump Lst
qtz lump sp skel (crin) Lst
VI qtz sp dolomite
I ool alg-micr sp lump Lst
II skel (crin) sp lump Lst
III skel sp lump Lst
IV qtz skel sp lump Lst
V sp skel Lst
lump Lst
a
b
c
d
e
f
g
h
i
j
k
l
m
n
o
p
q
r
s
t
oncol alg-micr ool Lst
sp lump Lst
solen lump Lst
skel calcis + dol lump Lst
sp lump Lst
skel (crin) sp lump Lst
lump sp skel Lst
sp lump Lst
qtz skel sp lump Lst
qtz lump sp skel Lst
qtz sp lump Lst
qtz lump Lst
silty crin Lst
qtz sp skel Lst
sp lump crin Lst
sp skel Lst
qtz dolomite
dolomite + qtz Sst
dol qtz Sst
M(G)93

Results

The output of the MULTBET programme is an agglomerative hierarchy (or dendrogram) of all the specimens, and a list of the mean values of attributes in each of the higher groups, from which the petrography and chemistry of each group may be found. After examination of the hierarchy, the lower part of which contains 58 groups*, the 20 higher groups (Table 8(1) and Fig. 22) were found to be the most useful ones for study, and they were labelled *a* to *t*. The groups ranged evenly from the extremes of *a*, comprising pure (non-terrigenous) sparry oolite and algal micrite (recognized as part of the reef facies), to *t*, a dolomitic quartz sandstone. No obvious misclassifications were found; on the contrary, the few suspected misclassifications showed the robustness of the programme in not being misled by attributes which are known to be of minor geological significance. For example, an apparent misclassification was the grouping in *a* of specimen 456-2, a dolomitic sparry oolite containing 28 percent dolomite. At first glance, its high content of dolomite would seem to require this specimen to be placed well away from the pure reef limestones towards the dolomitic and terrigenous side of the hierarchy, but the programme accepted geologically more significant attributes such as the very high oolith and very low insoluble residue content to classify it correctly with reef limestone.

Groups in the Famennian Sequence

As shown in Figures 23 and 24, the various facies in the Famennian sequence are characterized by particular assemblages of numerical groups. Thus, with one exception, all the specimens of the reef and vicinity are groups *a* and *b*; also with only one exception the back-reef is *c*, *d*, *e*, and *g*; the offshore lagoon is *i*, *j*, *l*, and *m*; and the inshore lagoon *h*, *n*, *s*, and *t*. As seen in Table 8(1), and Figure 22, groups *a* and *b* are sparry oolitic, oncolitic algal micrite, and lump limestones; *c-e* and *g* are red algal lump limestone, skeletal calcisiltite, and skeletal sparry lump limestone; *i*, *j*, *l*, and *m* are quartzose skeletal sparry lump limestone; and *h*, *n*, *s*, and *t* are lump sparry skeletal limestone, silty crinoidal limestone, and dolomitic quartz sandstone. (See also Table 13.)

The special feature of numerical classification lies in its power to distinguish groups by combinations, many of them subtle, of numerous attributes, not briefly described in words. In comparison, the petrographical names given above are clumsy oversimplifications useful only in summarizing the bulk composition of the groups. The petrography of the most distinctive groups was known intuitively before the classification was made, and the computer's special contribution was to refine this knowledge in all groups on a rigorous quantitative basis.

* See Table 13.

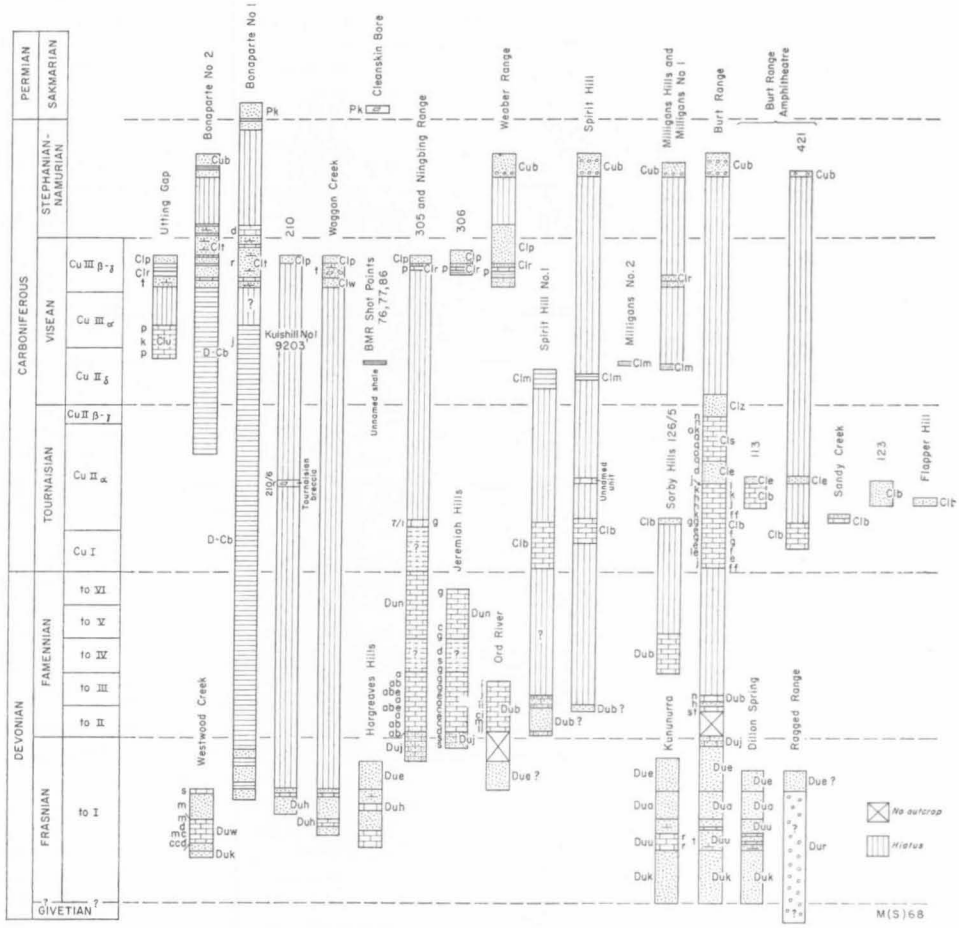

Figure 23. Stratigraphical distribution of groups. (Plotted on the correlation diagram of Veevers & Roberts, 1968, fig. 40). The carbonate formations contain the following groups:

Westwood Member (Duw): **c** and **d** (Supergroup I), **m** (IV), **s** (VI); Kununurra Member (Duu): **r** and **t** (VI); Jeremiah Member (Duj): **s** (VI); Ningbing Limestone (Dun): **a — e** (I), **g** (II), **s** (VI); Buttons Beds (Dub): **c** (I), **h** and **i** (III), **j, l, m** (IV), **n** (V), **s** and **t** (VI); Unnamed Tournaisian limestone (loc. 7-1): **g** (II); Burt Range Formation (Clb): **e** (I), **f** and **g** (II), **h** and **i** (III), **j — l** (IV); Enga Sandstone (Cle): **d** (I); Unnamed Tournaisian breccia (loc. 210-6): **r** (VI); Septimus Limestone (Cls): **k** (IV), **n, o,** and **q** (V); Utting Calcarenite (Clu): **k** (IV), **p** (V); Kulshill No. 1 (9201): **j** (IV); Burvill Beds (Clr): **p** (V), **t** (VI); Waggon Creek Breccia (Clw): **t** (VI); Tanmurra Formation (Clt): **d** (I), **r** (VI).

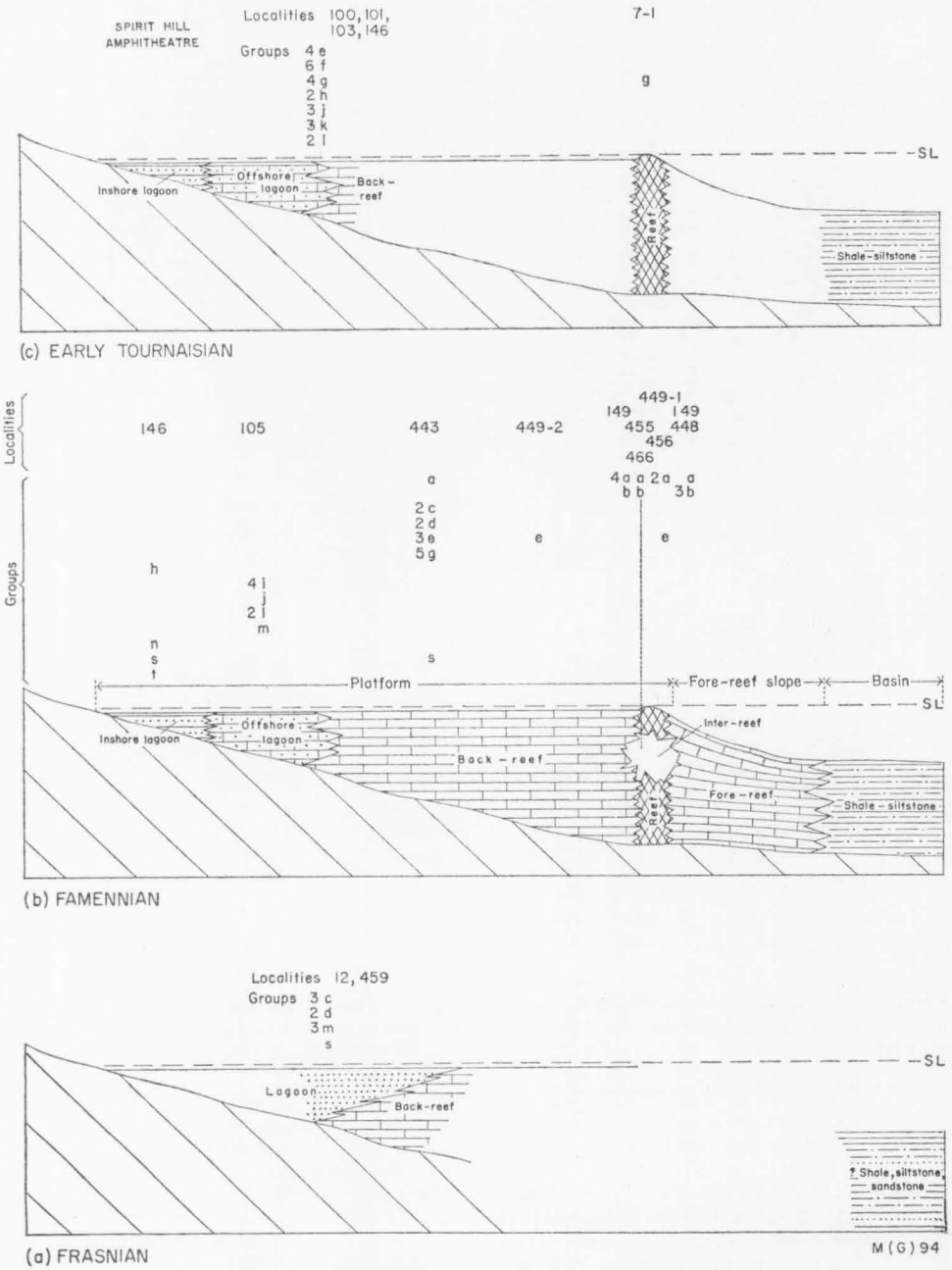

Figure 24. Distribution of groups in the reefal sequence

Interpretation of the Suspected Reefal Limestone of Frasnian Age

Veevers & Roberts (1968) suspected that the lower part of the Frasnian Westwood Member (locs 12, 459) was reefal because it contains a build-up of brecciated stromatolites in a matrix of micrite containing abundant *Renalcis,* a schizophyte alga common in the Upper Devonian reef limestone of the Canning Basin (Playford & Lowry, 1967). Being a breccia, it was tentatively classed as fore-reef.

In terms of the computer classification, this limestone sequence comprises groups *c, d, m,* and *s.* This group assemblage, clearly not that of a fore-reef, comes closest to those of the Famennian back-reef and lagoon, and is so identified. This is an attractive geological interpretation because the Frasnian limestone is interbedded with and finally overlain by calcareous quartz sandstone (Fig. 24), which is not common beyond the lagoonal facies. As shown in Figure 23, this sequence is interpreted as interfingering back-reef and lagoonal facies deposited during a marine regression. The *Renalcis*-bearing stromatolite breccia is regarded as part of a patch reef. The basinal facies shown on the right-hand side of Figure 24 is represented by shale, siltstone, and sandstone (Bonaparte Beds) of possible Frasnian age (Fig. 23), penetrated by wells in the axis of the Bonaparte Basin.

Interpretation of the Early Tournaisian Limestones

The early Tournaisian sequence (Figs 23, 24) is fragmentary, being known from isolated occurrences of subsurface basinal shale and siltstone (Bonaparte Beds), a single outcrop of reef or near-reef limestone (loc. 7-1), and an extensive outcrop of limestone (Burt Range Formation) (locs 100, 101, 103, 146, all in the Burt Range area), whose precise environment of deposition was unknown. As detailed by Veevers & Roberts (1968) the geological setting at locality 7-1 is complex, with a pocket of skeletal sparry lump limestone (group *g*) in a *Stromatactis* limestone. *Stromatactis* (Pl. 42, fig. 1), a problematical structure (Bathurst, 1964, p. 334), is restricted to reef limestone in the underlying Famennian sequence and in the equivalent reef limestone of the Canning Basin (Playford & Lowry, 1967), as elsewhere in the world. Its occurrence at locality 7-1 outweighs the classification of the enclosed pocket of group *g* limestone, which elsewhere is typically back-reef. This is not necessarily contradictory, because a nest of shelly fossils, highly prized for palaeontological correlation and prone to be over-sampled (as it was) at the expense of the enclosing rock, is rarer in reef than in back-reef limestone. The analysis of a representative suite of specimens would have clarified this point.

The specimens from the extensive outcrop of early Tournaisian Burt Range Formation (locs 100, 101, 103, 146) belong to groups *e-h* and *j-l,* which are skeletal to quartzose sparry lump limestones. Compared with the Famennian sequence, this assemblage has groups *e* and *g* in common with the back-reef, and *h, j,* and *l* with the lagoon, and is thus interpreted as representing interfingering back-reef and lagoonal limestones. In the light of this interpretation, the hitherto anomalous occurrence in the Burt Range Formation at locality 100-9 of a bed of stromatolites, with strong reefal affinities, is resolved. For reasons of economy, specimens from equivalent carbonate rocks at Spirit Hill and the Amphitheatre were not classified, but their high terrigenous content indicates their place in the inshore lagoonal facies, where they are shown in Figure 24.

Veevers & Roberts (1968) glimpsed the possibility that the Burt Range Formation at localities 100, 101, 103, and 146 was associated with a contemporary reef, but without the refined petrological information now available offered their views as plain speculation only.

Interpretation of later Lower Carboniferous (late Tournaisian and Visean) Limestones

The late Tournaisian and Visean limestones are dominated by groups *n* to *q* (sparry skeletal, mainly crinoidal, limestone), which, with one exception only, do not occur in the underlying reefal limestones (Fig. 24). This stratigraphical separation of older reefal groups and younger non-reefal ones can be interpreted unhesitatingly in terms of the tectonic history. In the Upper Devonian and Lower Carboniferous, a constant feature, varying only in intensity, was the influx of terrigenous sediment from the southeast in response to intermittent movement along the fault system that marked the southeast shore of the basin. The most intense movements occurred during the Frasnian, and consequently deposition was largely terrigenous, extensive Frasnian carbonates (locs 12, 459) being deposited only a considerable distance from the southeast shore. With the reduced but still appreciable supply of terrigenous sediment in the Famennian and early Tournaisian, the marine platform became the site of reefal deposition, which was continuous except where locally interrupted by uplift. A new tectonic element appeared in the mid-Tournaisian, at the boundary between the reefal and non-reefal limestones: the violent uplift, faulting, tilting, and deep erosion of the hitherto quiescent southwest part of the basin (Veevers & Roberts, 1966). The accompanying influx of terrigenous detritus into the basin, represented in outcrop by the 500 feet of Enga Sandstone that overlies the early Tournaisian limestone (Fig. 24), deeply buried the reefal sequence and smoothed out the formerly rugged seafloor to make it an unsuitable surface for reef building during later periods of carbonate deposition.

Summary

The Upper Devonian and Lower Carboniferous carbonate rocks fall into two major divisions: (a) Upper Devonian and early Tournaisian reefal limestones, comprising six facies, each distinguishable by a characteristic assemblage of numerical groups; and (b) late Tournaisian and Visean non-reefal limestones, dominantly skeletal (mainly crinoidal) limestones, distinguishable from the reefal limestones by a characteristic assemblage of groups.

The persistence of reefal limestones from the base of the Famennian to the end of the early Tournaisian and their earlier appearance during the dominantly terrigenous deposition of the Frasnian indicates the maintenance of a delicate balance of conditions in the sea favouring reef growth despite the intermittent influx of terrigenous sediment. The effects of the rapid uplift of the southwest margin of the basin in the mid-Tournaisian destroyed the balance, and reefs did not reappear in the later Lower Carboniferous sea.

These conclusions stem largely from the successful application of numerical classification to the lime[illegible]. If, instead of the numerical classification, a qualitative and unavoidably [illegible]classification had been made, it would almost certainly have failed to [illegible]e refined information required to solve this type of complex geological pi

Further Notes on the Groups

Group *a*, identified as reef or near-reef limestone, comprises 9 specimens containing mainly sparry calcite, oncoliths, algal micrite, and ooliths. As noted above, the ooliths are probably algal, so that except for the sparry calcite cement most constituents of the rocks were probably deposited under the influence of porostrome algae. Their content of insoluble residue, 2.6 percent, is the lowest of all the groups, and almost all the specimens contain conodonts. Group *b*, near-reef limestone, comprises 5 specimens of sparry lump limestone, likewise thought to be algal. Insoluble residue is 3.8 percent and conodonts occur in every specimen. Group *c*, mostly back-reef limestone, is more definitely algal, with 13 percent solenopore algae, 5 percent *Renalcis,* and 37 percent algal micrite. Following the trend already noted, it contains an increased content of insoluble residue of 5.3 percent.

Group *d*, dominantly back-reef limestone, is a mixed group of shelly and *Renalcis* calcisiltite and dolomitic lump limestone. Insoluble residue is 8.3 percent.

Group *e*, dominantly back-reef limestone, is a mixed group of 7 sparry lump limestones, a sparry oolite, and a lump sparry oncolite.

Groups *a-e* comprise supergroup I, which is almost exclusively algal, group *d* being the only one containing appreciable shelly matter (10%).

Groups *f* and *g*, constituting supergroup II, differ markedly from the preceding groups in containing as much as 30 percent shelly matter in skeletal sparry lump limestones. Ostracods occur in all 16 specimens of these groups, and conodonts in 12 of them.

The distinctions in the middle part of the hierarchy, between groups *h* and *i* (supergroup III) and their neighbours, are much less obvious, and this is where the advantages of computer classification over other methods are greatest. Group *h* consists of lump sparry skeletal limestone, and *i* of sparry lump limestone. Groups *j* to *m* (supergroup IV) are quartzose sparry lump limestone with or without skeletal material; groups *j* and *k* have 15 to 30 percent of skeletal material, *l* and *m* have less than 4 percent. Groups *n* to *q* (supergroup V) are sparry skeletal limestone; group *n* is silty crinoidal limestone in which crinoid ossicles constitute half of the rock; the specimens in group *p* also contain abundant crinoids, and in *q* crinoids, brachiopods, and bryozoans together make up 65 percent of the rock. Groups *r* to *t* (supergroup VI) contain quartzose dolomite (group *r*) dolomite and calcareous quartz sandstone (*s*), and dolomitic quartz sandstone (*t*).

Notes on the higher groups

Table 8(2) gives the mean values of attributes in the supergroups and higher groups. The highest agglomerations contain almost the same number of specimens. I and II are distinguished from the remainder (III to VI) by their low content of dolomite and insoluble residue. Almost all the dolomite in III to VI is contributed by VI (46.8%), the other supergroups averaging only 0.4 percent. Supergroup V is distinguished from III and IV by its high skeletal content (60%) and low lump content. IV is distinguished from III by its threefold greater amount of quartz. Finally, II is distinguished from I by its higher content of skeletal material (about 20% v. 4%) and spar (35% v. 23%), and by its lack of algae and ooliths.

TABLE 8: ANALYTICAL DATA ARRANGED IN GROUPS

1. MEAN VALUES OF ATTRIBUTES IN GROUPS a-t

REEF COMPLEX AND ASSOCIATED SEDIMENTS

Groups	N	Formations	Reef	Inter-reef	Fore-reef	Reef/Back Reef	Back Reef	Lagoon (offshore)	Inshore Lagoon
			R	IR	FR	R-BR	BR	Lo	Li
Gp Ia	9	Dun	2/9	1/9	1/9	4/9	1/9	—	—
Gp Ib	5	Dun	—	1/5	3/5	1/5	—	—	—
Gp Ic	6		—	—	—	—	5/6	1/6	—
Gp Id	6		—	—	—	—	4/6	—	—
Gp Ie	9		1/9	—	—	—	4/9	—	—
Gp IIf	6	Clb	—	—	—	—	—	—	—
Gp IIg	10		1/10	—	—	—	5/10	—	—
Gp IIIh	3		—	—	—	—	—	1	1/3
Gp IIIi	4		—	—	—	—	—	—	3/4
Gp IVJ	5	Dub	—	—	—	—	—	1/5	—
Gp IVk	5		—	—	—	—	—	—	—
Gp IVl	4		—	—	—	—	—	1/2	—
Gp IVm	4		—	—	—	—	3/4	1/4	—
Gp Vn	4		—	—	—	—	—	—	1/4
Gp Vo	3		—	—	—	—	—	—	—
Gp Vp	4		—	—	—	—	—	—	—
Gp Vq	3	Cls	—	—	—	—	—	—	—
Gp VIr	4		—	—	—	—	—	—	—
Gp VIs	5		—	—	—	—	2/5	—	1/5
Gp VIt	4		—	—	—	—	—	—	1/4

QUALITATIVE ANALYSIS

Groups	Solenopore alga 1	*Umbella* 2	Concidont 3	Ostracod 4	Bryozoan 5	Glauconite 6	Crinoid ossicle 7	Crinoid ossicle silicified 8	Brachiopod 9	Ostracod 10	Bryozoan/coral 11	Foram 12	Gastropod or pelecypod 13	Unidentified shell 14	Solenopore alga 15	*Umbella* 16	*Renalcis* 17	Calcisiltstone 18	Micrite lump 19	Micrite lump dolomite 20	Algal micrite 21	Coated grain 22	Oncolith 23	Oolith 24	Oolith, dolomite 25	Grapestone 26	Microspar or calcisilt 27	Granular calcite 28	Drusy mosaic 29	Birdseye 30	Dolomite filling 31	Quartz 32	Feldspar 33	Rock fragments 34	Glauconite 35	Undiff. dolomite 36
Gp Ia	—	—	6/7	—	—	0.4	2	—	0.5	—	—	—	—	0.2	—	—	—	0.2	—	—	25	—	6	27	0.7	0.8	—	27	6	—	—	.2	—	—	—	4
Gp Ib	0.6	—	1	—	—	—	2.6	—	1	—	—	—	0.2	—	0.8	—	—	—	60	—	—	—	—	—	—	—	—	32	0.8	—	—	2.6	—	—	—	3
Gp Ic	0.7	—	—	—	—	—	0.5	—	0.7	—	1.2	—	0.2	—	13	—	5	—	12	—	37	—	—	—	—	—	—	23	4	—	—	0.5	—	—	—	3
Gp Id	—	—	0.7	—	—	—	2.5	—	6.5	—	—	1	—	—	—	—	4	—	20	18	—	—	—	—	—	—	33	7	0.3	7	—	0.2	—	—	—	0.2
Gp Ie	1/9	—	1/8	4/9	1/9	—	1	—	—	.5	—	—	—	4	—	—	—	—	22	—	11	.5	—	—	—	—	1	25	.3	.2	—	3	—	—	—	—
Gp IIf	—	—	1	1	5/6	—	15	—	7	3	.3	—	—	—	—	—	—	—	40	.5	—	—	—	—	—	—	3	34	—	—	—	3	—	—	—	—
Gp IIg	1/10	—	6/10	1	1/10	1/10	13	—	2	4	—	—	—	—	—	—	—	—	21	—	—	—	—	—	—	—	—	40	.2	—	—	8	—	—	—	—
Gp IIIh	—	—	1	1	1/3	—	9	—	7	1	—	—	—	6	2	—	—	—	70	—	—	—	—	—	—	—	—	19	—	—	—	4	—	—	—	—
Gp IIIi	—	—	1/2	1/2	—	—	4	—	1.5	.05	—	—	—	—	1.5	—	—	—	—	—	—	—	—	—	—	—	—	—	—	—	—	—	—	—	—	—
Gp IVJ	—	—	2/5	1	—	—	2.6	—	7	0.2	5	1	—	2	0.2	—	—	—	20	—	2	2	—	2	—	—	—	29	7	—	—	18	—	—	—	2
Gp IVk	—	—	4/5	1	1	—	15	—	11	1	3	—	—	—	.4	—	—	—	13	—	0.2	—	—	—	—	—	—	31	0.2	—	—	24	—	—	—	1
Gp IVl	—	—	2/3	3/4	—	1	2	—	—	—	—	—	—	—	—	—	—	—	48	—	—	—	—	—	—	—	—	15	—	—	—	26	—	6	—	—
Gp IVm	—	—	1/3	1/2	3/4	1/4	48	10	3	—	.2	—	—	—	—	—	—	—	66	—	—	—	—	—	—	—	—	8	—	—	—	23	—	—	—	—
Gp Vn	—	—	—	—	—	—	27	—	38	—	1	1	—	—	—	—	—	—	2	—	—	—	—	—	—	—	20	8	2	—	—	9	—	—	—	—
Gp Vo	—	—	—	—	—	—	42	1	3	1	.2	3	—	—	.5	—	—	—	—	—	—	—	—	—	—	—	—	13	0.3	—	6	14	—	—	—	—
Gp Vp	—	—	1	1	1	—	25	—	18	1	21	—	—	—	—	—	—	—	23	—	—	—	—	—	—	—	—	17	1	—	—	7	—	—	—	.5
Gp Vq	—	—	1/4	—	—	0.5	.5	—	—	—	—	—	—	—	—	—	—	—	—	—	—	—	—	—	—	—	—	24	6	—	—	6	—	—	—	—
Gp VIr	—	—	1/3	—	—	—	—	—	—	—	—	—	—	—	—	—	—	—	—	—	—	—	—	—	—	—	—	—	—	—	—	—	—	—	—	62
Gp VIs	1/5	—	—	—	—	—	—	—	—	—	—	—	—	—	—	—	—	—	7	—	—	—	—	—	—	—	—	14	0.3	—	6	36	1	—	—	55
Gp VIt	—	—	—	—	—	1/2	—	—	—	—	—	—	—	—	—	—	—	—	—	—	—	—	—	—	—	—	14	4	—	—	—	19	1	.2	—	55
																												14	—	—	—	61	1	.2	.2	22

MODAL ANALYSIS

Groups	Micrite lump 19	Micrite lump dolomite 20	Algal micrite 21	Coated grain 22	Oncolith 23	Oolith 24	Oolith, dolomite 25	Grapestone 26	Microspar or calcisilt 27	Granular calcite 28	Drusy mosaic 29	Birdseye 30	Dolomite filling 31	Quartz 32	Feldspar 33	Rock fragments 34	Glauconite 35	Undiff. dolomite 36
Gp Ia	—	—	25	—	6	27	0.7	0.8	—	27	6	—	—	.2	—	—	—	4
Gp Ib	—	—	—	—	—	—	—	—	—	32	0.8	—	—	2.6	—	—	—	3
Gp Ic	—	—	37	—	—	—	—	—	—	23	4	—	—	0.5	—	—	—	—
Gp Id	—	—	—	.7	8	7	—	—	—	1	25	.3	.2	—	3	—	—	—
Gp Ie	—	—	—	.5	—	—	—	—	—	—	37	—	—	—	1	—	—	—
Gp IIf	—	—	3	34	—	—	—	—	—	—	—	—	—	—	3	—	—	—
Gp IIg	—	—	—	—	—	—	—	—	—	—	40	.2	—	—	8	—	—	—
Gp IIIh	—	—	—	19	—	—	—	—	—	—	—	—	—	—	4	—	—	—
Gp IIIi	—	—	—	—	—	—	—	—	—	—	—	—	—	—	—	—	—	—
Gp IVJ	—	—	2	2	—	2	—	—	—	29	7	—	—	18	—	—	—	2
Gp IVk	—	—	—	—	—	—	—	—	—	—	—	—	—	—	—	—	—	—
Gp IVl	—	—	—	—	—	—	—	—	—	—	—	—	—	24	—	—	—	1
Gp IVm	—	—	—	—	—	—	—	—	—	—	—	—	—	26	—	6	—	—
Gp Vn	—	—	—	—	—	—	—	—	—	—	—	—	—	23	—	—	—	—
Gp Vo	—	—	—	—	—	—	—	—	20	8	2	—	—	9	—	—	—	—
Gp Vp	—	—	—	—	—	—	—	—	—	13	0.3	—	6	14	—	—	—	—
Gp Vq	—	—	—	—	—	—	—	—	—	17	1	—	—	7	—	—	—	.5
Gp VIr	—	—	—	—	—	—	—	—	—	24	6	—	—	6	—	—	—	—
Gp VIs	—	—	—	—	—	—	—	—	—	—	—	—	—	36	1	—	—	62
Gp VIt	—	—	—	—	—	—	—	—	14	4	—	—	—	19	1	.2	—	55
	—	—	—	—	—	—	—	—	—	14	—	—	—	61	1	.2	.2	22

CHEMICAL ANALYSIS

Groups	CO_3 37	Ca 38	Mg 39	Fe 40	Pb 41	Zn 42	Mn 43	Insoluble residue 44	P 45	Sr 46	Ba 47	Distance from shore 48
Gp Ia	59.1	37.8	0.7	.024	10	4	140	2.6	.008	220	15	37
Gp Ib	57.6	38.3	0.3	.015	10	2	112	3.8	.017	180	24	35
Gp Ic	56.2	36.9	0.5	.047	10	7	210	5.3	.006	340	15	43
Gp Id	56.4	37.0	0.4	.044	10	1	150	6.1	.004	370	20	23
Gp Ie	57.2	37.5	0.4	.075	14	2	240	4.9	.007	770	14	11
Gp IIf	56.7	37.3	0.4	.035	13	1.6	150	5.3	.012	650	28	21
Gp IIg	49.6	32.6	0.3	.290	12	1	380	17.3	.008	500	30	11
Gp IIIh	52.4	34.1	0.5	.051	99	1	180	12.0	.009	575	110	28
Gp IIIi												
Gp IVJ	43.3	28.5	2.4	.072	4	2	235	27.8	.026	650	130	13
Gp IVk	35.1	24.8	0.2	.093	4	1	250	37.0	.021	300	90	18
Gp IVl	42.9	28.6	0.3	.233	5	2	450	26.7	.014	320	45	50
Gp IVm	45.7	29.9	0.3	.166	9	2	400	22.9	.021	400	180	15
Gp Vn	40.3	24.4	0.6	.380	2	1	360	33.8	.071	330	80	11
Gp Vo	52.1	34.1	0.4	.091	10	2	960	12.8	.032	190	35	22
Gp Vp	53.5	34.6	0.2	.160	8	1	850	11.7	.023	490	30	7
Gp Vq	46.4	19.7	5.2	.079	13	10	410	27.6	.012	90	35	30
Gp VIr	21.3	10.8	1.3	.311	2	1	740	66.8	.013	80	60	11
Gp VIs												
Gp VIt												

Rock Type	Ca/Mg	Sr/Ca × 1000
Oncolitic sparry algal micrite coolitic limestone	94.8	0.6
Sparry lump limestone	164.8	0.5
Solenopore lump limestone	88.9	0.9
Skeletal calcisiltite and dolomitic lump limestone	75.7	0.8
Sparry lump limestone	108.8	1.0
Skeletal sparry lump limestone	105.6	2.0
Skeletal sparry lump limestone	110.2	1.8
Lump sparry skeletal limestone	114.3	1.5
Sparry lump limestone	70.9	1.7
Quartzose skeletal sparry lump limestone	112.1	1.3
Quartzose lump sparry skeletal limestone	136.2	2.3
Quartzose sparry lump limestone	98.2	1.2
Quartzose lump limestone	104.0	1.1
Silty crinoidal limestone	97.2	1.3
Quartzose sparry skeletal limestone	64.4	1.7
Sparry lump crinoidal limestone	109.8	0.4
Sparry skeletal limestone	168.9	1.4
Quartzose dolomite	2.0	0.6
Dolomite/quartz sandstone	32.4	0.4
Dolomite/quartz sandstone	39.8	0.7

2. MEAN VALUES OF ATTRIBUTES IN MAJOR GROUPS

Group	N	1	2	3	4	5	6	7	8	9	10	11	12	13	14	15	16	17	18	19	20	21	22	23	24	25	26	27	28	29	30	31	32	33	34	35	36	CO_3 37	Ca 38	Mg 39	Fe 40	Pb 41	Zn 42	Mn 43	Insoluble residue 44	P 45	Sr 46	Ba 47	Distance from shore 48	Ca/Mg	Sr/Ca × 1000
I+II	51	.14	.04	.58	.4	.14	.06	5.5	—	2.2	1.26	0.18	0.12	.02	.5	1.61	—	1.14	.04	39.3	2.20	10.2	.18	2.26	6.08	1.12	.14	4.6	27.0	1.7	.90	—	1.63	—	—	—	5.12	57.0	37.1	0.5	0.06	11.5	2.5	204	5.1	.01	410	21.1	29	Oolitic skeletal algal micrite sparry lump limestone		
III+IV+V+VI	52	.11	.04	.47	.6	.35	.17	12.6	.9	6.0	0.33	2.11	0.37	—	.7	0.33	0.8	—	—	21.2	—	.25	.15	—	.21	—	—	2.4	17.6	1.4	—	.35	20.58	.23	.62	.02	27.99	43.5	26.2	1.4	0.17	7.8	2.5	488	28.0	.02	334	83.7	20	Quartzose dolomitic lump sparry skeletal (mainly crinoidal) limestone		
III+IV+V	39	.15	.05	.6	.8	.5	.13	16.8	1.2	8.0	.4	2.8	.5	—	.9	.4	.1	—	—	27.4	—	.3	.2	—	.3	—	—	2.1	20.6	1.9	—	.5	15.0	—	0.6	—	.4	45.8	29.9	.3	0.15	6.9	1.5	424	23.2	.02	418	96	20	Quartzose lump sparry skeletal (mainly crinoidal) limestone		
VI	13	—	—	.2	—	.31	.2	—	—	2.5	—	—	—	—	1.4	.6	.2	—	—	38.6	—	.5	.3	—	.4	—	—	3.6	8.8	—	—	—	37.3	.9	0.7	.1	46.8	36.6	15.1	4.6	0.23	10.5	5.4	680	42.4	.01	82	47	21	Quartzose sparry dolomite		
III+IV	25	.2	.1	.6	.9	.3	.2	5.8	—	4.8	.4	1.6	.2	—	—	.1	—	—	—	7.4	—	—	—	—	—	—	—	—	—	—	—	—	7.7	—	—	—	—	51.2	33.8	.41	.15	10.0	1.0	264	14.3	.01	541	77	21	Quartzose skeletal sparry lump limestone		
V	14	—	—	.4	.6	.8	.1	36.6	3.6	13.6	.6	5.0	1.1	—	—	—	—	—	—	48.6	—	—	—	—	—	—	—	—	—	—	—	—	22.6	—	1.3	—	.8	42.0	27.8	.27	.13	5.2	1.8	295	29.2	.02	425	113	24	Quartzose skeletal sparry lump limestone		
III	7	.6	—	.8	.9	.14	—	6.4	—	3.7	.6	—	—	—	2.7	1.7	—	—	—	34.7	—	.7	.4	—	.6	—	—	—	22.0	2.1	—	—	1.4	—	—	—	1.5	57.1	37.0	0.6	0.06	10.6	3.0	212	5.1	.01	281	20	34	Oolitic algal micrite sparry lump limestone		
IV	18	.1	.1	.6	.9	.39	.2	5.5	—	5.2	.3	2.2	.2	—	0.9	.2	.2	—	—	27.5	3.0	12.9	.17	3.3	8.9	.2	.2	5.9	23.4	2.5	1.3	—	1.4	—	—	—	—	56.9	37.4	0.4	0.05	13.4	1.6	185	5.1	.01	694	23	17	Skeletal (mainly crinoidal) sparry lump limestone		
I	35	.2	.03	.5	.1	.03	.06	1.7	—	1.5	.1	.2	.2	.03	.06	2.3	—	1.7	.06	27.5	3.0	12.9	.17	3.3	8.9	.2	.2	5.9	23.4	2.5	1.3	—	1.4	—	—	—	—														
II	16	.2	.06	.8	1.0	.40	.06	13.7	—	3.6	3.7	.1	—	—	1.60	—	—	—	—	33.4	.4	4.2	.19	—	—	—	—	1.9	35.0	—	—	—	2.2	—	—	—	—														

The data from which this table was compiled are available from the Bureau of Mineral Resources.

ORDINATION

An ordination programme adapted by Lance & Williams (1967) from a suggestion of Gower (1966) carries out a principal co-ordinate (or Q-factor) analysis of the data. In Q-factor analysis, the associations of the specimens in terms of their attributes are determined algebraically by vectors in n-dimensional space. Most of the variance in the data is accounted for by the first vector and successively less by higher vectors, so that vector 5, the last vector determined by the programme, probably reflects random variance and was not used. For convenience, and because of our lack of geometrical intuition beyond three dimensions, the positions of the specimens are projected on to the plane of two vectors. The projections of the 6 supergroups on the 6 planes obtained for 4 vectors taken 2 at a time are shown in Figure 26. These diagrams should be regarded as single views of 4-dimensional space. The programme also places the attributes in the order of their correlation coefficients with each vector. Only the values for the first four vectors are given in Figure 25 because for the fifth vector most of the variance accounted for is probably random. Also on Figure 25 are shown the values of the correlation coefficients with statistical significance at the 1 percent level ($r = 0.195$) and 5 percent level ($r = 0.250$) for $n = 103$. Correlation coefficients with absolute values greater than the significance values are statistically significant; those less are not.

These results should be interpreted cautiously. Firstly, correlation coefficients calculated between variables of a constant sum, as are most of those of this study, contain an intrinsic interlock reflecting the fact that the strong negative correlation between certain groups is caused by strong positive correlation within groups. Secondly, the vectors are not extrinsic, but are related to the attributes. Thus, vector 1 is defined by its high positive correlation with insoluble residue and quartz, and its high negative correlation with Ca and CO_3. In other words, vector 1 accounts for the varying content of terrigenous minerals; impure limestones are associated with the positive part of vector 1, and pure limestone with the negative part. The other vectors shown in Figure 25 are likewise identified by the attribute or attributes with which they have the strongest correlation.

A further point in interpretation is that the vectors are sequential, so that vector 2 accounts for most of the variance that remains after the extraction of vector 1, and so on. By the time vector 5 is reached, much of the variance is random.

Finally, in interpreting the correlations shown in Figure 25 we may place as much value on those attributes whose correlation with the vector is not significant as in those whose correlation is significant. For example, the concentrations of calcisilt, Zn, and drusy mosaic, to name a few, are independent of the $CaCO_3$ content of the limestone (vector 1), whereas the concentrations of Mn, Ba, and Pb are dependent.

Correlation of Attributes and Vectors

Many of the correlations shown in Figure 25 are geologically trivial, and this discussion is focussed on less obvious relationships.

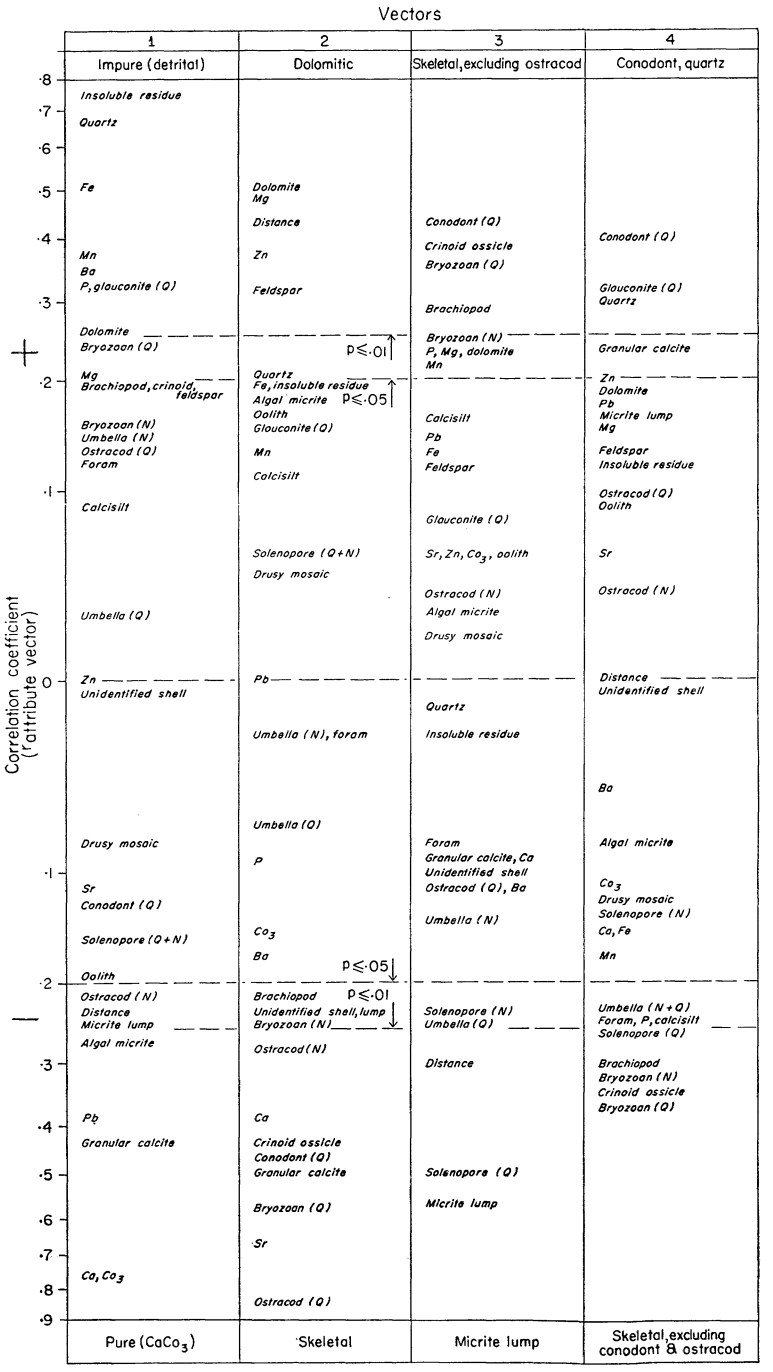

Figure 25. Correlation coefficients between attributes and vectors

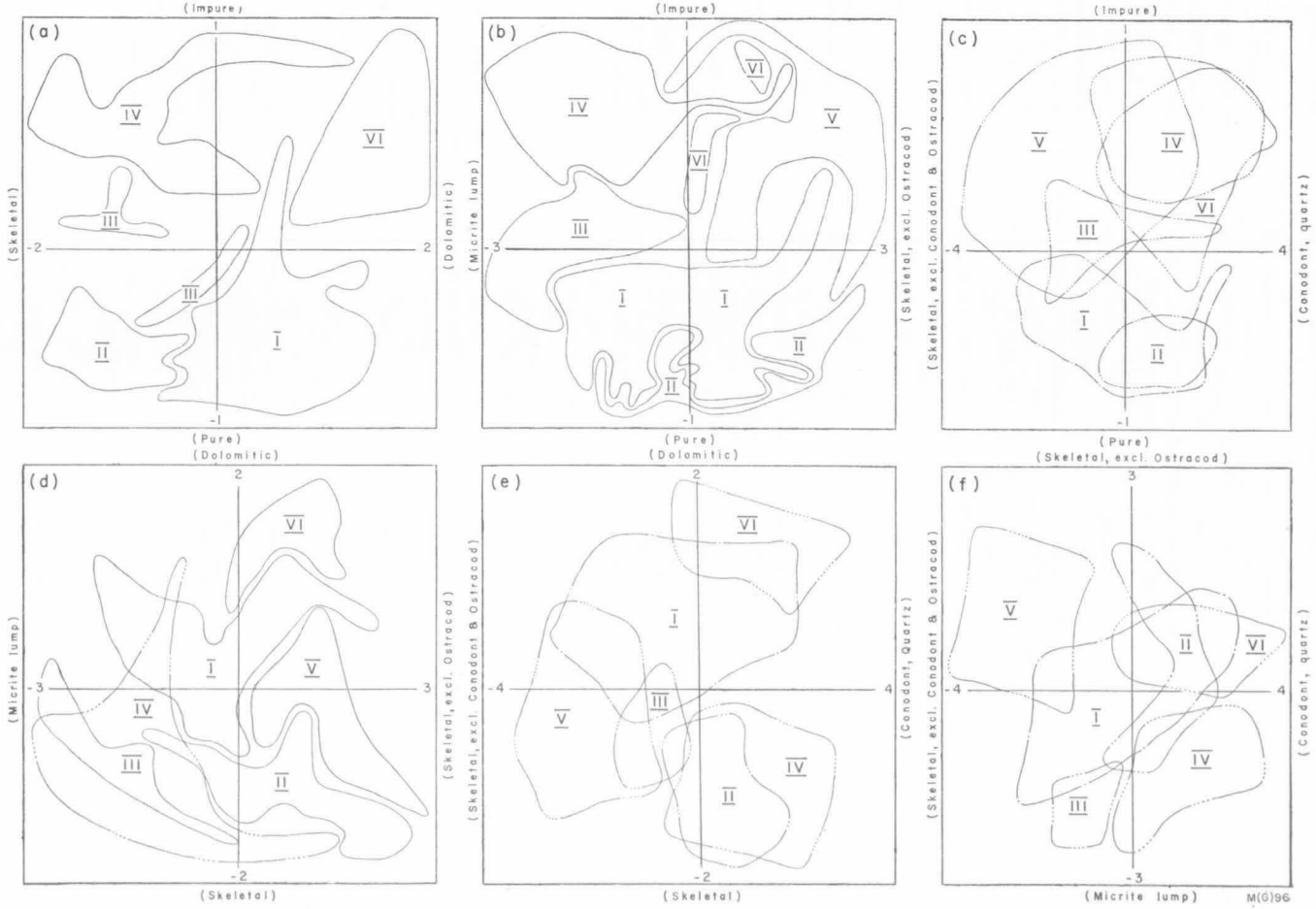

Figure 26. Plots of the specimens against the vectors

Vector 1

Glauconite (N), dolomite, and the chemical attributes Fe, Mn, Ba, and P are positively correlated ($p < 1\%$) with terrigenous impurities, and Pb and algal micrite negatively correlated. The chief contributors of skeletal matter (brachiopods, crinoids, bryozoans) are weakly positively correlated, and micrite lumps, distance, ostracods (N), and ooliths are negatively correlated. The negative correlation of distance with impurities confirms the intuitive notion that impurities in carbonate sediments decrease with distance from the shore. The implied negative correlation between algae (algal micrite, ooliths, micrite lumps, and possibly solenopore algae) and skeletal matter possibly indicates that they were deposited in environments which differed chiefly in distance from the shore. Ostracods (N) side with algae rather than with the other skeletal organisms. Zn and Sr are the only chemical attributes that lack correlation with vector 1.

These are the primary relationships to which those described below are secondary.

Vector 2

The positive correlation between dolomite and vector 1 shows up again in the positive correlation of feldspar, quartz, Fe, and insoluble residue with vector 2, identified as dolomite. In view of this association, the positive correlation of distance with vector 2 is at first sight disconcerting, but on examination is seen to be explained by its negative correlation with skeletal matter, which is most abundant near shore. Sr is the only attribute besides skeletal material that is negatively correlated with vector 2, indicating, as expected, that Sr is linked with skeletal material. The other elements and algae (except micrite lumps) are independent of vector 2.

Vector 3

Positively correlated with vector 3 are skeletal grains excluding ostracods ($p < 0.01$), dolomite, P and Mn ($p < 0.05$), and negatively correlated are algal grains—micrite lumps ($p < 0.01$) but also solenopore algae and *Umbella* ($p < 0.05$)—and distance ($p < 0.01$). Distance has the same relationship here as it has to vector 1; that is, it is associated with algae in negative correlation with skeletal matter and dolomite.

Vector 4

In vector 4, a further reduced assemblage of skeletal organisms (bryozoan, crinoid ossicle, and brachiopod) is negatively correlated with conodonts, glauconite, and quartz. Associated with the shells are solenopore algae (Q), *Umbella,* foraminifera, calcisilt, and P; and with the conodonts, granular calcite, and possibly Zn and dolomite. Insoluble residue, ostracods, and all the chemical attributes except P are independent.

Independent Attributes

Seven attributes—gastropod or pelecypod, *Renalcis,* calcisphere, oncolith, grapestone, birdseye, and glauconite (N) lack significant correlation with any of the vectors because of their rare occurrence and are not shown in Figure 25.

Drusy mosaic occurs in 17 specimens but nevertheless lacks significant correlation. This is a surprise because drusy mosaic seemed to me to occur generally in the cavity of brachiopods and would be correlated accordingly. The lack of correlation suggests that some of the cavity infillings were identified as granular calcite rather than drusy mosaic.

Five attributes—calcisilt, unidentified shell, oolith, coated grain, and rock fragments—are correlated with vectors at the 5 percent level of significance ($0.01 \leqslant p \leqslant 0.05$). Two of these (coated grain and rock fragments) occur in three specimens only, and are not shown in Figure 25. The rest occur frequently enough to have meaningful correlation coefficients. Ooliths are negatively correlated with vector 1, in association with distance and pure $CaCO_3$, confirming the notion that ooliths occur well away from the shore in reef complexes. Calcisilt is negatively correlated with vector 4, in association with a dominantly skeletal assemblage of bryozoans, crinoid ossicles, brachiopods, solenopore algae (Q), foraminifers, and *Umbella*. As expected, unidentified shell is associated with other skeletal grains in negative correlation with vector 2.

Dependent Attributes

The remaining attributes are more significantly correlated with one or other of the vectors.

Skeletal Grains

Crinoid ossicles, bryozoans, and brachiopods are associated in all four vectors. They correlate weakly with vector 1 (impurities), are associated with ostracods and conodonts in negative correlation with vector 2 versus dolomite, with conodonts versus micrite lumps and algae in vector 3, and alone in negative correlation with vector 4 against conodonts and quartz.

Of note in these associations is the independence of the ostracods. The weak negative correlation of ostracods (N) with impurities and brachiopods, crinoids, and bryozoans, and the independence of ostracods and vectors 3 and 4 suggests that ostracods inhabited a different environment from the other skeletal organisms. It is only in negative correlation with vector 2, versus dolomite, that the ostracods are associated with the other skeletal grains. The positive, dolomitic part of vector 2 possibly reflects a salinity higher than normal, and this explains the association of skeletal organisms, including ostracods, with a low tolerance of abnormal salinity, in negative correlation with dolomite. With the third and fourth vectors, ostracods become independent of the other skeletal organisms and algae.

Conodonts are independent of vector 1, are associated with all the skeletal types in vector 2, with all types but ostracods in vector 3, and occur alone versus brachiopods, bryozoans, and crinoid ossicles in vector 4. These results confirm the view that conodonts are independent of the content of terrigenous detritus, that they eschew dolomite, possibly because of the higher salinity, that they are associated with shelly invertebrates rather than with algae, and that they are associated with calcareous glauconitic quartz sandstone, as in the Lower Ordovician Pander Greensand of the Bonaparte Basin.

Foraminifers, mainly endothyrids, are independent of all the vectors except 4. In negative correlation with vector 4 ($0.01 < p < 0.05$), foraminifers are associated with bryozoans, crinoid ossicles, brachiopods, and *Umbella*.

Algae

Two attributes, solenopore algae and *Renalcis*, and probably a third, *Umbella*, are algae. Algal micrite and oncoliths were deposited by the activity of filamentous algae; and part, probably the greater part, of the micrite lumps, ooliths, grapestone, coated grains, calcispheres, and birdseyes were also deposited in the same way. Of these eleven attributes, *Renalcis*, calcispheres, oncoliths, birdseyes, coated grains, and grapestones occur too infrequently to have significant correlation, leaving solenopore algae, *Umbella*, algal micrite, micrite lumps, and ooliths. Associated in negative correlation with vector 1 are algal micrite ($p < 0.01$), micrite lumps and distance ($0.01 < p < 0.05$), and ooliths ($p = 0.05$). Algae, except lumps ($0.01 < p < 0.05$), are independent of vector 2, as is to be expected from organisms with a tolerance of different salinities. Micrite lumps and solenopores (Q) (both with $p < 0.01$) and *Umbella* (Q) are associated with negative correlation with vector 3. And in negative correlation with vector 4, *Umbella* (N and Q) and solenopores (Q) are associated for the first time with brachiopods, crinoid ossicles, and bryozoans. *Umbella* is associated with solenopore algae in vector 3 and 4 and with forams in vector 4, so that nothing new about its biological affinity—authors place it with the algae or foraminifers—is indicated by these associations.

The suspicion that micrite lumps and ooliths are at least in part poorly preserved algal micrite seems to be confirmed by the association of these attributes in vector 1. Their association in pure limestone deposited far from the shore reflects their chief occurrence in reef limestone.

Terrigenous Mineral or Rock Grains

Insoluble residue, quartz, and feldspar have significant correlation coefficients. Insoluble residue and quartz ($p < 0.01$) and feldspar ($p = 0.05$) are associated in positive correlation with vector 1, and also positively correlated with vector 2. They are independent of vector 3, and quartz is positively correlated with vector 4. The occurrence of terrigenous grains in impure limestone and dolomite is obvious, but the association of quartz, conodonts, and glauconite (Q) is not.

Diagenetic Minerals and Cement

Dolomite and glauconite (Q) are associated with impure carbonates (vectors 1, 2, and 4), as they are in the modern sediments of the Timor Sea (van Andel & Veevers, 1967, fig. 9.1). Granular calcite is obviously associated with the pure calcareous attributes of vector 1, and with the skeletal grains of vector 2, but less obviously with conodonts, glauconite, and quartz in vector 4.

Chemical Attributes

Table 8(2) contains the mean values of attributes in the supergroups and higher groupings up to the entire suite of specimens. The chemical analyses were compared with the compilations of Vinogradov & Ronov (1956), Graf (1960,

III, table 38), and Wolf, Chilingar, & Beales (1967, table III). The analyses compiled by these authors were made on whole samples, so that Ca, Mg, Ba, P, and Sr, also determined on whole samples of the Bonaparte material, are the only elements that are strictly comparable, because Cu, Fe, Mn, Pb, and Zn of the Bonaparte suite were determined on the fraction soluble in acetic acid. With the assumption that the elements in marine platform carbonates contain elements of the same order of magnitude, any notable discrepancies between analyses of the soluble fractions and those of whole samples are attributed to the differential concentration of elements in the insoluble residue.

Whereas the average Ca content of the Bonaparte suite (31.7%) roughly agrees with that of the Devonian and Carboniferous carbonate rocks of the Russian Platform (28%) (Vinogradov & Ronov, 1956, pp. 534-5), the average Mg content of the Bonaparte suite is much less (0.9% v. 6%); even the lowest Mg value of the Palaeozoic carbonates of the Russian Platform of about 2 percent (Vinogradov & Ronov, 1956, fig. 3), deposited during the quiet tectonic phase in the Upper Devonian (D_3) and Lower Carboniferous (C_1 and C_2), is twice the Mg value of the Bonaparte suite. A more sensitive index, the Ca/Mg ratio, underlines the contrast in Mg content: the average Bonaparte ratio is 35, that of the Devonian and Carboniferous of the Russian Platform and of North America (Vinogradov & Ronov, 1956, fig. 4), is about 8.

The average $\frac{Sr}{Ca} \times 10^3$ value of the Bonaparte suite is 1.2 ($\frac{Ca}{Sr} = 850$), and this value corresponds with that found in the Upper Devonian and Lower Carboniferous of the Russian Platform (Vinogradov & Ronov, 1956, fig. 6), which is a low value compared with that in earlier and later periods. This ratio also corresponds with those of North American limestones given by Wolf et al. (1967, table IX).

Ba and insoluble residue, which are strongly correlated, are slightly higher in the Bonaparte suite than in the contemporary suite of the Russian Platform, but Ba is some four to eight times lower than the average of the Illinois, Kansas, and Scottish suites listed by Wolf et al. (1967, table III).

Cu was not detectable (< 10 ppm) in the soluble fraction of any of the Bonaparte specimens. According to the various compilations of analyses, this is not an exceptionally low concentration, even for whole samples.

The Fe content of the Bonaparte suite is low (0.115%), some ten times lower than that of the Illinois carbonates listed by Wolf et al. (1967) and of the Russian carbonates (Vinogradov & Ronov, 1956, table 4); Mn is some two to four times lower than it is in the Russian, Kansas, and Illinois suites, and Zn fifteen times lower. These differences are taken as indicating that in order of increasing intensity Mn, Fe, and Zn are concentrated in the insoluble residue, and this is possibly borne out for Fe and Mn by their positive correlation with vector 1 (Fig. 25). In contrast, the average Pb value in the soluble fraction of 10 ppm is close to the mean values given by Wolf et al. (1967), though slightly lower than the values of the Kansas and Illinois suites, and this is interpreted as indicating that Pb is concentrated in the soluble fraction, confirmed by their positive correlation (Fig. 25). The Zn content of the soluble fraction, while independent of the content of insoluble residue (Fig. 25), is positively correlated with dolomite and Mg (vector 2), possibly because Zn substitutes for Mg.

From analyses of specimens classified as bahamites (pellet limestones), skeletal limestones, and oolites, Beales (1958, p. 1855) found that for Mg, Sr, Fe, and Mn, among other elements, skeletal limestones are intermediate between the bahamites and oolites, and that for Pb the bahamites are intermediate between the oolites and skeletal limestones. Table 9 shows that Beales' conclusions do not apply to the Bonaparte suite.

TABLE 9: TRACE ELEMENT COMPOSITION OF LIMESTONES

Limestone Type	Mg (%)	Sr (ppm)	Fe (%)	Mn (ppm)	Ba (ppm)	Pb (ppm)
Skeletal (supergroups II and V)	0.4	520	0.12	427	53	10
Oolites (specs. 456-1, 456-5B)	0.6	180	0.017	115	21	12
Bahamites (group *b*)	0.3	180	0.015	112	24	10

On the basis of these elements, the oolites and bahamites are virtually identical, and differ from skeletal limestones in containing less Sr, Mn, Fe, and Ba.

Compared with modern shelf carbonates (Stehli & Hower, 1961; Maxwell, Jell, & McKellar, 1964, app. II), the Bonaparte suite, in company with other ancient carbonates, contains much less Sr and much more Mn as the result of diagenesis and epigenesis.

Summary. Because the Precambrian to Tertiary limestones of the Russian Platform are the only suite that is well known geochemically, most of the comparisons made above necessarily refer to it. The Bonaparte suite and the contemporary part of the Russian Platform suite have similar Ca, Ba, and Sr contents; Mg is much lower in the Bonaparte suite; and insoluble residue higher. Greater tectonic activity of the neighbouring land, presumably responsible for the higher content of insoluble residue, cannot explain the lower Mg content, which is only explicable in terms of a factor preventing hypersalinity, such as a wet climate causing low evaporation, or continuous mixing of the shelf water with deeper oceanic water.

In comparison with other later Palaeozoic carbonate suites that have been chemically analysed—Carboniferous limestones from Illinois, Kansas, and Scotland (Wolf et al., 1967, table III)—the Bonaparte suite has much the same content of Sr and much less Ba. The Fe, Mn, and Zn in the soluble fraction of the Bonaparte suite are all much lower than they are in the whole samples from Illinois, Kansas, and Scotland, and this possibly indicates that these elements are concentrated in the insoluble residue. In contrast, the Pb of the soluble fractions of the Bonaparte suite has much the same value as the whole samples of the other suites, which indicates its concentration in the soluble fraction.

On the basis of these comparisons, the elements composing the Bonaparte carbonates have much the same proportions as those in the platform carbonates of Russia, Scotland, and the midcontinent of North America.

Individual Chemical Attributes

Barium. The correlation of Ba, determined on whole samples, with insoluble residue (vector 1) agrees with the relationships found by Vinogradov & Ronov (1956). Graf (1960, III, p. 6) notes that Ba is correlated with Mn, and this also

is borne out by this study (Fig. 25). As mentioned already, the average Ba content of 52 ppm is low, but it corresponds with that of the Upper Devonian and Lower Carboniferous carbonates of the Russian Platform (Vinogradov & Ronov, 1956), which were deposited during a period of tectonic calm. The insoluble residue content of the Russian carbonates ranges from 4 to 10 percent, and is appreciably lower than the 16.5 percent of the Bonaparte suite, which possibly reflects a slightly increased degree of tectonic activity.

Copper. The low concentration of Cu (< 10 ppm) in the soluble fraction parallels the low values of Beales' (1958) and others' whole samples (Graf, 1960, III, pp. 20-1).

Insoluble Residue is associated with quartz, Fe, Mn, Ba, P, glauconite, and dolomite in positive correlation with vector 1. Its associations with the various attributes are discussed separately.

Iron. As noted already, Fe in the soluble fraction of the Bonaparte suite (average 0.115%) is some ten times lower than it is in the whole samples of Illinois and Russian carbonates, which possibly indicates its concentration in the insoluble residue. Following the relationship in the Cedar Valley Formation of Iowa (Bisque & Lemish, 1959), Fe is weakly associated with dolomite in vectors 1 and 2, probably because part of the Fe is present in ferroan dolomite, as Oldershaw & Scoffin (1967) found in some British limestones. In vector 1, Fe is generally associated with insoluble residue, Mn, Ba, P, Mg, in antipathy to Ca, CO_3, and Pb, bearing out the conclusion of Seibold (1955), as quoted by Graf (1960, II, p. 32), that in the argillaceous limestone of the Lower Malm of southern Germany, Fe and P are associated in negative correlation with $CaCO_3$.

Lead. The Pb content of the soluble fraction of the Bonaparte suite (10 ppm) is similar to that of whole samples of other suites, and Pb and the soluble fraction (Fig. 25) are positively correlated, together indicating that Pb is concentrated in the soluble fraction, a conclusion opposite that of Wedepohl (1956), cited by Graf (1960, III, p. 24). Wedepohl found also that with some exceptions pure biogenic calcites normally contain no more than 1 ppm Pb. If the acid treatment effectively separates the detrital and non-detrital fractions, then the Bonaparte specimens contain an exceptional amount of Pb in their soluble fraction. The negative correlation of Pb and Mg in vector 1 and their independence in vector 2 contrasts with Wedepohl's (1956) result, reported by Graf (1960, III, p. 24), that the Pb contents of dolomite and limestone are of the same order of magnitude.

Magnesium. From the close association of Mg and dolomite (Fig. 25), it seems that most of the Mg is in the form of dolomite.

The strong negative correlation of Mg and the main skeletal types in vector 2 is probably due to two factors: first, skeletal organisms were inhibited by the high salinity that favours dolomitization (Ingerson, 1962, p. 829); and secondly, Mg was lost from the skeletons after death. That skeletons concentrated Mg during life is indicated by analyses of 7 to 16 percent $MgCO_3$ (2-5% Mg) in crinoids (Graf, 1960, II, table 2), and similar amounts in many other groups (see Lowenstam, 1963, table 1). Specimen 465-1, with 65 percent crinoid ossicles, has only 0.4 percent Mg, and a $\frac{Ca}{Mg}$ ratio of 106.0, presumably because most of the original Mg has been lost.

TABLE 10: CONCENTRATION OF CALCIUM AND MAGNESIUM IN FOSSILS AND ENCLOSING MATRIX

Specimen No.	Material	Ca	Ma	Ca/Ma	Average Ca/Ma
(1) 107-1	matrix	33.6	0.39	86.2	85.7
(2) 107-1	matrix	33.2	0.39	85.1	
(3) 107-1	crinoid columnal	36.7	0.65	56.5	
(4) 107-1	crinoid crown plates	37.8	0.18	210.0	
(5) 107-1	crinoid crown plates	39.0	0.25	156.0	
(6) 107-1	crinoid crown plates	39.3	0.11	353.7	255.5
(7) 107-1	crinoid crown plates	38.9	0.10	389.0	
(8) 107-1	crinoid crown plates	38.8	0.23	168.7	
(9) 100-7C	crinoidal limestone ('orthomarble')	38.7	0.35	110.6	
(10) 104-5	crinoidal limestone ('orthomarble')	30.3	0.25	121.2	109.0
(11) 104-12	crinoidal limestone ('orthomarble')	32.4	0.34	95.3	
(12) 105-850	matrix	33.5	0.51	65.7	
(13) 105-850	solenopore alga	39.6	0.50	79.2	77.5
(14) 105-850	solenopora alga	38.6	0.51	75.7	

TABLE 11: CONCENTRATION OF CALCIUM, MAGNESIUM AND STRONTIUM IN FOSSILS AND ENCLOSING MATRIX

Specimen No.	Material	Ca (%)	Mg (%)	Ca/Mg	Average Ca/Mg	Sr (%)	Sr/Ca x10³	Average Sr/Ca x10³
(1) 102-4	matrix	24.1	0.20	120.5		0.04	1.6	
(2) 102-4	matrix	14.4	0.28	51.5	68.7	0.005	0.3	1.0
(3) 102-4	matrix	24.8	0.73	34.0		0.025	1.0	
(4) 102-4	*Leptagonia* wtih sparry calcite infilling	31.5	0.20	157.5		0.08	2.5	
(5) 102-4	*Leptagonia* with sparry calcite infilling	32.7	0.18	181.7		0.04	1.2	
(6) 102-4	*Leptagonia* with sparry calcite infilling	32.2	0.18	178.9	161.5	0.06	1.9	1.7
(7) 102-4	*Leptagonia* with sparry calcite infilling	33.6	0.21	160.0		0.035	1.4	
(8) 102-4	*Leptagonia* with sparry calcite infilling	29.8	0.23	129.6		0.05	1.7	
(9) 107-6A	matrix	37.6	0.47	80.0		0.02	0.5	
(10) 107-6A	*Delepinea*	36.5	0.34	107.4	116.6	0.04	1.1	1.3
(11) 107-6A	*Delepinea*	39.0	0.31	125.8		0.06	1.5	
(12) 107-7	matrix	27.5	0.34	80.9		0.02	0.7	
(13) 107-7	*Rhipidomella*	38.6	0.31	124.5		0.055	1.4	
(14) 107-7	*Rhipidomella*	39.0	0.36	108.3		0.065	1.7	
(15) 107-7	*Rhipidomella*	39.3	0.30	131.0	123.1	0.065	1.6	1.6
(16) 107-7	*Rhipidomella*	38.9	0.34	114.4		0.07	1.8	
(17) 107-7	*Rhipidomella*	38.4	0.28	137.1		0.05	1.3	

TABLE 12: VECTOR COMPONENTS OF SUPERGROUPS

Vectors	Supergroup	Main Components
1	I	pure (non-terrigenous), dolomitic
	II	pure, skeletal
and	III	pure to impure, skeletal
	V	impure, skeletal
2	VI	impure, dolomitic
1	I, II	pure, lump, skeletal
and	III	lump
	IV	impure, lump
3	V	impure, skeletal (excl. ostracods)
	VI	impure
1	IV, VI	impure, conodonts and quartz
and 4	V	impure, skeletal (excl. ostracods and conodonts)
2	I	dolomitic
	II, V	skeletal
and	III, IV	lump, skeletal
3	VI	dolomitic, skeletal
2	IV	skeletal, conodonts and quartz
and	II, III	skeletal
4	V	dolomitic, skeletal (excl. ostracods and conodonts)
3	V	skeletal (excl. ostracods and conodonts)
and	IV	lump, conodonts and quartz
4	III	lump, skeletal (excl. ostracods and conodonts)

Notes: Specimens belonging to supergroup V are widely scattered on the plot of vectors 1 and 2, and are not shown on Figure 26. Supergroups that overlap each other in the other plots are not listed in Table 9.

Specific analyses of fossils and their enclosing matrix (Tables 10, 11) were made to study this question further. A crinoid columnal, five crinoid crown plates, and the enclosing matrix were analysed from specimen 107-1 (Table 10). The results are equivocal. Proportional to Ca the crown plates contain only one-third as much Mg as the matrix, while the single crinoid columnal has more than one and a half times as much Mg. It is unlikely that the crown plates concentrated less Mg than the columnals, and one can only conclude that the crown plates have lost a greater amount of Mg, but as both kinds of plates have the same crystal structure this is anomalous. The three crinoidal limestones analysed (Table 10) have the same $\frac{Ca}{Mg}$ ratio as specimen 465-1, and like that specimen show no obvious enrichment in Mg. Nor do the two specimens of solenopore algae (Table 10), which have $\frac{Ca}{Mg}$ ratio only slightly greater than that of the matrix. Even if dilution by the sparry calcite matrix within the thallus is allowed for in a generous proportion, say two parts matrix to one part thallus, the Mg enrichment is trivial compared to the high values of Mg (from 2.3 to 8.6%) in their modern representatives, the coralline algae (Graf, 1960, II, table 2). Once again we must conclude that any Mg concentrated by this solenopore alga has been subsequently lost.

Essentially the same results for Mg were found with the brachiopods whose analyses are shown in Table 11. If allowance is made for some dilution by the sparry calcite infilling in the *Leptagonia,* then proportional to Ca the three forms analysed are seen to contain about two-thirds as much Mg as the matrix. The additional analysis for Sr in these specimens narrows the range of interpretation, for, in line with the same kind of experiment by Kulp et al. (1952), proportional to Ca the brachiopods contain roughly twice as much Sr as the matrix, showing that at least some of the fossil calcite is not recrystallized. Averages for both species and matrices are larger than those of Kulp et al. (1952):

	$\frac{Sr}{Ca} \times 10^3$	
	Kulp et al. (1952)	*This Study*
Average of species	1.0	1.5
Average of matrices	0.5	0.8

The $\frac{Sr}{Ca} \times 10^3$ ratio of species analysed in this study is closer to the figure of 1.36 found by Thompson & Chow (1955). Prokofiev's (1964, p. 33) determination of 0.3 to 0.8 percent (3,000-8,000 ppm) Sr in brachiopods is suspiciously high.

In summary, this work bears out the comment of Wolf et al. (1967, p. 70) on the concentration of Sr in limestones that 'original differences may well be reduced (or completely erased) by differential solution recrystallization, or some other process'. The original ratio of Ca/Mg in crinoid plates has thus been changed, but in the brachiopods analysed the preservation of Sr, if only in a regular reduction of content, implies little recrystallization, so that their lower concentration of Mg than the matrix is possibly original.

In vector 1, Mg and dolomite are correlated with insoluble residue and negatively with distance from the shore, in harmony with the relationships found by Fairbridge (1957, fig. 10) in the Lower Ordovician carbonates of Pennsylvania, by Harbaugh & Demirmen (1964) in the Americus Limestone (Permian) of Kansas and adjacent states, by Bisque & Lemish (1959) in the Cedar Valley Limestone (Devonian) of Iowa, and by Lucchi (1964) in the Miocene of north Italy. Graf (1960, II, pp. 24-5) pointed out firstly that this relationship is not general, and secondly that the Pennsylvanian example may be explained by the kind and amount of authigenic silica rather than by the detrital content. Authigenic silica, including chert, is volumetrically unimportant in the Bonaparte specimens, so Graf's second point does not apply.

Mg is concentrated in two supergroups: VI with 4.6 percent, I with 0.6 percent. The specimens included in these supergroups came from markedly different depositional environments: inshore, including the littoral dolomites of the Waggon Creek Breccia (VI), and near-reef (I). It is the inshore carbonates, and not the reef carbonates, that are positively correlated with insoluble residue. The concentration of Mg in inshore carbonates is indicated in vector 1 by the negative correlation of Mg and distance, and in reef carbonates by the positive correlation of Mg and distance in vector 2.

The concentration of Mg probably comes from the higher salinity due to restricted marine circulation in these two depositional environments. In most

other ways these environments and their deposits are poles apart, and failure to make the distinction would lead to confusion.

Manganese. As noted above, Mn in sympathy with Fe and Zn seems to be concentrated in the insoluble residue. Mn is concentrated less intensely than the others—its average content in the soluble fraction of the Bonaparte suite (346 ppm) is two-thirds the concentration of 530 ppm in the whole samples of Russian Platform carbonates (Ronov & Ermishkina, 1959, table 1) and virtually the same as in the Upper Devonian and Lower Carboniferous part of the Russian suite, as read from Ronov & Ermishkina's figure 2.

As shown in Figure 25, Mn is strongly associated with insoluble residue, quartz, Fe, Ba, P, glauconite, and dolomite in positive correlation with vector 1, and less strongly associated with the main skeletal types (excluding ostracods), P. Mg, and dolomite in positive correlation with vector 3. In both vectors, Mn is negatively correlated with distance from the shore. The strong association of Mn with insoluble residue, Ba, and Fe, and its negative correlation with distance from the shore parallel the relationships found by Ronov & Ermishkina (1959, fig. 5) in the Russian Platform carbonates. Ronov & Ermishkina (1959) further relate the concentration of Mn in carbonate rocks to climate: higher concentration (840 ppm) in the humid zone, caused by greater leaching of the continent, and lower (330 ppm) in the arid zone. Without analyses of Mn on whole samples, the place of the Bonaparte suite in Ronov & Ermishkina's scheme cannot be determined.

The correlation of Mn and P is discussed below.

Phosphorus. The average P content of 0.015 percent of whole samples of the Bonaparte suite is the same as that in carbonates of the Russian Platform (Ronov & Korzina, 1960, *in* Wolf et al., 1967, pp. 125-7). The correlations of P in the Bonaparte suite are complex, probably reflecting the interplay of many factors: P is strongly positively correlated in vector 1 with insoluble residue, quartz, Fe, Mn, Ba, glauconite, and dolomite, and less strongly with the main skeletal types. It is weakly positively correlated with the main skeletal types in vectors 3 and 4 also, in vector 4 being negatively correlated with conodonts, the only attribute known to concentrate P, and with glauconite. The correlation between P and glauconite (in vector 1) is well documented for carbonates that commonly contain appreciable quartz (Graf, 1960, II, pp. 30-2). It is surprising therefore that P is not positively correlated with vector 4, in association with conodonts, glauconite, and quartz. Instead, in association with the main skeletal types, it is negatively correlated with these attributes.

The lack of correlation between P and conodonts is not surprising in view of the commonly very low volume of conodonts in limestone. In a personal communication to Graf (1960, II, p. 32), C. W. Collinson estimated 'that there is a 50 percent chance of recovering 15 or more conodonts in any 1,000 grams of marine limestone of Ordovician through Pennsylvanian age in the midwestern United States. Fifteen conodonts would correspond to about 1 ppm $Ca_3(PO_4)_2$' (which is equivalent to 0.2 ppm P).

As mentioned already, the association in German Mesozoic limestone of P and Fe in negative correlation with $CaCO_3$ (Seibold, 1955, *fide* Graf, 1960, II, p. 32) is repeated in the Bonaparte suite.

The correlation of P with the main skeletal types in vectors 1, 3, and 4, and with Mn and Mg in vectors 1 and 3, the only consistent relationships of P, suggests that the skeletons contribute most of the P. This hypothesis is supported by the high average P content of living bryozoans (0.4%) and articulate brachiopods (0.04%) (Graf, 1960, II, table 1). The further positive correlation of P with Mn has an interesting interpretation in view of Ingerson's (1962, p. 841) remarks on the concentration of these elements in bones and in the shells of the inarticulate brachiopod *Lingula*. And the correlation of Mg and P with the main skeletal types in vector 3 bears out Vinogradov's (1953) conclusion, reported by Wolf et al. (1967, p. 61), that P and Mg are positively correlated in certain groups, including brachiopods and bryozoans.

Strontium was determined on the whole sample in this study, and is thus directly comparable with published analyses. As noted earlier, the $\frac{Sr}{Ca} \times 10^3$ ratio of 1.2 corresponds with that of the Upper Devonian and Lower Carboniferous carbonates of the Russian Platform.

According to Graf (1960, III, p. 32), most Sr is substituted for Ca in calcite. Sr is correlated with Ca and the main skeletal types in vector 2, but is not correlated with Ca in vector 1; this indicates that Sr is concentrated in skeletons, as confirmed by the special study of brachiopods and matrices reported above. Most of the Sr is probably concentrated in crinoid ossicles, brachiopods, and bryozoans, which are the most abundant skeletons. Harbaugh & Demirmen (1964) found that in the Americus Limestone Sr correlated with bryozoans and fusulinids. In modern forms, these groups have a ratio range from 1.36 to 3.41 (Wolf et al., 1967, table VII). Kulp et al. (1952, tables 4, 7) found $\frac{Sr}{Ca} \times 10^3$ ratios of 0.20 to 0.80 in Silurian to Carboniferous crinoids, and 0.36 to 1.97 (average 1.03) in Palaeozoic brachiopods. The matrix enclosing the brachiopods was also analysed, and its ratio was 0.51, which shows (as does Figure 25) that the Sr is concentrated in skeletons. This result was found again in the study reported on pages 70 and 74. The strongest negative correlate with vector 2 is osrtacods. I have not been able to find analyses of the tests of ostracods to find out if, as Figure 25 suggests, ostracods concentrate Sr. According to Odum (1957, fig. 2), the crustaceans, a group near ostracods, have a high $\frac{Sr}{Ca} \times 10^3$ ratio of 6, and according to Richards' (1956, table 1) analyses of living specimens, the King Crab (*Limulus polyhemus*), admittedly a long way biologically from the ostracods, has a ratio of 30 to 300. Ostracods are volumetrically unimportant in the specimens analysed, except one, 443-14, which contains 20 percent. The lower Sr content (240 ppm) and $\frac{Sr}{Ca} \times 10^3$ ratio of 0.6 of this specimen shows that the ratio in these ostracods cannot exceed 3.

As illustrated by Wolf et al. (1967, fig. 6), Sternberg et al. (1959) found a progressive lowering of the Sr content of calcite from the basin through the fore-reef to the back-reef of the Steinplatte reef complex of Austria, and attributed this distribution to more thorough recrystallization away from the basin. Flügel &

Flügel-Kahler (1962) found a similar situation in the Sauwand limestone. The distribution of $\frac{Sr}{Ca} \times 10^3$ from the Famennian fore-reef across the reef complex to the associated inshore lagoonal deposits is more complex (Fig. 27). The highest concentration of Sr is in the offshore lagoonal deposits, probably due at least in part to their high skeletal content. This is confirmed by the high $\frac{Sr}{Ca} \times 10^3$ ratio of 2 in group *f*, all Burt Range Formation, interpreted as offshore lagoonal deposits.

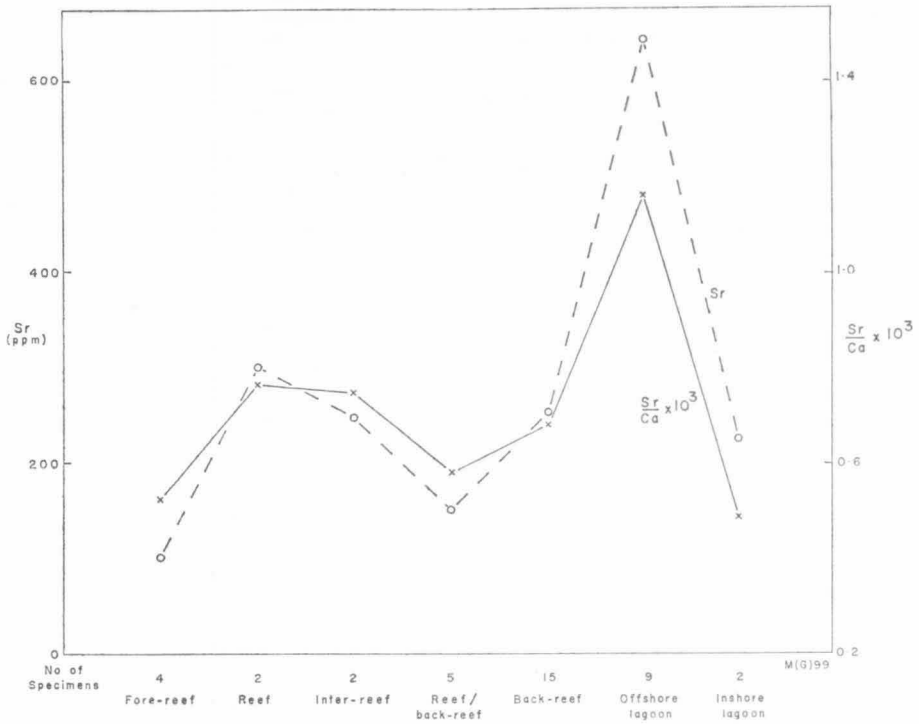

Figure 27. Distribution of Sr, and the $\frac{Sr}{Ca} \times 10^3$ ratio in the Famennian reef complex and associated deposits

The lowest contents are in the inshore lagoonal deposits, reef, back-reef, and fore-reef. In this reef complex, factors other than recrystallization evidently played a part in determining the Sr content. Certainly the slightly higher values of $\frac{Sr}{Ca} \times 10^3$ ratio in the reef and inter-reef compared with the fore-reef and reef/back-reef seem to contradict our field observations that the reef is more recrystallized than the other facies. Of course, a greater number of samples would be required to confirm these trends. In any case, the different pattern of distribution of Sr in the Austrian and Bonaparte reef complexes is not unexpected. Ingerson (1962, pp. 24-5) points out that 'it is extremely unlikely that geochemical criteria that were developed by studies of Pacific atolls for recognising reef facies would

apply to the fringing reefs of the Permian Basin or to Bahaman type reefs', and suggests that 'development of criteria should be by studies of a single type of reef and applied to that type only'. Because the Upper Devonian reefs of the Bonaparte and Canning Basins are the same type (Playford et al., 1966), criteria from the Bonaparte Basin will be applicable to the Canning Basin reefs and to any reefs that may be found by drilling beneath the Timor Sea (Veevers, 1967).

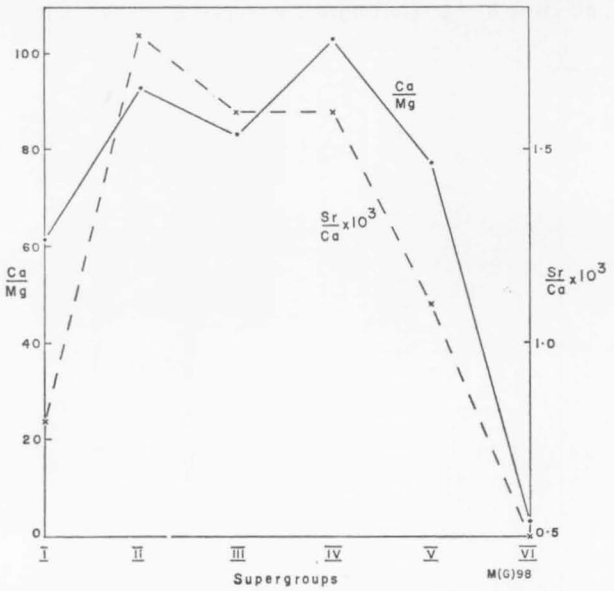

Figure 28. Ratios of $\frac{Ca}{Mg}$ and $\frac{Sr}{Ca} \times 10^3$ in the supergroups

The distribution of $\frac{Sr}{Ca} \times 10^3$ in the supergroups (Fig. 28) shows the concentration of Sr in skeletal limestones (decreasing from II to V). The correlation of $\frac{Sr}{Ca}$ with $\frac{Ca}{Mg}$ is partly due to the strong negative correlation between Sr and Mg. A strong negative correlation between Sr and Mg is found also in Scottish carbonates (*in* Graf, 1960, III, table 19) and in Recent carbonates of Florida (Siegel, 1961), but not in Indiana limestones (Kulp et al., 1952, table 1) or in the Sauwand limestone (Flügel & Flügel-Kahler, 1962). Wolf et al. (1967, p. 112) provide an apt comment: 'The final trace-element composition after diagenesis and epigenetic recrystallization, therefore, may be very complex and difficult to interpret'. What is, however, becoming clear is the light recrystallization of the Bonaparte specimens, so that their trace element composition is a fair reflexion of the original deposit.

The negative correlation between Sr and Mg in the Bonaparte suite as in the Americus Limestone (Harbaugh & Demirmen, 1964) agrees with Pilkey & Hower's (1960) conclusions that in echinoids Mg is directly related to both water temperature and salinity, and that Sr is inversely related to water temperature and is independent of salinity. Lowenstam (1963, pp. 156-7), however, found that in articulate brachiopods Sr correlates with salinity and temperature.

Zinc. The average value of Zn in the soluble fraction of the Bonaparte suite is 2.5 ppm, which is an order of magnitude lower than that of other suites (Wolf et al., 1967, table III; Graf, 1960, III, table 20), and probably indicates that most of the Zn is in the insoluble residue, possibly on clay minerals, or because of the positive correlation of Zn in the soluble fraction with Mg it may substitute for Mg in dolomite. Zn in the soluble fraction is independent of insoluble residue, and its only strong correlations are in vector 2 (Fig. 25): positive with Mg and dolomite, negative with the main skeletal types and Sr. Zn is possibly lacking in ancient skeletons, as shown by Prokofiev's (1964, p. 33) failure to detect Zn in Upper Carboniferous to Upper Permian brachiopods. The wide range of the Zn content of existing skeletal organisms (Graf, 1960, III, table 20, *after* Wedepohl, 1953), from 1 ppm in *Arca* to 180 ppm in *Globigerina,* indicates that the biochemistry of Zn is complex, and deserves more detailed study. Ingerson (1962, pp. 841-42) has pointed out that Zn is an essential part of an enzyme that may be involved in the formation of calcium carbonate by marine organisms. 'If a zinc-bearing enzyme is essential, or at least active, in the formation of organic carbonate, then we might expect that limestone of organic origin would contain zinc, whereas an inorganically precipitated one should be essentially free of it.' Prokofiev's (1964) and the present study discourage this hope.

My study is open to Ingerson's (1962, pp. 840-41) criticism that interpretation of chemical analyses of carbonate rocks is weakened by lack of data on the exact part of the rock in which the various trace elements are concentrated. The statistical analysis of the data and the discrimination for some elements between the acid-soluble fraction and the insoluble residue were made as a compromise between cost on the one hand and scientific return on the other. Many questions necessarily remain unanswered.

Distance

Distance is significantly correlated with three vectors: negatively with vectors 1 (impurities) and 3 (skeletal matter) and positively with vector 2 (dolomite). The apparently contradictory association of distance with dolomite and impurities in vector 2 probably arises from its antipathetic association with the main skeletal types, which are negatively correlated with vector 2, and from the occurrence of dolomite in reef limestone distant from the shore.

Relationships Between Supergroups and Vectors (Fig. 26)

As expected, the separation of the supergroups is greatest on the plot of the first two vectors and least on plots of the highest vectors. The main components of the supergroups as indicated by the plots of Figure 26 are listed in Table 12.

In summary, the composition of the analysed specimens may be expressed in varying proportions of four vectors or factors, each of two negatively correlated attributes or sets of attributes, in the following order of importance:

1 — impurity (terrigenous minerals) versus purity (pure calcite, or lack of terrigenous minerals).

2 — dolomite versus skeletal matter.

3 — skeletal matter, excluding ostracods, versus lumps and algae.

4 — conodonts and quartz versus skeletal matter, excluding conodonts and ostracods.

The information given in Table 12 can be condensed thus:

Supergroup	*Components*
I	pure calcite, dolomite
II	pure calcite, skeletal matter
III	skeletal matter, lumps
IV	impurities, skeletal matter, lumps, conodonts and quartz
V	impurities, skeletal matter excluding ostracods and conodonts
VI	impurities, dolomite, conodonts and quartz

Some of these conclusions require explanation. The vectors are important both relatively and absolutely. Supergroup I, influenced by vector 2 (dolomite), has a mean content of only 1.5 percent dolomite, but this is at least twice the dolomite content of all the other supergroups except VI. Supergroup III, with 48.6 percent lumps, and IV (34.7%) are the only ones dominated by lumps, yet II contains 53.4 percent and I 27.5 percent. The negative part of vector 3 is, however, not defined by lumps alone—solenopore algae (qualitative) are also important; in fact, the other attributes negatively correlated with vector 3 (*Umbella* (Q), solenopore (N)) are also algal, and it is the addition of this algal component to the lumps that sets III and IV apart from the others.

SUMMARY AND CONCLUSIONS

The Upper Devonian and Lower Carboniferous shelf sequence comprises four basic elements: (1) carbonates; (2) flat-bedded quartz sandstone deposited along a shifting shore; (3) cross-bedded quartz sandstone distributed across the platform by tidal currents; and (4) siltstone and shale deposited in the basinal part of the shelf. The chief single factor governing the proportions and distributions of these elements was the rate of vertical movement in the source and deposi-

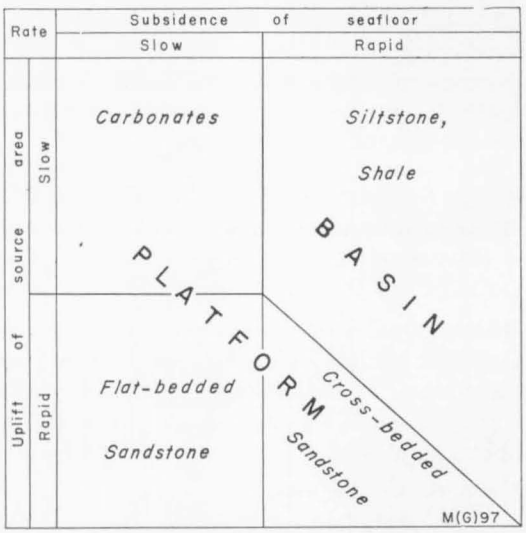

Figure 29. Bonaparte Basin Shelf sediments related to vertical movements in the source and depositional areas

tional areas (Fig. 29). The second factor was distance from the shore; this determined (a) the lateral terrigenous sequence, from shore to open basin, of conglomerate, pebbly quartz sandstone, quartz sandstone, shale, and siltstone

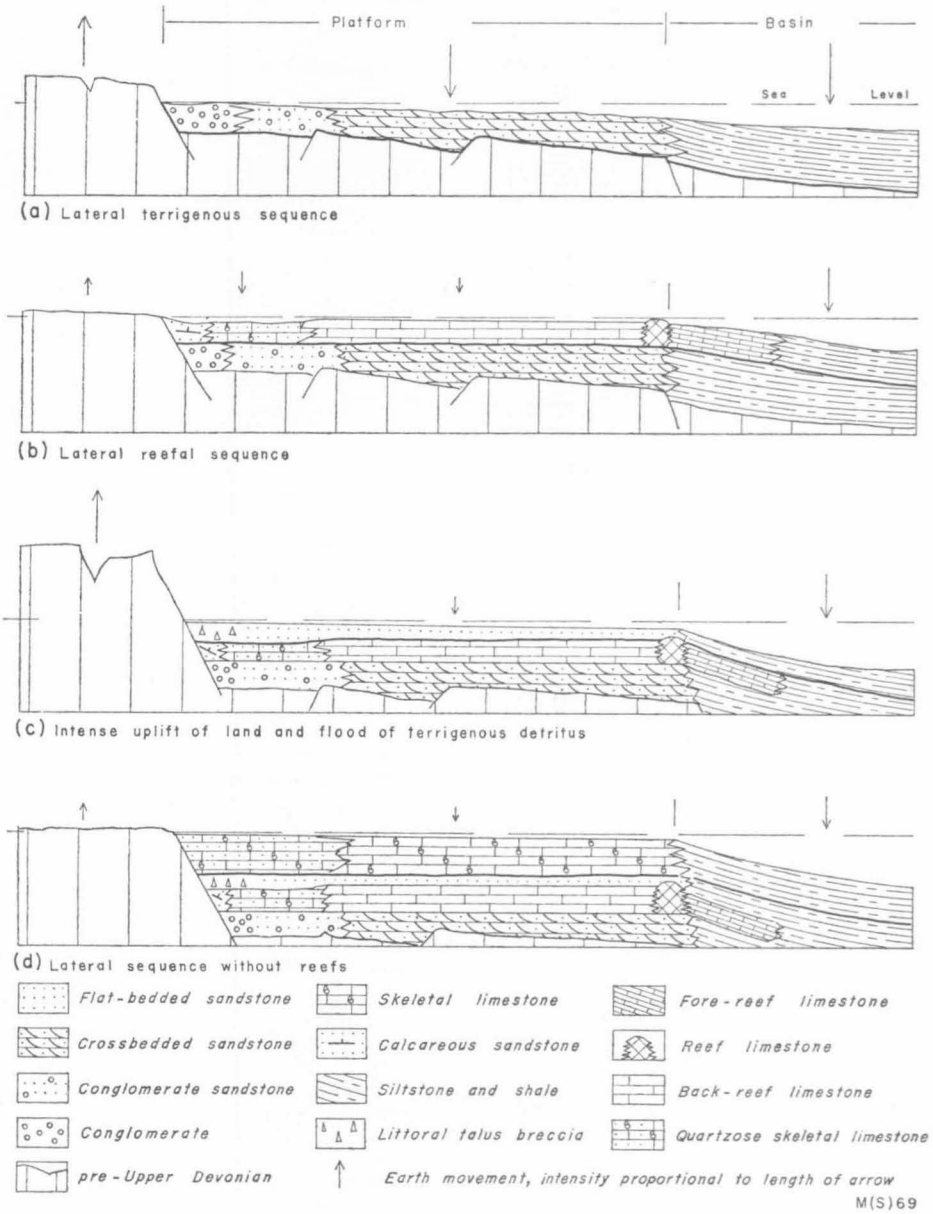

Figure 30. Evolution of the Upper Devonian and Lower Carboniferous sequence

(Fig. 30a); (b) the lateral reefal facies sequence of inshore lagoon, offshore lagoon, back-reef, reef and inter-reef, fore-reef, and basinal shale and siltstone (Fig. 30b); and (c), in the late Tournaisian and Visean, the simpler lateral sequence, without reefs, of inshore quartzose skeletal limestone, offshore skeletal limestone, and basinal siltstone and shale (Fig. 30d). The third factor, causing an end to reef deposition, was the mid-Tournaisian disruption of the pre-existing steady state by an intense uplift of the land and accompanying influx of detritus levelling out the sea floor (Fig. 30c).

All the chief vertical and horizontal facies variations in the shelf sequence are accounted for by these three factors.

The carbonate rocks were deposited in two broad environments:

(a) A marine environment in which circulation of the sea water was restricted by barrier reefs. Reef and back-reef sediments were deposited in very shallow water, fore-reef sediments on the fore-reef slope down to a depth of several hundred feet, inter-reef sediments in channels that cut across the reef, and lagoonal sediments in water deep enough to cover most of the lagoon even at low tide. Marine circulation was greatest over the fore-reef slope, less over the lagoon, and least over the back-reef. The salinity was lowest in parts of the inshore lagoon because of dilution from rivers, high in other very shallow parts, near-normal over the rest of the lagoon and over the fore-reef and inter-reef, and highest over the reef/back-reef. All but a few specimens of supergroups I to IV (Frasnian to early Tournaisian) were deposited in this environment.

(b) A shallow marine environment open to the sea, in which supergroup V (late Tournaisian and Visean) was deposited.

The remaining carbonates with a considerable proportion of terrigenous material (group VI) were deposited close inshore.

The basinal siltstone and shale were deposited in front of the fore-reef deposits in water whose depth must have exceeded several hundred feet.

ACKNOWLEDGMENTS

I have drawn heavily on the assistance of colleagues in the Bureau of Mineral Resources both for information on particular subjects and for criticism. R. L. Folk, University of Texas, made stimulating comments in the field and the laboratory, as did P. E. Playford, Geological Survey of Western Australia. I owe thanks for criticism of the manuscript to J. R. Conolly and W. G. H. Maxwell, University of Sydney, and C. E. B. Conybeare, Australian National University. R. C. Moore made available to me the facilities of the Paleontological Institute of the University of Kansas, in which I made the modal analyses of limestone. I thank G. N. Lance and W. T. Williams, CSIRO Division of Computing Research, for the use of their programme, and Dr Williams in particular for help in all aspects of the classification.

The photomicrographs, except for three taken by R. Helby of the Geological Survey of New South Wales, were taken by J. E. Zawartko, BMR.

REFERENCES

ALLEN, J. R. L., 1963a—The classification of cross-stratified units, with notes on their origin. *Sedimentology*, 2, 93-114.

ALLEN, J. R. L., 1963b—Asymmetrical ripple marks and the origin of water-laid cosets of cross-strata. *Liverpool Manchester geol. J.*, 3(2), 187-236

ALLEN, J. R. L., 1966—On bed forms and palaeocurrents. *Sedimentology*, 6, 153-90.

BANNER, F. T., and WOOD, G. V., 1964—Recrystallization in microfossiliferous limestones. *Geol. J.*, 4(1), 21-34.

BATHURST, R. G. C., 1958—Diagenetic fabrics in some British Dinantian limestones. *Liverpool Manchester geol. J.*, 2(1), 11-36.

BATHURST, R. G. C., 1964—Diagenesis and paleoecology: a survey, *In* IMBRIE, J., and NEWELL, N.D. (Eds), APPROACHES TO PALEOECOLOGY, 319-44. *N.Y., Wiley.*

BATHURST, R. G. C., 1966—Boring algae, micrite envelopes and lithification of molluscan biosparites. *Geol. J.*, 5(1), 15-32.

BEALES, F. W., 1958—Ancient sediments of Bahaman type. *Bull. Amer. Ass. Petrol. Geol.*, 42(8), 1845-80.

BISQUE, R. E., and LEMISH, J., 1959—Insoluble residue—magnesium content relationship of carbonate rocks from the Devonian Cedar Valley Formation. *J. sediment. Petrol.*, 29(1), 73-6.

BONHAM-CARTER, G. F., 1956—A numerical method of classification using qualitative and semi-qualitative data, as applied to the facies analyses of limestones. *Bull. Canad. Petrol. Geol.*, 13, 482-502.

CARROLL, Dorothy, 1947—Heavy residues of soils from the lower Ord River Valley, Western Australia. *J. sediment. Petrol.*, 17(1), 8-17

CROOK, K. S. W., 1965—The classification of cross-stratified units, comment on a paper by J. R. L. Allen. *Sedimentology*, 5, 249-54.

CURRAY, J. R., 1956—The analysis of two-dimensional orientation data. *J. Geol.*, 64(2), 117-31.

DICKINS, J. M., ROBERTS, J., and VEEVERS, J. J., 1968—Permian geology of the northeastern part of the Bonaparte Gulf Basin. *Bur. Miner. Resour. Aust. Rep.* (in prep.).

DUNBAR, C. O., and RODGERS, J., 1957—PRINCIPLES OF STRATIGRAPHY. *N.Y., Wiley.*

DUNHAM, R. J., 1962—Classification of carbonate rocks according to depositional texture. *Amer. Ass. Petrol. Geol. Mem.* 1, 108-21.

FAIRBRIDGE, R. W., 1957—The dolomite question. *In* R. J. LEBLANC and J. G. BREEDING (Eds)—Regional aspects of carbonate deposition. *Soc. econ. Paleont. Miner. spec. Publ.* 5, 80-99.

FLÜGEL, E., and FLÜGEL-KAHLER, E., 1962—Mikrofazielle und geochemische Gliederung eines obertriadischen Riffes der nördlichen Kahlalpen. *Mitt. Mus. Bergb. Geol. Techn. Landesmus. 'Joanneum', Graz*, 24, 1-128.

FOLK, R. L., 1955—Student operator error in determination of roundness, sphericity, and grain size. *J. sediment. Petrol.*, 25, 297-301.

FOLK, R. L., 1961—PETROLOGY OF SEDIMENTARY ROCKS. *Austin, Hemphill.*

FOLK, R. L., 1962—Spectral subdivision of limestone types. *Amer. Ass. Petrol. Geol. Mem.* 1, 62-84.

FOLK, R. L., 1966—A review of grain-size parameters. *Sedimentology*, 6, 73-93.

FOLK, R. L., and WARD, W. C., 1957—Brazos River bar, a study in the significance of grain-size parameters. *J. sediment. Petrol.*, 27, 3-27.

FRIEDMAN, G. M., 1958—Determination of sieve-size distribution from thin section data for sedimentary petrological studies. *J. Geol.*, 66, 394-416.

FRIEDMAN, G. M., 1967—Dynamic processes and statistical parameters compared for size frequency distribution of beach and river sands. *J. sediment. Petrol.* 37, 327-54.

GLOVER, J. E., 1963—Studies in the diagenesis of some Western Australian sedimentary rocks. *J. Roy. Soc. W. Aust.*, 46(2), 33-56.

GOWER, J. C., 1966—Some distance properties of latent root and vector methods used in multivariate analysis. *Biometrika*, 53, 325-38.

GRAF, D. L., 1960—Geochemistry of carbonate sediments and sedimentary carbonate rocks. I. Carbonate mineralogy. Carbonate sediments. II. Sedimentary carbonate rocks. III. Minor element distribution. IV.A. Isotopic composition. Chemical analyses. IV.B. Bibliography. *Ill. State geol. Surv. Circ.* 297, 298, 301, 308, 309.

HARBAUGH, J. W., and DEMIRMEN, F., 1964—Application of factor analysis to petrologic variations of Americus Limestone (Lower Permian), Kansas and Oklahoma. *Kansas geol. Surv. spec. Publ.* 15.

HARVEY, J. G., 1966—Large sand waves in the Irish Sea. *Mar. Geol.*, 4(1), 49-55.

HIRST, D. M., and NICHOLLS, G. D., 1958—Techniques in sedimentary geochemistry: (1) separation of the detrital and non-detrital fractions of limestones. *J. sediment. Petrol.*, 28, 468-81.

IMBRIE, J., and PURDY, E. G., 1962—Classification of modern Bahamian carbonate sediments. *Amer. Ass. Petrol. Geol. Mem.* 1, 253-72.

INGERSON, E., 1962—Problems of the geochemistry of sedimentary carbonate rocks. *Geochim. cosmochim. Acta*, 26, 815-47.

JONES, P. J., 1962—The ostracod genus *Cryptophyllus* in the Upper Devonian and Carboniferous of Western Australia. *Bur. Miner. Resour. Aust. Bull.* 62(3).

JONES, P. J., 1968—Upper Devonian Ostracoda and Eridostraca from the Bonaparte Gulf Basin, northwestern Australia. *Bur. Miner. Resour. Aust. Bull.* 99.

JORDAN, G. F., 1962—Large submarine sand waves. *Science*, 136 (3519), 839-48.

KARCZ, I., and BRAUN, M., 1964—Sedimentary structures and palaeocurrents in the Triassic sandstone of Makhtesh Ramon. *Israel geol. Surv. Bull.* 38.

KRYNINE, P. D., 1948—The megascopic study and field classification of sedimentary rocks. *J. Geol.*, 56, 130-65.

KULP, J. L., TUREKIAN, K. K., and BOYD, D. W., 1952—Sr contents of limestones and fossils. *Bull. geol. Soc. Amer.*, 63, 701-16.

LANCE, G. N., and WILLIAMS, W. T., 1967—Mixed-data classificatory programs. I. Agglomerative systems. *Aust. Computer J.*, 1, 15-20.

LEE, G. W., 1912—The British Carboniferous Trepostomata. *Geol. Surv. Great Britain, Palaeont.*, 1(3).

LOEBLICH, A. R., and TAPPAN, H., 1964—Sarcodina. *In* MOORE, R. C., Ed., TREATISE ON INVERTEBRATE PALEONTOLOGY. Part C, Protista 2. *Geol. Soc. Amer. & Univ. Kansas Press.*

LOWENSTAM, H., 1963—Biological problems relating to the composition and diagenesis of sediments. *In* DONNELLY, T. W., Ed., THE EARTH SCIENCES. *Rice University, Semicentennial Publ., Univ. Chicago Press*, 137-95.

LUCCHI, F. R., 1964—Ricerche sedimentologiche sui Lembi Alloctoni della Val Marechia. *G. Geol. Ann. Mus. Geol. Bologna*, Ser. 2., 32(2), 543-626.

MASLOV, V. P., 1966—On the umbellas. *Trudy geol. Inst. ANSSSR*, 143, 221-2 (in Russian).

MASON, C. C., and FOLK, R. L., 1958—Differentiation of beach, dune, and aeolian flat environments by size analysis, Mustang Island, Texas. *J. sediment. Petrol.*, 28, 211-26.

MAXWELL, W. G. H., JELL, J. S., and MCKELLAR, R. G., 1964—Differentiation of carbonate sediments in the Heron Island Reef. *J. sediment. Petrol.*, 34(2), 294-308

MCKEE, E. D., 1940—Three types of cross-lamination in Palaeozoic rocks of northern Arizona. *Amer. J. Sci.*, 238, 811-24.

MCKEE, E. D., REYNOLDS, M. A., and BAKER, C. H., 1962—Laboratory studies on deformation in unconsolidated sediment. *U.S. geol. Surv. prof. Pap.* 450-D, 151-60.

MOSS, A. J., 1962—The physical nature of common sandy and pebbly deposits. Pt I. *Amer. J. Sci.* 260, 337-73.

NELSON, H. F., BROWN, C. W., and BRINEHAN, J. H., 1962—Skeletal limestone classification. *Amer. Ass. Petrol. Geol., Mem.* 1, 224-52.

NIEHOFF, W., 1958—Die primär gerichteten Sedimentstrukturen insbesondere die Schrägschichtung im Koblenzquarzit am Mittelrhein. *Geol. Rdsch.*, 47(1), 252-321, 469.

ODUM, H. T., 1957—Biochemical deposition of strontium. *Texas. Univ., Inst. mar. Sci.*, 4, 39-114.

OFF, T., 1963—Rhythmic linear sand bodies caused by tidal currents. *Bull. Amer. Ass. Petrol. Geol.*, 47(2), 324-41.

OLDERSHAW, A. E., and SCOFFIN, T. P., 1967—The source of ferroan and non-ferroan calcite cements in the Holkin and Wenlock Limestones. *Lpool Manchester geol. J.*, 5(2), 309-20.

PETTIJOHN, F. J., 1957—SEDIMENTARY ROCKS. 2nd Ed. *N.Y., Harper.*

PIA, J., 1937—Die wichtigsten Kalkalgen des Jung Palaeozoikums und ihre geologische Bedeutung. *C.R. 2nd Congr. Strat. Carb.*, 2, 765-856.

PILKEY, O. H., and HOWER, J., 1960—The effect of environment on the concentration of skeletal magnesium and strontium in *Dendraster*. *J. Geol.*, 68, 203-16.
PLAYFORD, P. E., and LOWRY, D. C., 1967—Devonian reef complexes of the Canning Basin, Western Australia. *Geol. Surv. W. Aust. Bull.* 118.
PLAYFORD, P. E., VEEVERS, J. J., and ROBERTS, J., 1966—Upper Devonian and possible Lower Carboniferous reef complexes in the Bonaparte Gulf Basin. *Aust. J. Sci.*, 28(11), 436-7.
POTTER, P. E., and PETTIJOHN, F. J., 1963—PALEOCURRENTS AND BASIN ANALYSIS. *N.Y., Academic Press.*
POWER, M. C., 1953—A new roundness scale for sedimentary particles. *J. sediment. Petrol.*, 23, 117-19.
POYARKOV, B. V., 1966—Devonian charophytes in Tien-Shan. *Trudy geol. Inst. ANSSSR*, 143, 161-200 (in Russian).
PROKOFIEV, V. A., 1964—Spectrographic determination of trace elements in Palaeozoic brachiopod shells. *Geochem. Int.*, 1, 32-6.
QUIRKE, T. T., 1930—Spring pits; sedimentation phenomena. *J. Geol.*, 38, 88-91.
REITLINGER, E. A., 1966—On the umbellas in the European part of the USSR and in Transcaucasia. *Trudy geol. Inst. ANSSSR.*, 143, 213-220 (in Russian).
RICHARDS, A. G., 1956—Studies in arthropod cuticle. XII. Ash analyses and microincineration. *J. Histochem. Cytochem.*, 4, 140-52.
RONOV, A. B., and ERMISHKINA, A. I., 1959—Distribution of manganese in sedimentary rocks. *Geochemistry (USSR)* (Engl. trans.), 1959(3), 254-78.
RONOV, A. B., and KORZINA, G. A., 1960—Phosphorus in sedimentary rocks. *Geochemistry (USSR)* (Eng. trans.), 1960(8), 805-29.
SAKSMAN, G. G., TOLBERT, W. H., and VILLARS, R. G., 1966—Sand-ridge migration in St Andrew Bay, Florida. *Mar. Geol.*, 4, 11-19.
SEIBOLD, E., 1955—Zum Phosphat-, Eisen- und Kalkgehalt einiger Horizonte des süddeutschen Jura. *Geol. Jb. geol. Landesanst.*, 70, 577-610.
SHEPARD, F. P., 1963—SUBMARINE GEOLOGY. 2nd Ed. *N.Y., Harper & Row.*
SHROCK, R. R., 1948—SEQUENCE IN LAYERED ROCKS. *N.Y., McGraw-Hill.*
SIEGEL, F. R., 1961—Variations of Sr/Ca ratios and Mg contents in Recent carbonate sediments of the northern Florida Keys area. *J. sediment. Petrol.*, 31, 336-42.
STEHLI, F. G., and HOWER, J., 1961—Mineralogy and early diagenesis of carbonate sediments. *J. sediment. Petrol.*, 31(3), 358-71.
STERNBERG, E. T., FISCHER, A. G., and HOLLAND, H. D., 1959—Strontium contents of calcites from the Steinplatte Reef Complex, Austria. *Bull. geol. Soc. Amer.*, 70(12, 2), 1681.
STRIDE, A. H., 1963—Current-swept sea floors near the southern half of Great Britain. *Quart. J. geol. Soc. Lond.*, 119, 175-99.
STRIDE, A. H., 1965—Preservation of some marine current-bedding. *Nature*, 206 (4983), 498-9.
THOMAS, G. E., 1962—Grouping of carbonate rocks into textural and porosity units for mapping purposes. *In* HAM, W. E., Ed., Classification of carbonate rocks. *Amer. Ass. Petrol. Geol. Mem.* 1, 193-223.
THOMPSON, T. G., and Chow, T. J., 1955—The Sr/Ca atom ratio in carbonate-secreting marine organisms. *Deep-Sea Research*, 3 *(Suppl. Paps Mar. Biol. Oceanogr.)*, 20-30.
TRAVES, D. M., 1955—The geology of the Ord-Victoria Region, northern Australia. *Bur. Miner. Resour. Aust. Bull.* 27.
VAN ANDEL, T. H., and VEEVERS, J. J., 1967—Morphology and sediments of the Timor Sea. *Bur. Miner. Resour. Aust. Bull.* 83.
VEEVERS, J. J., 1967a—Combined analysis of size, shape and compositional mode of grains in altered sandstones. *J. sediment. Petrol.*, 37(4), 1251.
VEEVERS, J. J., 1967b—The Phanerozoic geological history of northwest Australia. *J. geol. Soc. Aust.*, 14(2), 253-71.
VEEVERS, J. J., and MAFFI, C., 1968—Jointing related to structure in sandstones of the Bonaparte Gulf Basin. *Appendix to* Veevers & Roberts, 1968.
VEEVERS, J. J., and ROBERTS, J., 1966—Littoral talus breccia and probable beach rock from the Visean of the Bonaparte Gulf Basin. *J. geol. Soc. Aust.*, 13(2), 387-403.
VEEVERS, J. J., and ROBERTS, J., 1968—Upper Devonian and Carboniferous geology of the Bonaparte Gulf Basin, northwest Australia. *Bur. Miner. Resour. Aust. Bull.* 97.

VINOGRADOV, A. P., 1953—THE ELEMENTAL CHEMICAL COMPOSITION OF MARINE ORGANISMS. *New Haven, Yale Univ. Press.*

VINOGRADOV, A. P., and RONOV, A. B., 1956—Composition of the sedimentary rocks of the Russian Platform in relation to the history of its tectonic movements. *Geochemistry (USSR)* (English Transl.), 195(6), 533-559.

VON DER BORCH, C. C., 1965—Distribution of detrital minerals in Recent carbonate sediments from the Sahul Shelf, northern Australia. *J. geol. Soc. Aust.*, 12(2), 333-9.

WALKER, T. R., 1957—Frosting of quartz grains by carbonate replacement. *Bull. geol. Soc. Amer.*, 68, 267-68.

WALKER, T. R., 1967—Formation of red beds in modern and ancient deserts. ***Bull. geol. Soc. Amer.***, 78, 353-68.

WARNE, S. ST J., 1962—A quick field or laboratory staining scheme for the differentiation of the major carbonate minerals. *J. sediment. Petrol.*, 32(1), 29-38.

WEDEPOHL, K. H., 1953—Untersuchungen zur Geochemie des Zinks. *Geochim. cosmochim. Acta*, 3, 93-142.

WEDEPOHL, K. H., 1956—Untersuchungen zur Geochemie des Bleis. *Ibid.*, 10, 69-148.

WERMUND, E. G., 1965—Cross-bedding in the Meridian Sand. *Sedimentology*, 5, 69-79.

WOLF, K. H., 1965a—Petrogenesis and palaeoenvironment of Devonian algal limestones of New South Wales. *Sedimentology*, 4, 113-178.

WOLF, K. H., 1965b—Gradational sedimentary products of calcareous algae. *Ibid.*, 5, 1-37.

WOLF, K. H., 1965c—Littoral environment indicated by open-space structures in algal limestones. *Paleogeogr., Paleoclimat., Paleoecol.*, 1, 183-223.

WOLF, K. H., CHILINGAR, G. V., and BEALES, F. W., 1967—Elemental composition of sedimentary carbonates. *In* CARBONATE ROCKS, ed. CHILINGAR, G. V., BISSELL, H. J., and FAIRBRIDGE, R. W. *N.Y., Elsevier.*

WOOD, A., 1943—The algal nature of the genus *Koninckopora* Lee, its occurrence in Canada and western Europe. *Quart. J. geol. Soc. Lond.*, 98(3-4), 205-221.

WRAY, J. L., 1967—Upper Devonian calcareous algae from the Canning Basin, Western Australia. *Prof. Contr. Color. Sch. Mines*, 3.

TABLE 13. DETERMINATIONS OF SPECIMENS IN TERMS OF GROUPS, FORMATIONS, PARTS OF REEFAL OR NON-REEFAL SEQUENCES, AND ROCK TYPE.

Field Number	Groups[1]	Formation[2]	Reef Complex and Associated Sediments[3]							Non-Reefal	Rock Type
			Reef	Inter reef	Fore reef	reef Back reef	Back reef	Lagoon	Inshore Lagoon		
			R	IR	FR	R-BR	BR	L	Li		
456-2	I a 1	Dun				1					dolomitic sparry oolite
443-11							1				
456-6B	2		1								sparry algal micrite limestone
455-2			1								
446-5B	3					1					sparry oolite
456-1	4					1					
448					1						skeletal sparry algal micrite
455-3B	5					1					algal micrite limestone
455-1B				1							sparry oncolite
456-7A	b 6	Dun			1						quartzose skeletal sparry lump limestone
466-2	7			1							sparry lump limestone
149-3B					1						
149-3A	8				1						
149-2B						1					
459-75	c 9	Duw					x	x			skeletal solenopore sparry lump limestone
105-575		Dub						1			solenopore sparry lump limestone
443-6	10	Dun					1				crinoidal algal micrite limestone
12-3		Duw					x	x			**Renalcis** sparry lump limestone
459-2A	11	Duw					x	x			solenopore algal micrite limestone
443-9		Dun					1				dolomitic solenopore algal micrite limestone
Bonaparte No. 1											
687′	d 12	Clt								NR	skeletal calcisiltite
443-20	13	Dun					1				dolomitic sparry lump limestone
459-200	14	Duw					x	x			dolomitic lump limestone
443-3		Dun					1				dolomitic birdseye limestone
459-15	15	Duw					x	x			**Renalcis** calcisiltite
103-17C		Clb					x	x			brachiopodal calcisiltite
443-23A	I e 16	Dun					1				sparry oolite
146-17		Clb						x			lump limestone
449-2	17	Dun					1				lump sparry oncolite
100-16	18	Clb					x	x			sparry lump limestone
100-9		Clb					x	x			
443-12	19	Dun					1				
443-8		Dun					1				
100-8A	20	Clb					x	x			
449-1		Dun	1								
100-7xA	II f 21	Clb									skeletal sparry lump limestone
100-17		Clb					x	x			
100-11	22	Clb					x	x			skeletal sparry algal micrite limestone
100-6A		Clb					x	x			
100-22	23	Clb					x	x			lump sparry skeletal limestone
100-20		Clb					x	x			
443-25	g 24	Dun					1				skeletal sparry lump limestone
443-16		Dun					1				
443-17	25	Dun					1				
7-1	26	Tournaisian	1				x				skeletal sparry silty lump limestone
443-22	27	Dun					1				skeletal sparry lump limestone
443-14		Dun					1				
100-19A	28	Clb					x	x			lump sparry skeletal limestone
100-13B		Clb					x	x			skeletal sparry lump limestone
100-18C	29	Clb					x	x			
100-14A		Clb					x	x			
100-30	III h 30	Clb					x	x			quartzose lump sparry skeletal limestone
100-25		Clb					x	x			lump sparry skeletal limestone
146-12	31	Dub							1		
105-890	III i 32	Dub						1			solenopore sparry lump limestone
105-505		Dub						1			quartzose lump limestone
105-735	33	Dub						1			skeletal sparry lump limestone
105-620		Dub						1			
AAP Kulshill		D-Cb									
No. 1 9203′	IV j 34									NR	quartzose skeletal oolitic sparry lump limestone
105-830		Dub						1			bryozoal sparry lump limestone
100-27	35						x	x			quartzose skeletal sparry lump limestone
146-15	36	Clb					x	x			quartzose algal micrite skeletal sparry lump limestone
103-14C		Clb					x	x			
101-20A	k 37	Clb					x	x			quartzose skeletal sparry lump limestone
100-21A		Clb					x	x			
108-3	38	Clu								NR	
104-11B	39	Cls								NR	quartzose sparry skeletal limestone
101-21		Clb					x	x			
146-18	l 40	Clb					x	x			quartzose sparry lump limestone
103-13		Clb					x	x			
105-320	41	Dub						1			
105-65B		Dub						1			
459-390	m 42	Duw					x	x			quartzose lump limestone
13-6		Duw					x	x			
459-160	43	Duw					x	x			
105-230		Dub						1			
146-13	V n 44	Dub							1		silty crinoidal limestone
5-2		Clr								NR	quartzose silty crinoidal limestone
104-17A	45	Cls								NR	quartzose sparry crinoidal limestone
104-16		Cls								NR	silty crinoidal limestone
104-12	o 46	Cls								NR	quartzose dolomitic sparry skeletal limestone
627-1	47	Permian								NR	brachiopodal limestone
104-7B		Cls								NR	quartzose sparry skeletal limestone
465-1	V p 48	Clr								NR	lump crinoidal limestone
458-0		Clr								NR	quartzose sparry lump crinoidal limestone
108-5	49	Clu								NR	sparry lump crinoidal limestone
108-0		Clu								NR	
104-10	q 50	Cls								NR	sparry skeletal limestone
104-6	51	Cls								NR	
104-4		Cls								NR	
406-15	VI r 52	Duu								NR	quartzose dolomite
210-6	Cl	(breccia)								NR	
AOD Bonaparte No. 1											
1,264′	53	Clt								NR	
438-1		Duv								NR	
442-9	s 54	Duj								NR	calcisilty quartz sandstone
146-9		Dub							1		quartzose silty lump limestone
13-1	55	Duw					x	x			sparry dolomite
443-18	56	Dun					1				dolomite
442-5		Duj								NR	
455-2	t 57	Clw								NR	dolomitic quartz sandstone
146-6		Dub							1		
108-6	58	Clu								NR	dolomitic sparry quartz sandstone
28-10		Duu								NR	

NOTES: 1. Taken from Figure 22. The lowest group (1-58) is not shown in Figure 22.

2. For explanation of letter symbols, see Figure 3.

3. Reef determination of Famenian sequence based on field evidence, shown by 1.
Reef determination of other sequences based on petrographic evidence, shown by x.